THE GENETICS, GENOMICS AND PHYSIOLOGY OF THE RESPONSE OF *POPULUS* TO ELEVATED OZONE

In one volume

James Tucker

School of Biological Sciences

University of Southampton

Submitted for Doctor of Philosophy, August 2006

Abstract

Faculty of Medicine, Health and Life Sciences, University of Southampton

Doctor of Philospohy

THE GENETICS, GENOMICS AND PHYSIOLOGY OF THE RESPONSE OF *POPULUS* TO ELEVATED OZONE

James Tucker

The genetic basis of susceptibility of *Populus* to ozone damage was investigated using a combination of phenotyping, QTL mapping and microarray analysis on an F_2 mapping population, Family 331, bred from a cross between *Populus trichocarpa* (93-968) and *P. deltoides* Bart (ILL-129).

P. trichocarpa and *P. deltoides* exposed to an acute ozone treatment in growth chambers showed highly divergent physical symptoms, with *P. trichocarpa* developing necrotic lesions within 9 hrs of treatment and *P. deltoides* remaining undamaged. This provided the basis for a large-scale QTL mapping and phenotyping experiment in open-top chambers on 164 individuals of the F_2 mapping population, and also for gene expression studies in the grandparental species. A total of 20 ozone-specific QTL were mapped for numerous physiological traits, several of which displayed marked transgressive segregation. This wide range of sensitivity allowed selection of two groups of ozone sensitive and tolerant genotypes with contrasting patterns of visible damage. cDNA microarrays were used to uncover genes that showed altered expression in response to an acute ozone treatment, and included those encoding antioxidants and also those involved in photosynthesis and the phenypropanoid pathway. Furthermore, genes that were differentially expressed between the grand-parental species and between the two sensitivity groups of F_2 genotypes were identified. The recent completion of the physical genome sequence allowed the position of these candidate genes to be compared to QTL locations, a field termed "genetical genomics". Differentially expressed genes that co-located with QTL for visible damage to ozone were considered to be encouraging candidates for mediating the response. These included genes encoding arginine decarboxylase, SAM synthetase, and a plasma membrane intrinsic protein, which can be targeted for further investigation.

Acknowledgements

First, I should like to thank my supervisors, Professor Gail Taylor and Professor John Hall, for their help and guidance throughout my PhD, and to the Natural Environment Research Council for providing funding.

I am grateful to all members of the Plants and Environment group; in particular Caroline Dixon, Harriet Trewin, Mike Cotton, Laura Graham, Sarah Elhag, Penny Tricker Sera Bowden and Nicole Harris for their help with data collection at the field trial. I also extend gratitude to Dr. Matthieu Pinel for performing the hormone profiling described in Chapter 4 at the University of Helsinki. I am particularly indebted to Dr. Nathaniel Street for both his help with data collection and work in the laboratory, and also for inspiring discussions on aspects of this work.

Franco Miglietta and Alessandro Zaldei were very helpful in the task of constructing an ozone enrichment system, and provided valuable advice on the problems which I encountered, both during their visit and subsequently.

I extend my gratitude to Jaakko Kangasjärvi and Mikael Brosché from the University of Helsinki for the use of their microarray facility for a full month, and for help with laboratory methods and data analysis.

The field trial would not have been possible without Dr Mark Broadmeadow and the staff at Headley Nurseries, who spent considerable time constructing the ozone enrichment system and maintaining the open-top chambers.

Table of contents

List of abbreviations

ABA	Abscisic acid
ADC	Arginine decarboxylase
AFLP	Amplified fragment length polymorphism
ANOVA	Analysis of variance
CAD	Cinnamyl Alcohol Dehydrogenase
cGMP	Cyclic GMP
CHISAM	Chloroform isoamyl alcohol (24:1)
CIM	Composite interval mapping
cM	Centimorgan
d	Day
DNA	Deoxyribonucleic acid
DRE	Dehydration responsive element
EST	Expressed sequence tag
FDR	False discovery rate
FWER	Family-wise error rate
GC-MS	Gas chromatography mass spectrometry
GO	Gene Ontology
HR	Hypersensitive response
hr	Hour
HRGP	Hydroxproline rich glycoprotein
JA	Jasmonic acid
L	Litre
LG	Linkage group
Ln	Leaf number
LOD	Likelihood of odds
Lowess	Locally weighted regression
LOX	Lipoxygenase
m	Metre
MA plot	Plot of log-intensity ratios (M-values) versus log-intensity averages (A-values)
MAPK	Mitogen activated protein kinase
MGDG	Monogalactosyl diglycerides
min	Minute
mm	Millimetre
mol	Mole
MQ	Milli-Q
NO	Nitric oxide
OTC	Open-top chamber
PAL	Phenylalanine ammonia lyase
PAR	Photosynthetically active radiation
PB	Phosphate buffer
PCD	Programmed cell death
PCR	Polymerase chain reaction
PLS-DA	Partial least squares discriminant analysis
PMT	Photomultiplier tube
ppb	Parts per billion
PPFR	Photosynthetic photon fluence rate
PR	Pathogenicity related
QT	Quantitative trait
QTL	Quantitative trait locus

RAPD	random amplified polymorphic DNA
RFLP	Restriction fragment length polymorphism
RI	Ratio intensity
RIL	Recombinant inbred line
RIL	Recombinant inbred line
RIPK	ROS induced protein kinase
RLK	Receptor-like kinase
RNA	Ribonucleic acid
ROS	Reactive oxygen species
RT-PCR	Real-time PCR
RT-qPCR	Real-time quantitative PCR
s	Second
SA	Salycylic acid
SAG	Senescence associated gene
SAR	Systemic acquired resistance
SDS	Sodium dodecyl sulphate
SE	Standard Error
SIPK	Salicylate induced protein kinase
SNP	Single nucleotide polymorphism
SSC	Saline sodium citrate
SSR	Simple sequence repeat
TIFF	Tagged image file format
TUNEL	Terminal deoxynucleotidyl Transferase Biotin-dUTP Nick End Labeling
VIP	Variable importance
WB	Wash buffer

Chapter 1: General introduction

1.1 Poplar as a model tree species

Many biological processes exhibit considerable similarity across diverse taxonomic groups. It is therefore not usually necessary to study such processes in every species; rather, a "model" organism can be selected. All model organisms possess the common feature of being amenable to experimental research, for example exhibiting short generation time or facile genetic transformation. When work is focussed on a particular organism, it is possible to develop a co-ordinated network of research and centralised resources, greatly accelerating the progression of biological understanding. Examples of model organisms include the fruit fly *Drosophila melanogaster* Meigen (Ashburner & Bergman, 2005) and the nematode worm *Caenorhabditis elegans* Maupas (Kaletta & Hengartner, 2006).

The first plant to be accepted as a genetic model was *Arabidopsis thaliana* L.(thale cress) and is widely used (Glazebrook et al., 1997; Hays, 2002; Koornneef et al., 2004). It possesses numerous advantages, including short generation time, ease of growth, the ability to self-fertilise, a short life cycle, and a small genome. It was in fact the first plant to have its genome fully sequenced (The Arabidopsis Genome Initiative, http://www.arabidopsis.org/), and a myriad of genomic resources are now available. Although *Arabidopsis* has proved useful as a model for biological processes, there are features present in other plants that are not found in *Arabidopsis*. For example, rice is now an accepted model for monocotyledonous food plants,

(International Rice Genome Sequencing Project, 2005), where the dicotyledonous Arabidopsis was not considered suitable.

Trees can be distinguished from annual herbaceous species such as Arabidopsis by long lifespan, wood production, seasonal senescence, secondary cambium, dormancy and branching. Trees must also be able to cope with diverse environmental stresses throughout their lifespan. Due to these distinct differences in morphological and life history traits, the use of *Arabidopsis* in modelling such features is questionable (Taylor, 2002).

Poplar has long been a commercially important species, with diverse uses such as timber, pulp and paper, carbon sequestration and bioremediation. More recently, its value as a model tree has been considered, and it has since joined the league of accepted model organisms (Taylor, 2002; Brunner et al., 2004; Tuskan et al., 2004).

The genus *Populus* comprises approximately 40 species located throughout the Northern hemisphere from the tropics to the Arctic Circle. This wide geographical range is in itself advantageous for analysing adaptation to contrasting environments. For example, McCamant & Black (2000) demonstrated differences in cold hardiness of *P. trichocarpa* Marsh from diverse habitats. Poplar is among the fastest growing trees, and can also be clonally propagated. These features are of tremendous advantage in the production of large volumes of experimental material, and in maintaining populations (Taylor, 2002).

Since the acceptance of poplar as a model, considerable genetic and genomic resources have been developed, perhaps most important being the completion of the

physical genome sequence of *P. trichocarpa* to an 8X depth (i.e. it is sequenced 8 times, reflecting the accuracy of the final sequence). The poplar genome is relatively short in comparison to other trees, containing 50 times less base pairs than pine. This not only aided the sequencing effort, but will also facilitate subsequent studies. The sequence is available on-line at the Joint Genome Institute (JGI) site (http://genome.jgi-psf.org/Poptr1/Poptr1.home.html), and annotation of the sequence is currently underway.

Large EST collections have also been developed. In particular, the Swedish *Populus* Genome Project has identified 25,000 unigenes (http://poppel.fysbot.umu.se/). Other collections include an 8,000 EST set from the University of Helsinki (http://sputnik.btk.fi/), and a 20,000 set from Genome British Columbia (http://www.genomebc.ca). Such projects are proving invaluable in aiding annotation of the genome through identification of coding regions, and also in gene expression studies through cDNA microarrays. Commercial organisations are also involved, for example Picme (http://www.picme.at) are now producing custom poplar microarrays from current EST collections, and Affymetrix (www.affymetrix.com) are planning the release of a poplar oligonucleotide array.

A number of poplar genetic maps have been developed, for example Family 331 (Bradshaw et al., 1995), a Belgian cross of *P. trichocarpa, P. nigra and P. deltoides* (Cervera et al., 2001), and a French cross of *P. nigra* and *P. deltoides* (Cervera et al., 1997). These populations have been used to map many QTL, and the high congruency between the genetic and physical maps (Bradshaw et al., 2000) will allow further elucidation of the genetic basis of many important traits.

Poplar was the first tree to be successfully transformed, and transgenes have been shown to be relatively stable (Peña et al., 2001). Agrobacterium-mediated transformation is now a routine procedure in a number of poplar species, and knockout studies using RNA interference are currently under development.

It can therefore be seen that poplar possesses numerous features that render it suitable as a model tree, and the genetic and genomic resources are becoming comparable to those available to Arabidopsis.

1.2 Ozone- a damaging tropospheric pollutant

Ozone (O_3) concentrations in the troposphere (the lowermost region of the atmosphere) have increased by approximately four-fold in the last century, and summer concentrations can exceed 150 parts per billion (ppb). Whilst ozone in the stratosphere (the atmospheric layer above the troposhere) serves an important protective role through filtering harmful UV radiation, tropospheric ozone is extremely toxic, and there is mounting concern regarding its detrimental effects on organisms from humans to plants. It is formed largely from nitrogen oxide gases and volatile organic compounds contained in industrial emissions and car exhausts, which can interact with oxygen to form ozone in the presence of ultraviolet light and favourable temperatures.

Heggestad (1959) first documented the phytotoxic effects of ozone, describing the lesions seen as "weather flecks", and it is now known that sensitive species can be affected by concentrations as low as 40 ppb. It can damage wild and cultivated plants alike, and has a huge impact on crop yield. In the USA, a 1-2% per year increase in

tropospheric ozone concentration is anticipated for the next fifty years (Morgan et al., 2004). In Europe, the UN-ECE critical threshold has been exceeded in recent years (Führer et al., 1997), and in the UK, August 2003 saw the highest ozone concentrations for over a decade (www.defra.gov.uk).

Considerable progress has been made concerning the physiological, biochemical and underlying genetic responses to ozone, and this is the subject of the following sections.

1.3 Acute ozone treatment as an abiotic elicitor of the hypersensitive response

The HR as a defence mechanism

The hypersensitive response (HR) is mounted by resistant plants when inoculated with avirulent pathogens. It encompasses both localised cell death and induction of defence genes. The extent of cell death is interspecifically variable and can range from one cell to formation of visible lesions. The cell death observed is thought to be a form of PCD. Evidence for this includes the presence of hallmarks of animal apoptosis, such as DNA laddering, and the fact that death requires active plant metabolism, such as translation and/or transcription (Heath et al., 1997; Mansfield et al., 1997; Mould and Heath, 1999). It is therefore considered that the response is under control of the plant. In light of this, it has been proposed that cell death aids in pathogen containment. There is a considerable body of research indicating that the ozone-induced response overlaps with that of plant-pathogen interactions, therefore acting as an abiotic elicitor of the HR.

Physiological assessment provides a first line of evidence for an HR-like response to ozone. Guderian (1985) described "classical" ozone symptoms in tobacco BelW3. This ozone-sensitive plant exhibits lesions on the adaxial side of the leaf, which result from death of palisade cells. Such lesion formation has been documented in other sensitive species (Strohm et al., 1999; Langebartels et al., 2002), and bears striking similarity to those seen during the HR. Furthermore, lesions have been found to appear in periveinal regions (Wohlgemuth et al., 2002), a feature also seen in "micro-HR" responses to pathogens.

Markers of PCD (and therefore the HR) have also been reported, including DNA laddering (indicated by Transferase-mediated dUTP Nick-End Labelling (TUNEL) analysis) (Koch et al., 2000), and chromatin condensation (Rao et al. 2000).

Ozone also upregulates many HR and defence-associated gene products, such as those involved in salicylic acid and jasmonic acid biosynthesis (Kangasjärvi et al., 2005), pathogenicity related (PR) proteins (Sharma and Davis, 1996; Agarwal et al., 2002), hydroxyproline-rich glycoproteins (HRGPs) (Eckeykaltenbach et al., 1994), phytoalexins (Rosemann et al., 1991; Grimmig et al., 2003), and enzymes of the phenylpropanoid pathway (Cabane et al., 2004).

The considerable similarity between acute ozone response and the HR has caused current opinion to favour ozone as an abiotic elicitor of the response.
Recently, progress has been made concerning the signal transduction pathways involved in the ozone-induced HR, with attention focussed largely on reactive oxygen

species (ROS), salicylic acid (SA), nitric oxide (NO), ethylene and jasmonic acid (JA), which will be discussed in turn in the following sections. It is now thought that the pathways involved are far from linear, with extensive interactions, or "cross-talk" occurring between them.

Death upregulators

Reactive oxygen species (ROS) and the oxidative burst

Ozone possesses very powerful oxidising properties, which can result in the production of reactive oxygen species (ROS) such as $\cdot O_2^-$ (superoxide), H_2O_2 (hydrogen peroxide) and O (singlet oxygen) upon contact with apoplastic fluid. In sensitive species, endogenous ROS production follows, resulting in a self-perpetuating amplification of ROS levels, known as the "oxidative burst". An analogous response occurs in plants inoculated with avirulent pathogens, and is thought to be involved in initiating the hypersensitive response (HR) (reviewed in Doke et al., (1996)).

The source of ROS for the ozone-induced oxidative burst has proved enigmatic, although it is likely that plasma membrane NADPH oxidases, which produce superoxide, play an important role (Laloi, Apel and Danon, 2004). Wohlgemuth et al. (2002) reported upregulation of two NADPH oxidase transcripts and, furthermore, showed that an inhibitor of flavin containing oxidases (such as NADPH) could curb both the oxidative burst and hypersensitive cell death in tomato. Other candidate

enzymes include amine oxidases, oxalate oxidase, and cell wall peroxidases (Bolwell, 1999; Corpas et al., 2001; Wohlgemuth et al., 2002).

Which ROS play the most prominent role in the oxidative burst? This has also been a point of controversy, and is particularly difficult to investigate due to the ability of ROS to interconvert between forms (e.g. $\cdot O_2^-$ is rapidly converted to H_2O_2 both spontaneously and through the action of superoxide dismutase (SOD)). However, in light of a comprehensive analysis by Wohlgemuth et al. (2002), it seems likely that there are interspecific differences. H_2O_2 accumulated in all ozone-treated tobacco and tomato cultivars, whilst $\cdot O_2^-$ was the most abundant in two *Rumex* species.

Debate has also surrounded the precise function of the oxidative burst, particularly whether it is necessary and sufficient for death induction. A wealth of research involving use of antioxidants, radical quenchers and catalase show that death can be blocked by decreasing ROS concentrations in plants exposed to avirulence signals. Similarly, inhibition of the $\cdot O_2^-$ producing NADPH oxidase reduced cell death in ozone stressed plants (Wohlgemuth et al., 2002). Conversely, Glazener et al. (1996) demonstrated that cell death in response to avirulent bacteria could be blocked by mutation of a gene in the Hrp cluster (involved in bacterial type III secretion systems), despite the presence of an oxidative burst. It is therefore considered that a variety of other signalling molecules are required for a full response to both pathogens and ozone, and these will now be discussed.

Salicylic acid (SA)

It is well established that the phenylpropanoid compound salicylic acid (SA) plays an important role in plant defence. Transgenic *Arabidopsis* expressing the bacterial salicylate hydroxylase gene NahG, the product of which breaks down SA, are defective in pathogen containment and do not mount an HR (Delaney et al., 1994); they also exhibit impaired induction of defence genes for pathogenesis-related proteins and antioxidants (Sharma and Davis, 1996).

Although the complete mechanism is yet to emerge, SA is now known to act as a positive regulator of cell death. Research has suggested that SA acts downstream of the oxidative burst (Hammond-Kossack, 1996; Dangl et al., 1996; Delaney, 1997), although it has become apparent that SA can also act to increase production of ROS (Kauss and Jeblick, 1995; Mur et al., 1996; Ganesan and Thomas, 2001). A proposed mechanism by which this occurs is through inhibition of antioxidant enzymes such as catalase (Durner and Klessig, 1996), ascorbate peroxidase (Durner and Klessig, 1995), and certain peroxidase isoforms (Ganesan et al 2001), resulting in impaired quenching of ROS. This is proposed to result in a positive feedback loop of SA and ROS production, increasing hypersensitive cell death (Rao and Davis, 2001).

Mitogen-activated protein kinases (MAPKs) are known to modulate ROS production and cell death patterns (Kovtun et al., 2000). Zhang and Klessig (1997) identified a MAPK (named SIPK, for Salicylate Induced Protein Kinase) that is rapidly induced by SA treatment. However, Samuel et al. (2000) found that NahG plants under oxidative stress are not compromised in SIPK activation, although the response can be inhibited by radical quenchers. The authors suggest that SA may not play a direct role

in activation, and that SIPK would be more appropriately named RIPK (for ROS-induced protein kinase).

Several receptor-like kinases (RLKs) are induced by salicylic acid treatment (Ohtake et al., 2000). These are known to be involved in many signal transduction pathways, and it has been suggested that they play a role in cell death and defence gene induction. Interestingly, the genes contain a TTGAC sequence in the promoter region, a motif known to be important for defence gene expression. They may therefore be involved in the salicylic acid induced signal transduction pathway.

Ozone is capable of inducing large increases in SA levels, first demonstrated by Yalpani et al. (1994) in tobacco plants. Puzzlingly, ozone-induced cell death has been found to be greater in NahG plants. However the death in this case is thought to be due to severely compromised antioxidant defences seen in such plants resulting in uncontrolled death rather than an HR-like response (Sharma et al., 1996). It has since been demonstrated in an ozone sensitive Arabidopsis ecotype, Cvi-0, that SA accumulation is indeed associated with increased ozone-induced cell death (Rao and Davis, 1999; Rao et al., 2000), similar to the hypersensitive response. As with the HR, SA has also been shown to be required for upregulation of a number of HR-associated genes during ozone treatment, including *PR-1* and *GST-1*(Sharma and Davis, 1996).

Nitric oxide (NO)

Nitric oxide is also thought to play a role as a positive regulator of death and defence gene induction during acute ozone exposure. It first attracted attention as an early-response signal molecule that acts to potentiate cell death during the HR in soybean

cells, and was found to act in synergy with ROS (Delledonne et al., 1998). Its ability to induce phenylalanine ammonia lyase (PAL) (Durner et al., 1998), production of which is unaffected in NahG transgenics, suggests that it can operate on SA-independent pathways. Similar to mammalian systems, it appears that NO exerts its effects at least partly through cyclic GMP (cGMP). cGMP is inducible by NO and, furthermore, inhibitors of mammalian guanylate cyclase (the enzyme which produces cGMP) abolish NO-induced PAL upregulation (Durner et al., 1998). Its ability to induce SIPK (Klessig et al., 2000) also leaves open the possibility that it may also act via MAP kinases, although inhibitors of mammalian MAPKs have no effect on NO induced cell death.

Ozone has been found to increase NO synthase activity prior to SA accumulation (Rao et al. 2001) suggesting an early role for NO signalling in the ozone-induced response. As discussed, PAL is inducible by NO and cGMP, but independent of SA. PAL represents the first enzyme in the phenylpropanoid pathway, of which SA is a product. It is therefore possible that an early rise in NO-induced cGMP results in an increase in SA biosynthesis via upregulation of PAL. Additionally, NO is able to react with superoxide, forming the peroxynitrite radical. This highly reactive species may cause increased ROS production and therefore amplify SA concentrations (Bolwell, 1999).

Ethylene

Increased ethylene concentrations have long been known to be associated with ozone exposure in sensitive plants (Mehlhorn and Wellburn, 1987; Tuomainen et al., 1997).

It is involved in many plant developmental processes including those involving PCD, for example root aerenchyma formation (Drew et al., 2000) and carpel senescence (Orzaez and Granell, 1997). It is also plays a key role in responses to pathogens, inducing a number of defence genes, including PR proteins (Deikman, 1997) and enzymes involved in phytoalexin synthesis (Ecker and Davis, 1987). More recent work revealed its importance in the cell death response itself. Ciardi et al. (2000) demonstrated that overexpression of *NR* (a gene in tomato which shows homology to ethylene receptors) in *Arabidopsis* rendered plants less sensitive to ethylene, with an associated decrease in lesion spread. It is therefore thought that ethylene acts as a positive regulator of cell death.

The correlation between ozone sensitivity and ethylene production was originally thought to be due to formation of ROS and aldehydes from reaction between the two compounds, resulting in uncontrolled necrotic cell death through membrane damage (Elstner, 1987). However, it is now thought that ethylene is involved in a controlled, HR-like response. Correlative evidence suggested that ethylene was involved in exacerbation of $\cdot O_2^-$ levels (Mittelstrass et al. unpublished). Furthermore, Overmyer et al. (2000) demonstrated that exogenous ethylene results in increased $\cdot O_2^-$ levels in *Arabidopsis radical induced cell death 1* (*rcd1*) mutants. The authors also demonstrated a requirement for functional ethylene perception, as *rcd1/ein2* (*ethylene insensitive 2*) double mutants were impaired in $\cdot O_2^-$ accumulation and lesion spread. Interestingly, ozone still induced lower levels of $\cdot O_2^-$ together with "micro-lesions" in these mutants. The authors therefore suggest that it is lesion propagation as opposed to initiation that requires ethylene. Consistent with this is the observation that lesions

fail to spread following ozone exposure in *rcd1/ein2* double mutants, whereas propagation continued in *rcd1* plants.

There is some evidence to suggest that ethylene can serve a protective role against ozone damage. Treating pea and mung bean with ethylene prior to ozone exposure has been found to increase resistance to damage (Mehlhorn, 1990). It is therefore possible that the timing of ethylene accumulation is important in governing the response. In support of this, Vahala et al. (2003) found that blocking ethylene perception after ozone treatment decreased cell death, implying that ethylene action is required late in order to promote damage. The authors suggest that sensitivity may in part be governed by differential transcript accumulation of ACC synthase at the time of damage, as BP-ACS2 was detected at this time in an ozone sensitive birch clone, but not in an ozone tolerant clone.

Recently, it has been demonstrated that functional ethylene perception is required to protect against ozone induced cell death. It has been found that blocking ethylene production completely inhibits cell death in ozone sensitive birch, whilst ethylene insensitive plants still exhibit some damage. When ACC is oxidised to ethylene, hydrogen cyanide (HCN) is produced as a by-product, which is normally detoxified by β-cyanoalanine synthase (β-CAS). However, ozone treated ethylene insensitive birch clones exhibited lower levels of β-CAS, whilst maintaining rates of ethylene synthesis and therefore HCN. This could allow accumulation of HCN and concomitant cell death (Vahala et al., 2003). It may be argued that these results are not relevant to wildtype plants, as ethylene insensitivity was induced by transformation with the dominant negative *Arabidopsis* ethylene receptor gene *etr1-1*.

It has, however, been found that plants can alter their ethylene sensitivity in response to ozone (Tuominen et al., unpublished). Also, Moeder et al. (2002) demonstrated the existence of ozone-inducible ethylene receptor genes in tomato plants. It may be the case, therefore, that HCN plays a role in eliciting the cell death response.

A death inhibitor: Jasmonic acid (JA)

Jasmonic acid (JA) and its methyl ester (Me-JA) are widely distributed throughout plants, and are thought to be involved in diverse developmental processes and stress responses. It has been found to induce certain defence genes independently of SA, although recent studies have indicated that there is also a great deal of "cross-talk" between SA- and JA-dependent pathways. JA can act to synergise or antagonise SA dependent gene expression, with interspecific differences being observed (Niki et al., 1998; Xu et al., 1994). Interaction between the pathways has been corroborated by discovery of "cross-talk nodes", for example Shah et al. (1999) presented evidence that the gene product of *SSI1* may act as such an interface for SA and JA dependent pathways.

Ozone treatment rapidly (within hours) upregulates JA synthesis in *Arabidopsis* and hybrid poplar (Koch et al., 2000; Rao et al., 2000). A possible mechanism involves lipoxygenase (LOX), which has been found to be upregulated by ozone (Maccarrone et al., 1997) and liberates linolenic acid from the plasma membrane. Linolenic acid is the precursor for JA biosynthesis. JA has therefore attracted considerable attention regarding its role in the ozone-induced response. Exogenous JA application has been found to inhibit ozone-induced cell death in tobacco (Orvar et al., 1997) and hybrid poplar (Koch et al., 2000), and also diminishes H_2O_2 production in tobacco

(Schraudner et al., 1999). It has therefore become accepted that JA acts as a negative regulator of cell death in ozone treated plants. Work by Rao et al. (2000) has provided an insight into the mechanisms of JA action, and suggests that it negatively regulates the SA-mediated death pathway. Treatment of the ozone-sensitive Arabidopsis ecotype Cvi-0 with exogenous Me-JA prior to ozone treatment reduced H_2O_2 and SA production, with a concomitant decrease in lesion formation. Consistent with this, a *jar1* mutation renders the ozone tolerant ecotype Col-0 insensitive to JA, with ozone treatment resulting in elevated H_2O_2, SA and PR1 levels, together with lesion formation. The authors hypothesised that JA negatively regulates ROS accumulation, with a resulting decrease in SA synthesis. Their results also suggest existence of an additional cross-talk node downstream of SA synthesis. Col-0 plants treated with Me-JA and ozone showed a greater increase in SA and H_2O_2 accumulation than in plants treated only with ozone, whilst *PR-1* gene expression, which is induced by SA, was significantly lower in the former. It therefore seems likely that JA can act as a negative regulator at two points on the pathway.

It is of note that in some cases high JA levels have been found to correlate with ozone induced cell death, for example in the ozone-sensitive Arabidopsis *rcd1* mutant, and an ozone sensitive birch clone (Vahala et al., 2003). However, the authors note that this does not necessarily imply a death promoting role for JA. JA production has been found to be limited by availability of α-linolenic acid, a fatty acid found in the cell membrane. It is likely that this is liberated from the membrane during cell death, providing additional substrate for JA synthesis. Therefore JA levels may increase after cell death has occurred, and subsequently act to contain the response.

The interplay between ROS and hormonal cues in an acute ozone response is shown in Figure 1.1.

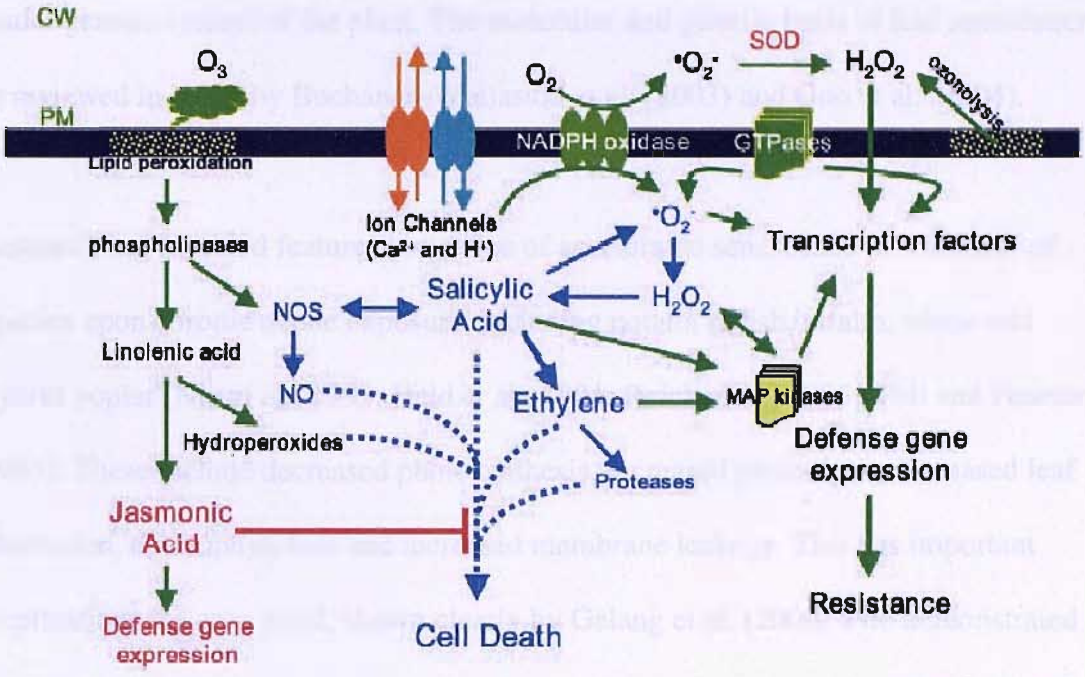

Figure 1.1: The interplay between hormonal cues and reactive oxygen species signalling in response to an acute ozone treatment. Taken from Rao & Davies (2001)

1.4 Chronic ozone exposure- accelerated senescence

Ozone treatment and accelerated senescence

Senescence represents the final stage of leaf development, and is thought to be a form of programmed cell death. It is an age dependent process, being initiated after a defined period of photosynthetic activity, and can also be triggered by factors such as shading, temperature and pathogen infection (Pons and Pearcy, 1994; Benbella and Paulsen, 1998). The leaf's role as a source of photosynthate decreases and salvage pathways are initiated, allowing remobilisation and hence redistribution of key nutrients, such as nitrogen, phosphorous and metals, to juvenile leaves or seeds. The program proceeds in a stereotyped order. Chloroplasts are broken down first, whilst

the nucleus and mitochondria remain intact until the final stages. Thus the metabolic and transcriptional activity of the cell is maintained throughout, essential for a process under genetic control of the plant. The molecular and genetic basis of leaf senescence is reviewed in detail by Buchanan-Wollaston et al. (2003) and Guo et al. (2004).

Research has revealed features indicative of accelerated senescence in a number of species upon chronic ozone exposure, including potato, radish, alfalfa, wheat and hybrid poplar (Nie et al., 1993; Held et al., 1991; Reich et al., 1985; Pell and Pearson, 1983). These include decreased photosynthesis, increased proteolysis, increased leaf abscission, chlorophyll loss and increased membrane leakage. This has important implications for crop yield, shown clearly by Gelang et al. (2000) who demonstrated that reduced grain yield in spring wheat in response to ozone treatment was primarily due to accelerated senescence.

Downregulation of photosynthetic components

Senescence involves downregulation of photosynthetic components, including ribulose 1,5 bisphosphate carboxylase oxygenase (Rubisco). A decrease in photosynthesis and Rubisco content has certainly been documented in ozone-treated plants (Farage et al., 1991; Glick et al., 1995; Farage, 1996; Miller et al., 1999). However, the predominant mechanism of loss has remained somewhat unclear. Pell et al. (1997) noted that, although nuclear run-on experiments have demonstrated that transcription of *RbcS* decreases with ozone treatment, it is not sufficient to account for the large drop in mRNA content, indicating that RNase activity may also play a role. Evidence for proteolysis has also been presented, with Rubisco first aggregating and then being degraded (Brendley and Pell, 1998). Eckardt and Pell (1994) used light and

dark grown potatoes to allow separation of transcription and degradation, as *Rubisco* transcription is light regulated. A decrease in Rubisco level was only seen during the dark treatment, suggesting that degradation may in fact be the main mechanism for loss of the protein.

A decline in levels of other photosynthetic proteins has also been reported, including photosystem II chlorophyll a/b binding protein, involved in light harvesting and D1, a core protein of the PSII reaction centre (Ranieri et al., 2001). Thus ozone fumigation results in decreased activity of electron transport chain components and decreased photosynthetic protein content.

A possible mechanism: oxidative stress in the chloroplast

As ozone cannot penetrate into the cytosol, another mechanism must exist by which it can cause oxidative damage to the chloroplast. Pell et al. (1997) proposed that ozone fumigation induces lipase activity, which acts on plastidic monogalactosyl diglycerides (MGDGs) giving increased fatty acids available for lipid peroxidation, resulting in an oxidative burden on the chloroplast.

Gene induction during ozone-induced senescence

A battery of genes is induced during leaf senescence. These senescence associated genes (SAGs) encode proteins involved in salvage pathways and execution of death, such as proteases, RNases, Gln synthetase, metallothioneins, protease regulators, ACC oxidase, lipases, glyoxylate cycle enzymes, catalase, endoxyloglucan transferase, pathogenesis-related proteins, ATP sulfurylase, glutathione *S*-transferase, Cyt P450,

and polyubiquitin. A comprehensive analysis by Miller et al. (1999) revealed that ozone is capable of upregulating a number of senescence-associated genes, including *ACC oxidase* (involved in ethylene production), *Cch* (a copper chaperone), *BCB* (blue copper-binding protein), *ERD1* (a protease regulator) and other SAGs of uncertain function. The spatial pattern of induction of certain SAGs was also affected. For example *SAG13* is normally induced first at the leaf borders, whilst ozone treatment induces expression throughout the leaves. Interestingly, four of the SAGs studied, including *MT1* (metallothionein) and *Atgsr2* (Glutathione synthetase) were not induced by ozone fumigation, indicating an incomplete overlap between senescence and ozone treatment. Also, as these genes are associated with salvage pathways, this could have profound implications for plant productivity in elevated ozone.

A role for ethylene

Considerable evidence exists that ethylene acts as a positive regulator of senescence. Arabidopsis *etr1* (defective in an ethylene receptor) and *ein* (ethylene insensitive) mutants exhibit both delayed senescence and chlorophyll loss (Bleecker et al., 1988; Zacarias and Reid, 1990; Grbic and Bleecker, 1995), as do plants treated with silver thiosulphate, an ethylene inhibitor (Davies and Grierson, 1989). It is likely that ethylene plays a role in accelerating senescence as opposed to causing it, as the process occurs in *etr1-1* plants, but with a delay.

Acute ozone treatment is capable of inducing ethylene production in sensitive plants (Tingey et al., 1976, Mehlhorn and Wellburn 1987, Tuomainen et al., 1997). There is evidence that low-level ozone exposure can induce ethylene production, with ethylene emission occurring in advance of senescence symptoms (Reddy et al., 1993). Also,

Schlagnhaufer et al. (1995) demonstrated an increase in *ACC synthase* mRNA and ethylene levels with chronic ozone fumigation, and a study by Glick et al. (1995) revealed that 0.08 μLL^{-1} ozone for five hours per day causes ethylene production, correlating with a loss of *RbcS* mRNA.

The effect of leaf age

It has become apparent that sensitivity to ozone depends on the age of the leaf, with older leaves being more prone to accelerated senescence. Leaf antioxidant content is known to decline with age, and it is therefore possible that older leaves are less able to cope with the oxidative burden caused by ozone treatment (Pell et al., 1997).

Possible roles for ABA, calcium and SA?

A number of questions still remain to be addressed concerning the similarity between natural and ozone-induced senescence, and analysis of natural senescence provides an important basis for investigating the ozone-induced response. ABA is a well-known promoter of senescence, and a number of ozone responsive SAGs can be induced by ABA treatment (Weaver et al., 1998). However, it is at present unknown whether ABA plays a role in the ozone-induced response. Calcium is a key second messenger in many plant responses, including to acute ozone treatment. The role of calcium in the response to chronic ozone fumigation represents an important avenue for future research.

Morris et al. (2000) demonstrated a role for salicylic acid, well known for its role in the HR, in governing expression of SAGs during natural senescence. Using NahG plants and mutants defective in SA synthesis, it was found that expression of *SAG12*

(encoding a cysteine protease) was completely dependent on SA, and glutamine synthetase exhibited partial dependence. Small differences were also seen in chlorosis and cell death patterns.

1.5 Overlap between the responses to acute and chronic ozone stress

Although it is yet to be established that SA plays a role in the response to chronic ozone treatment, this highlights an important question: how much overlap exists between the acute and chronic responses? As discussed, both acute and chronic ozone treatment result in production of ROS, and it is likely that they are involved in both responses. It is known that a threshold level of ROS is required for elicitation of the HR. Pell et al.(1997) proposed that the lower concentrations achieved during chronic ozone treatment are insufficient to trigger the HR, but instead result in accelerated senescence. It is therefore likely that the response of the plant not only depends on the presence of a signalling molecule, but also on its concentration. As discussed, salicylic acid represents a potential point of overlap between the responses, and again its effects are thought to be concentration dependent. PR1a, an SA induced protein, was found to reach low levels during natural senescence in comparison to during an HR, correlating with the level of SA in each response (Morris et al., 2000). Future work could address the extent of overlap between the responses to acute and chronic treatment.

1.6 The role of antioxidants

The ability of antioxidants to quench ROS has led to a wealth of research concerning whether they play a role in determining the outcome of a plant's response to ozone.

Ascorbate is a candidate for providing the first line of antioxidant defence, as it is located in the apoplast. Increased ascorbate levels have been found to stem ozone flux to the apoplast (van Hove et al., 2001), potentially intercepting up to 30-40% (Turcsanyi et al., 2000), and has also been shown to ameliorate photosynthetic decline (Zheng et al., 2000). However, its importance in determining resistance to ozone has been challenged, with a study by Kollist et al. (2000) suggesting that ozone flux to the plasmalemma is governed more by stomatal conductance. Also, Jakob and Heber (1998) infused leaves with oxidation sensitive dyes, and demonstrated that treatment with ascorbate did not protect the dyes from degradation by ozone.

Pell et al. (1997) assayed total soluble antioxidant concentrations, and sensitivity to ozone could not be explained by this in sugar maple or cherry. In fact, sugar maple had the highest antioxidant content, but the lowest resistance. Similarly, Strohm et al. (1999) demonstrated that hybrid poplar overexpressing glutathione synthetase or glutathione reductase did not exhibit enhanced resistance to ozone. However, Guzy and Heath (1993) concluded that antioxidant content played an important role in the determining the sensitivity of 12 varieties of *Phaseolus vulgaris*, and Loreto et al., (2001) revealed the importance of isoprene in quenching ozone.

The discrepancies within the research are likely to result from interspecific variation, the relative importance of the antioxidants studied, and differences in experimental

procedure. For example, Pell et al. (1997) acknowledge that their experiment may have omitted key antioxidants, as they only assayed for those that were soluble.

1.7 The effect of ozone on stomata

Stomata are essential in regulating CO_2 flux to photosynthetic tissues, and are the end point of the transpiration stream. Therefore any alteration in their behaviour by a stress will necessarily affect plant photosynthesis and water relations, and hence productivity. It is therefore paramount to understand their response to pollutants. It has become established that stomata act to determine ozone flux to the underlying tissues, and are therefore likely to be important in governing the nature of the response (Kollist et al., 2000).

Ozone effects on stomatal aperture

It has been known for some time that ozone can affect stomatal aperture, with the majority of studies showing increased resistance (Table 1.1). Interspecific differences have however been observed, with a number of studies showing no change, or even decreased resistance in response to ozone (Table 1.1). A study by Taylor and Dobson (1989) even revealed differences within the same plant, with first flush leaves exhibiting increased resistance, with the opposite response occurring in second flush leaves. Table 1.1 summarises the stomatal responses of a number of species:

Species	Author	Ozone conc. (ppb)	Effect on conductance
Pisum sativum	(Olszyk and Tibbitts, 1981)	130	Increase
Fagus sylvatica (SECOND FLUSH LEAVES)	(Taylor and Dobson, 1989)		Increase
Populus euramericana	Furukawa et al (1990)	540-720	No change
Helianthus annus	Furukawa et al (1990)	200	No change
Hordeum vulgare	(Ashmore and Onal, 1984)	180	Decrease
Pisum sativum	Olszyk & Tibbitts (1981)	270	Decrease
Glycine max	(Chevone and Yang, 1985)	200	Decrease
Fagus sylvatica (FIRST FLUSH LEAVES)	(Taylor and Dobson, 1989)		Decrease
Fagus sylvatica	(Pearson and Mansfield, 1993)	60-120	Decrease
Picea abies	(Lethiec et al., 1994)		Decrease
Plantago major		70	Decrease
Commelina communis	(McAinsh et al., 1996)		Decrease, +decreased opening
Vicia faba	(Torsethaugen et al., 1999)	180	Decrease
"	"	100	Decreased opening
Leontodon hispidus	(DeSilva et al., 1996)	100	Decrease

Table 1.1: Summary of research on the effects of ozone upon stomatal conductance.

Mechanisms for change in aperture

Decreased photosynthesis?

Considerable progress has been made concerning the underlying mechanisms that govern the stomatal response to ozone. It has been hypothesised that downregulation of photosynthesis caused by ozone results in raised intercellular CO_2 concentrations

(C_i), which are known to bring about stomatal closure. Downregulation of photosynthetic components has certainly been documented (Pell and Pearson, 1983), although ozone induced stomatal closure has been observed independently of changes in photosynthesis (Lehnherr et al., 1987; Torsethaugen et al., 1999), indicating that another mechanism operates.

Changes in ion flux?

As the plasma membrane is critical in turgor regulation, its role in the ozone-induced response has been examined. Guard cell turgor is regulated by flux of osmotically active solutes, primarily K^+ and its counter-ion Cl^-. K^+ channels are of two distinct types: inward-rectifiers, which allow influx of K^+ and hence stomatal opening, and outward rectifiers which allow efflux of K^+ and therefore stomatal closure. Changes in guard cell K^+ levels have been reported upon ozone exposure, giving an indication that these channels are involved in the response. Direct evidence for this came from a by Torsethaugen et al. (1999). The authors used patch clamping techniques to demonstrate that inward rectifying K^+ channels, and therefore K^+ influx, are inhibited by ozone treatment. Furthermore, no such effect was seen for outward rectifiers, indicating that, in this case, it is stomatal opening that is inhibited, as opposed to stomatal closure being stimulated. It is important to note, however, that these results do not preclude a role for altered photosynthesis, as at higher ozone concentrations the authors found a direct effect on photosynthesis, along with stimulation of stomatal closure.

Calcium is a ubiquitous second messenger in plant signal transduction and its role in stomatal responses, particularly to the drought stress hormone abscisic acid (ABA), is well documented. Ozone and H_2O_2 are known to result in increased whole plant Ca^{2+} (Price et al., 1994). Clayton et al. (1999) also characterised the ozone induced calcium signature, showing that the second peak of the biphasic response is required for induction of the defence gene glutathione-S-transferase (*GST*). Fink (1991) demonstrated that calcium oxalate crystals accumulate in guard cells and subsidiary cells in response to ozone, giving an indication that Ca^{2+} may indeed play a role in the ozone-induced stomatal response. Subsequently, Lethiec et al. (1994) demonstrated that Ca^{2+} accumulation in the guard cell cytosol of Norway spruce correlated with decreased stomatal aperture. Evidence for the importance of extracellular calcium comes from a study on calcicoles (plants that grow in soil with high Ca^{2+} concentrations). These plants are known to sequester calcium in trichomes, allowing maintenance of low apoplastic [Ca^{2+}] (DeSilva et al., 1996). Ozone treatment was found to disrupt this storage, resulting in changes in stomatal behaviour (DeSilva et al., 1996). More direct evidence for the importance of calcium came from work by McAinsh et al. (1996), demonstrating that H_2O_2 inhibits stomatal opening and promotes closure in *Commelina communis* in a dose-dependent manner, along with an increase in cytosolic Ca^{2+}. Importantly, both the increase in calcium and the decrease in stomatal conductance were inhibited by application of EGTA (a calcium chelator), implying a causative role for calcium in the response. Furthermore, Pei et al. (2000) presented evidence that H_2O_2 activates a Ca^{2+} channel in the guard cell plasma membrane, with a concomitant rise in cytosolic calcium. Additionally, it was shown

that ABA induces H_2O_2 production in guard cells, and radical quenchers abolish the calcium channel response. This leaves open the possibility that ozone induced oxidative stress may act as an elicitor of the ABA pathway, utilising ROS for signal transduction. Figure 1.2 depicts a putative mechanism by which ozone affects stomatal signal transduction and ion fluxes.

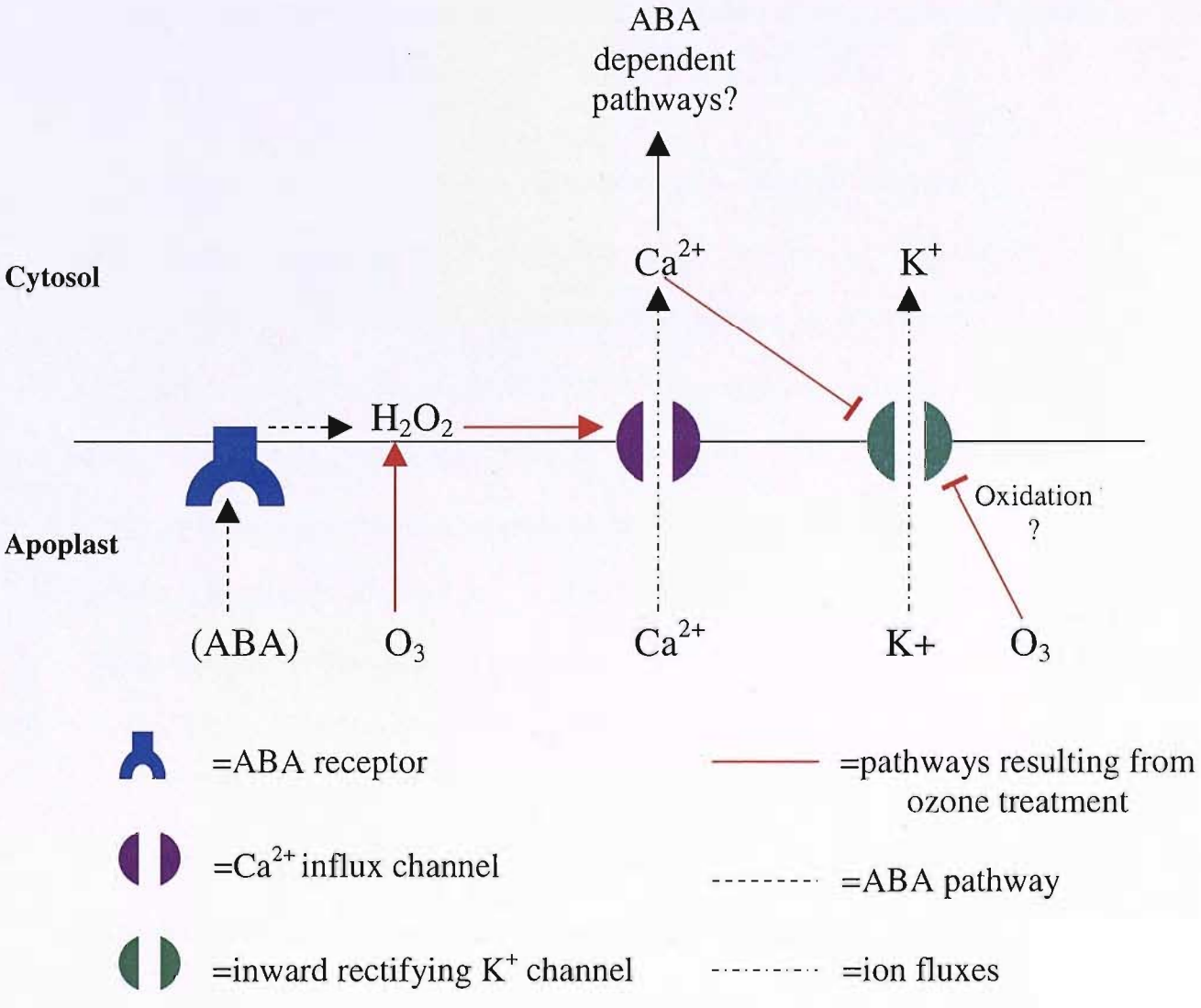

Figure 1.2: Putative pathways for ozone action on plasma membrane ion channels. Adapted from Torsethaugen et al. (1999) and Pei et al. (2000).

Although the results for H_2O_2 present encouraging evidence for a role for calcium in the ozone induced stomatal response, is important to note that the ROS produced by ozone is interspecifically variable, with $\cdot O_2^-$ being more prevalent in some species. Further work is also required to address which mechanisms operate in such plants.

1.8 QTL Mapping

Much research has focussed on closing the gap between genotype and phenotype, allowing physiological traits to be understood at the level of the gene. This is readily achieved in model organisms, for which researchers have a selection of powerful genomic and genetic tools at their disposal. The following sections examine two of these techniques, QTL mapping and microarrays, in detail, as they are pivotal to the work in this thesis.

The majority of trait variation within a population is quantitative, statistically approaching a normal distribution, rather than qualitative, with individuals falling into discrete phenotypic categories. Such variation is unlikely to be under control of one or a few loci, meaning that the relationship between genotype and phenotype will not be simple. For example, Dudley and Lambert (1992) predicted that around 173 genetic factors were involved in governing protein and starch concentrations in maize kernels. In these cases, phenotypic analysis is not likely to be informative about the underlying genetic factors important in governing the trait. Alternative methods must therefore be employed for genetic dissection of complex traits.

A Quantitative Trait Locus (QTL) can be defined as a locus containing alleles which affect the expression of a quantitative trait (QT). A quantitative trait is likely to be under control of multiple QTL, and it was traditionally thought that QTs were affected by many QTL of roughly equal but small effect. More recent research suggests that the effects of each are not equal, with a small number of QTL often having a large

effect on the trait. This has been demonstrated in *Populus* by Bradshaw & Stettler (1995), who found between 1 and 5 QTL of large effect for traits such as stem growth and spring flush, which accounted for up to 44.7 % of the genetic variance. This has become known as the "oligogenic" model. QTL mapping provides a method for analysis of such complex traits, and can be used to discover multiple genetic factors involved in trait expression.

Genetic mapping

The creation of genetic maps has provided the foundation upon which QTL mapping is based. The principles and procedures of genetic mapping will now be reviewed.

In the early twentieth century, it was believed that each chromosome was inherited as a unit, and as a consequence of this, genes were either inherited together if on the same chromosome, or independently if on different chromosomes. This was later found not to be the complete picture, and it is the phenomenon of partial linkage that has made genetic mapping procedures possible. Partial linkage can be explained by the behaviour of chromosomes during meiosis, and the crossing over (also known as recombination) that occurs during the process. Recombination between two genes will result in pairs of alleles for these genes being inherited as separate rather than single units, and the number of meioses in which this occurs is referred to as the recombination frequency, which represents the degree of linkage.

Under the assumption that recombination events occur randomly across the chromosome, recombination frequency can be used as a surrogate for the genetic distance between two genes. This is based on the principle that genes that are further

apart will undergo more recombination events between them. Therefore, recombination frequencies can be used to construct a genetic map, containing the positions of genes (or genetic markers) on the genome. It is of note that recombination events are not always randomly distributed, with recombination "hotspots" existing in certain locations. Nevertheless, a good correlation between genetic and physical maps is generally found (Oliver et al., 1992).

Genetic maps and DNA markers

In the early stages of genetic mapping, genes themselves were used as markers for map construction. This method is very limited in the level of resolution achievable, due to existence of large non-genic regions, and because most genes do not exist in allelic forms that can easily be deduced. It is this caveat that led to the development of DNA markers. The recombination frequencies of these can be used to calculate genetic distance and produce higher resolution genetic maps.

Marker information content.

A marker is described as informative when it can be used to deduce whether a recombination has occurred. For a marker to be fully informative, it is therefore essential to be able to deduce the parental origin of each marker allele in the offspring. The information content of a marker is related to its degree of polymorphism (i.e. the number of allelic variations of the marker). Highly polymorphic markers are more likely to show distinct alleles in the parents, allowing the origin of the alleles displayed in the offspring to be deciphered. High polymorphism also reduces the likelihood of two parents being heterozygous for the same alleles. Half the offspring

of such a cross would exhibit the same genotype as both parents, and would therefore be uninformative.

The information content of a marker is governed by its mode of inheritance. For certain markers, for example Randomly Amplified Polymorphic DNA (RAPDs), a marker genotype is determined by the presence or absence of a band on a gel. Due to this, a heterozygous individual with the "present" allele will be indistinguishable from an individual homozygous for the "present" allele. Such markers are said to have a dominant mode of inheritance. For co-dominant markers, for example microsatellites, it is possible to identify both alleles, and therefore distinguish homo- and heterozygotes. As such, co-dominant markers are generally the more informative type.

Restriction Fragment Length Polymorphisms (RFLPs), and Amplified Fragment Length Polymorphisms (AFLPs)

RFLPs were the first DNA markers used. They are identified by cutting DNA with a restriction enzyme, and allelic forms are represented by the presence or absence of a cut at a particular site, visualised as the length of DNA fragment produced. As both alleles will therefore be visible on a gel, they are co-dominant markers. Their popularity has waned, mainly due to technical difficulties in detection, as many fragments must be analysed simultaneously by Southern hybridisation. AFLPs are an improvement on this technique, using PCR to amplify the region containing the polymorphism prior to cutting, therefore aiding visualisation of the desired fragments against the background of unwanted fragments.

An inherent disadvantage of restriction fragment based markers is that they are biallelic, as the genotype is based on the presence or absence of a cut at a particular site. This results in lower polymorphism which may compromise the information content of the marker.

Randomly Amplified Polymorphic DNA (RAPD)

This technique uses random 10 base primers to amplify regions of the genome. Polymorphisms are detected as the presence or absence of a PCR product when analysed by gel electrophoresis, meaning that the markers are dominant. This issue has been circumvented somewhat by breeding strategies, discussed later. RAPDs have been used to generate maps for a variety of tree species, for example white spruce (Tulsieram, 1992), Eucalyptus (Grattapaglia and Sederoff, 1994) and slash pine (Nelson et al., 1993).

Simple sequence repeats (SSRs)

There are two main categories of SSR: minisatellites and microsatellites. Microsatellites have proved more useful for mapping purposes due to their more even distribution throughout the genome, and easier genotyping due to their shorter length. SSRs carry an advantage, in that they are highly polymorphic and are co-dominant. As such they are likely to have high information content. These advantages have led to their increased popularity in construction of tree genetic maps, for example *Pinus* species (Devey et al., 1996) and eucalyptus (Kirst et al., 2004). All four populations

used in the Popyomics project contain SSR markers. The release of the poplar genome sequence has made SSR detection considerably easier, as repetitive sequences can be easily located on the genome sequence and their polymorphism assessed. An additional advantage of SSRs is their use in aligning maps produced in different populations, as their position can be unambiguously identified and exhibits high homology across closely related species. This approach has been used to produce an integrated map of the soybean genome (Cregan et al., 1999), and to align the maps of the Popyomics populations. Map alignment is extremely useful as it allows data collected from different populations, in particular QTL location, to be compared. SSR sequences can also be located on the physical genome sequence, allowing alignment of physical and genetic maps. This has proved useful in identifying candidate genes underlying QTL regions (Street et al., in press).

Single nucleotide polymorphisms (SNPs)

SNPs are single nucleotide variants at a particular locus, and their discovery has had a positive impact on genetic map production. This is not least due to their abundance throughout the genome, allowing construction of high resolution maps. They are also amenable to high throughput discovery and genotyping techniques, for example through oligonucleotide microarrays (Wang et al., 2005). The large EST collections available for a number of tree species facilitate SNP detection, as sequences from genotypes or related species can be screened for polymorphisms. This process can be automated, and has been used to detect SNPs in maritime pine (Le Dantec et al., 2004), the EUFORGEN *Populus nigra* collection, and for poplar and spruce in the TreeSNP European Consortium as part of the Treenomix project

(http://www.treenomix.com/bioinformatics/candidate-gene-SNP.aspx). SNPs are of particular use in natural populations that are used for association mapping, where other markers cannot provide a linkage map of sufficient density.

QTL methodology

A requirement for QTL mapping is a mapping population with high density polymorphic molecular markers linked to regions of the genome, which exhibits continuous variation for the trait under investigation.

The individuals of the mapping population are first phenotyped for the trait in question, and genotyped at each of their marker loci. This allows phenotypic means to be calculated for each marker genotype. A significant difference in phenotypic means between marker genotypes at a particular locus indicates that the region of the genome linked to it contains a genetic factor or factors important in governing the trait. Simple statistical tests, such as ANOVA, can be used to test for such differences, although this is limited in that it cannot differentiate between QTLs of small effect that lie near to the marker, and those of large effect that lie distant to the marker. Modern software packages, for example MAPMAKER, QTL Cartographer and QTL Express overcome this problem through more advanced mapping techniques.

Mapping techniques

Interval mapping allows computation of the position of a QTL between 2 markers using maximum likelihood methods, resulting in a likelihood of odds (LOD) score, which corresponds to the probability of the QTL being located in a given location

against its probability of it arising by chance. It is possible to construct confidence intervals from these results by imposing cut-off limits on LOD scores. This technique offers considerably higher resolution than a simple comparison of means. Composite Interval Mapping (CIM) improves on this technique by taking into account variation created by non-target QTL, which would otherwise falsely contribute to the target QTL (Jansen & Stam, 1994; Zeng, 1994).

Applications of QTL mapping

QTL mapping has been used to dissect a number of quantitative traits in plants, including stress susceptibility and tolerance, for example drought, salinity, and cold stress in rice (Price et al., 1999; Koyama et al., 2001; Andaya et al., 2003). The technique has also been applied to *Populus*, with QTLs for traits such as leaf area, leaf pigmentation, petiole length, stem volume and basal area (Bradshaw et al 1994), phenology (Bradshaw and Stettler 1995), and stomatal initiation and density, and epidermal cell size and number in response to elevated CO_2 (Ferris et al 2002) . In *Populus*, this has largely been made possible by a mapping population known as Family 331, originally constructed by Bradshaw et al (1994). This was created by mating the female *P. trichocarpa* clone 93-968 from western Washington and the male *P. deltoides* clone ILL 129 to produce an F_1 family, Family 53. Two clones from this family, namely 53-246 and 53-242, were mated, resulting in an inbred F_2 population. The genetic map consists of high density AFLP and SSR markers well spaced throughout the genome. This family has recently been used to map QTL for osmotic potential, which is important in determining drought tolerance (Tschaplinski et al., 2006), and also for the response to chronic drought stress (Street et al., in press).

"Robustness" of QTL

It is of note that QTL are susceptible to environmental influences. QTL that are identified across environments can be considered to be "robust", and are more likely to be of fundamental importance. A similar principle applies to QTL that are consistently identified across different mapping populations. For Family 331, QTL for height have been mapped to corresponding locations in both USA and UK. Currently efforts are being made to align the genetic maps of the populations that form the Popyomics project, with a goal to identify robust QTL that are present across a variety of mapping pedigrees and environments.

Mapping populations

A number of mapping populations exist for *Arabidopsis thaliana*, the majority of which are composed of Recombinant Inbred Lines (RILs). These populations are produced by mating homozygous parents, and self fertilising the F_2 generation until homozygosity is achieved, typically after around nine generations (F_9). These populations are highly suitable for QTL mapping, as a large number of meioses will have taken place increasing the chance of recombination. The homozygosity also removes the problems associated with dominance and recessiveness, therefore increasing the information content of the markers.

Other mapping techniques include the test-cross, which involves mating a heterozygous parent with a homozygous recessive parent. This method allows the parental origin of each allele to be discerned, increasing the marker information content.

For out-crossing trees, production of such populations is not possible due to high genetic load (a large number of deleterious recessive alleles), and the inability to self fertilise. Therefore alternative mapping strategies are used. The two-way pseudo-testcross involves crossing heterozygous parents with the assumption that the testcross configuration (heterozygous in one parent and homozygous recessive in the other) will arise at a subset of loci. This technique has been implemented by Grattapaglia and Sederoff (1994) in Eucalyptus using RAPD markers. The technique results in production of a genetic map for each parent, and circumvents the problem of dominance associated with RAPDs.

F_2 populations are bred from parents that exhibit highly divergent phenotypes. Highly polymorphic markers are favoured to ameliorate the problem of heterozygosity by allowing the parental origin of each allele to be discerned. Family 331 (POP1) represents one such population, and is used in this thesis.

The suitability of Family 331

Continuous variation in a trait within a mapping population is likely to result if the parents of the population have highly divergent phenotypes. This is not always a necessity however, as the parents may possess a balance of positive and negative QTL which will segregate in the population to produce a variety of phenotypes (transgressive segregation). It is of note that *P. deltoides* and *P. trichocarpa* possess contrasting differences in their habitat and physiology. *P. deltoides* originates east of the Rocky Mountains in North America, whilst *P. trichocarpa* originates from the

west (Figure 1.3). *P. trichocarpa* possesses thicker, ovate leaves, whilst those of *P. deltoides* are thinner and deltoid. Habitat differences seem to have resulted in adaptive differences in physiology, with *P. trichocarpa* possessing a thick layer of spongy mesophyll that is likely to aid in interception of diffuse light travelling through the canopy, which is common on cloudy days. *P. deltoides* , in contrast, has palisade mesophyll on both the ad- and abaxial sides, and long flat petioles that are likely to aid in heat loss which is required in the hotter, drier climate in which they reside. Their responses to stress have also been found to differ. For example, *P. trichocarpa* is highly sensitive to drought, whilst *P. deltoides* is comparatively resistant (Street et al., in press). This difference is likely to be due at least in part to the decrease in stomatal conductance seen in *P. deltoides* in comparison to *P. trichocarpa*, which would result in reduced water loss due to transpiration. It can be seen, therefore, that these two species exhibit highly divergent phenotypes and responses, which underpins the success of Family 331 as a mapping population. As yet, Family 331 has not been used for mapping QTL for the response to ozone treatment. Woo et al. (2005) discovered that clones from the F_2 family exhibited differing sensitivity to chronic, low level ozone exposure, although this has not yet been confirmed for the response to acute ozone stress, and was not performed on enough individuals to allow QTL mapping.

Populus trichocarpa (Black Cottonwood) *Populus deltoides* (Eastern Cottonwood)

a) b)

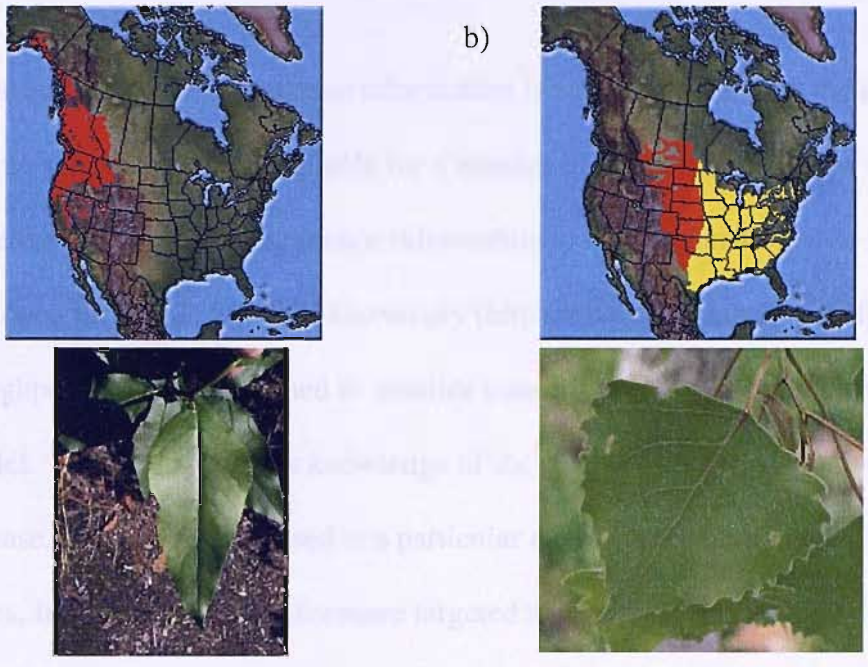

Figure 1.3: The distribution in North America and appearance of a) *P. trichocarpa* (Black Cottonwood) and b) *P. deltoides* (Eastern Cottonwood). Source: www.cnr.vt.edu.

It is important to note that although QTL mapping can identify a chromosomal subregion that is important in governing a response, this region is likely to encompass many genes. Microarray analysis is capable of identifying genes that are differentially expressed between the parents of a mapping population, and it is these differences in expression patterns that contribute to a quantitative trait. Therefore, if genes that are differentially expressed between the parents co-localise to a QTL, they represent encouraging candidates for being important in the response, and can be targeted for further investigation.

1.9 Microarray technology

A vast amount of gene sequence information is now available, with the complete genome sequences being available for a number of organisms. It is now necessary to capitalise on this and use sequence information to deduce function. The microarray, developed in 1995 at Stanford University (http://www.microarray.org/sfgf/), is a high throughput technique designed to monitor transcription of large numbers of genes in parallel. Such data provides knowledge of the spectrum of genes involved in a response, or of those expressed at a particular developmental stage or in certain tissues. It also gives a basis for more targeted studies once genes of interest have been identified.

Microarray platforms and production

The most commonly used microarray platforms are fragment based arrays and oligonucleotide arrays. The former will be discussed in detail, as they are used in this thesis.

Microarrays are produced by robotic deposition of fragments of cDNA onto indexed locations on a glass slide. The cDNA contained in each spot corresponds to a known sequence of a particular gene, and is referred to as a "probe". Through the principles of complementary base pairing, the array can be used to assess the relative abundance of transcripts in two biological samples. First, RNA must be extracted from each sample, and the samples labelled with contrasting fluorescent dyes. This is achieved

through reverse transcription in the prescence distinct fluorophore-dUTP conjugates, most commomly Cy3-dUTP (green, used in control samples) and Cy5-dUTP (red, used in experimental samples). The resulting labelled cDNA from both samples is then applied to the array, and allowed to hybridise with the probes. When excited by a laser, each fluorophore emits a distinct wavelength, and the ratio of the fluorescence intensity of the two dyes corresponds to the relative expression of each gene between the two samples. The procedure is summarised in Figure 1.4.

Oligonucleotide arrays still rely on hybridisation but, as their name implies, use oligonucleotides of approximately 70 bases as probes. These are synthesised *in situ* by photolithography, eliminating problems of incorrect deposition of probes. They also possess the advantage of being very sensitive to single nucleotide differences, and are thus useful for genotyping purposes. Studies have also indicated that they are more consistent between arrays than the fragment-based type.

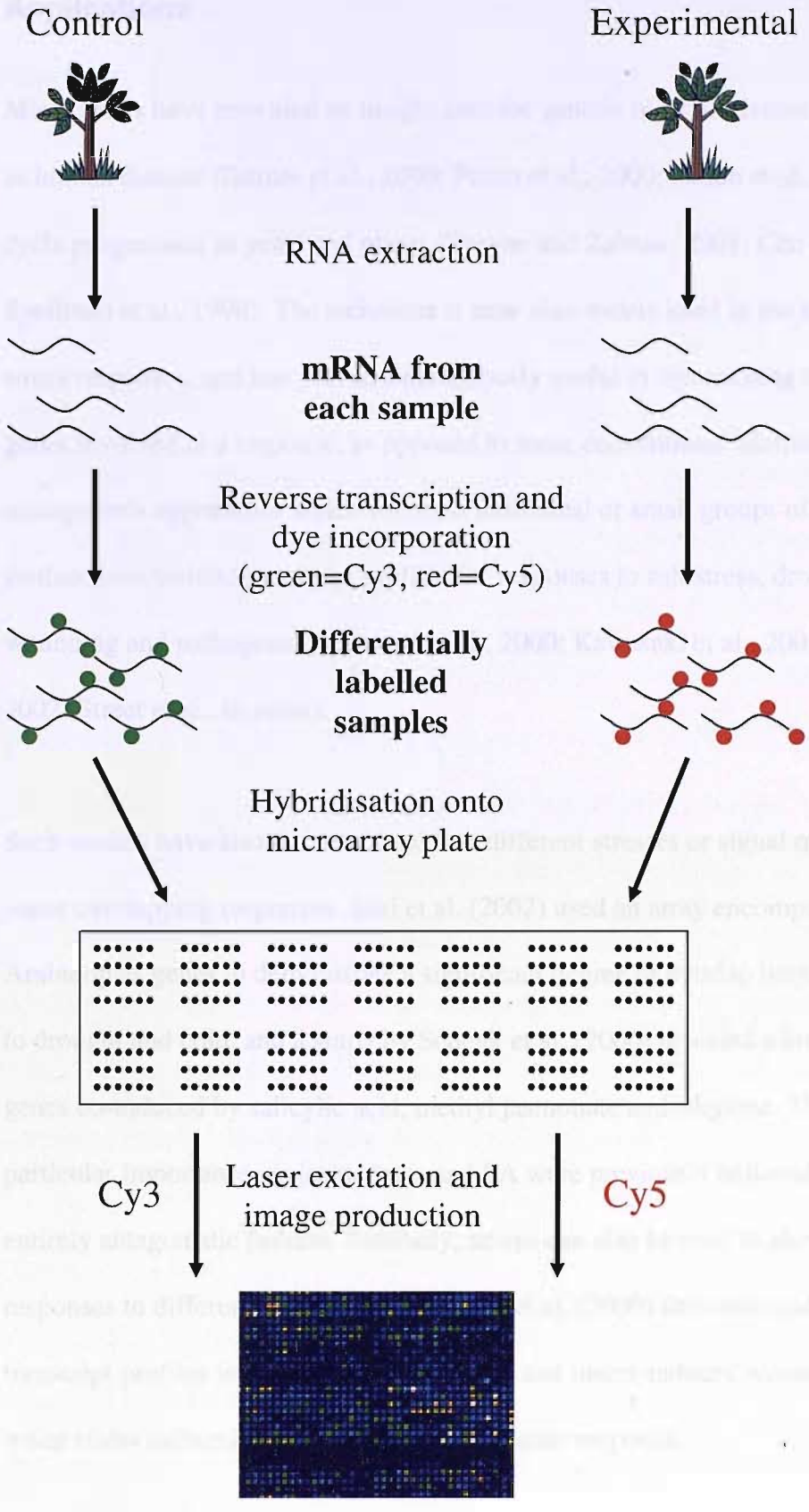

Figure 1.4: A summary of the microarray hybridisation procedure, depicting the processes of RNA extraction, reverse transcription and dye incorporation, and hybridisation.

Applications

Microarrays have provided an insight into the genetic basis of diverse processes such as human disease (Bittner et al., 2000; Perou et al., 2000; Golub et al., 1999), and cell cycle progression in yeast and plants (Breyne and Zabeau, 2001; Cho et al., 1998; Spellman et al., 1998). The technique is now also widely used in the study of plant stress responses, and has proved tremendously useful in determining the spectrum of genes involved in a response, as opposed to more conventional blotting and mutagenesis approaches which focus on individual or small groups of genes. Such studies have yielded transcript profiles for responses to salt stress, drought stress, wounding and pathogens (Reymond et al., 2000; Kawasaki et al., 2001; Seki et al., 2002; Street et al., in press).

Such studies have also demonstrated that different stresses or signal molecules can cause overlapping responses. Seki et al. (2002) used an array encompassing 1300 Arabidopsis genes to demonstrate a significant degree of overlap between responses to drought and cold, and a study by Schenk et al. (2000) revealed a large number of genes co-induced by salicylic acid, methyl jasmonate and ethylene. This is of particular importance, as jasmonates and SA were previously believed to act in an entirely antagonistic fashion. Similarly, arrays can also be used to show distinct responses to different treatments. Reymond et al. (2000) demonstrated contrasting transcript profiles in response to mechanical and insect-induced wounding, with less water stress induced gene expression in the latter response.

Time course studies have allowed gene expression to be categorised temporally. Kawasaki et al. (2001) revealed that, during salt stress, stress related transcripts

accumulate within hours, with defence related genes being induced later. The pattern of gene expression at one week indicated recovery from the stress. Kim et al. (unpublished) have also examined the temporal pattern of gene expression in Arabidopsis exposed to oxidative stress.

Time course studies, and also those involving multiple treatments, allow grouping of genes that behave in a similar fashion. This technique, known as cluster analysis, has proved particularly useful in identifying genes under common regulation, called regulons. In a landmark study, Maleck et al., (2000) applied clustering algorithms to genes induced during systemic acquired resistance (SAR). This research uncovered a group of coregulated genes that included *PR1*. Genes in this "*PR1* regulon" contained an unusually high number of W-box promoter elements, indicating that they may be all be regulated by WRKY type transcription factors. As mentioned, Seki et al. (2002) demonstrated an overlap between drought- and cold-inducible genes. Amongst these, 12 were identified as containing a dehydration responsive element (DRE). Furthermore, these were found to be under control of a specific transcription factor, DREB1A. Recent software advances allow expression patterns of clustered genes to be placed on chromosome maps, which can aid in the search for regulatory elements.

Kim et al. (unpublished) used cDNA microarrays representing nearly 4400 genes on Arabidopsis chromosome 2 to probe the response to H_2O_2 induced oxidative stress. They revealed regulation of genes involved in a number of processes, including defence, hormone synthesis, calcium signalling, MAPK signalling, and programmed cell death. They also performed cluster analysis on their results according to timing and level of expression, and revealed groups of genes exhibiting similar patterns,

including *PAL1* and *GST6*. Desikan et al. (2001) investigated the response of Arabidopsis cell cultures to H_2O_2. Again, genes of diverse function were induced, including heat shock proteins (known to be important in survival of oxidative stress in animals, plants and yeast), a tyrosine phosphatase (involved in protein phosphorylation and possibly signal transduction, and many transcription factors. In light of the proposed role of calcium in mediating the response to oxidative stress, it is particularly interesting that a calmodulin gene was induced in response to H_2O_2. They also noted induction of a syntaxin. An ABA induced syntaxin is known to play a role in control of guard cell ion channels, and it is possible that this is involved in the oxidative stress mediated guard cell response. This highlights the potential of microarrays in identifying genes of interest, which can then be used as a basis for proposing testable hypotheses. Vranova et al. (2002) used microarrays to probe the response of *Nicotiana tabacum* leaves acclimated to oxidative stress, and were able to demonstrate that pre-treatment was able to potentiate increased transcription following a second bout of stress. Again, significant changes in transcript levels occurred for a variety of genes, including those involved in the phenylpropanoid pathway, photosynthesis, detoxification and signal transduction. Cluster analysis revealed two groups of coregulated genes, categorised as early- and late-response, suggestive of at least two pathways of gene induction. Transcript levels of WRKY11 (a transcription factor) correlated with tolerance to oxidative stress, leading the authors to hypothesise that this factor may be involved in regulating transcription of genes involved in tolerance.

It is of note that the above studies involve artificially induced oxidative stress. To date, only two studies have used microarrays in conjunction with ozone treatment.

Matsuyama et al. (2002) used small, customised arrays diagnostically, to allow UVB and ozone stress to be distinguished, and Ludvikow et al. (2004) performed a global expression analysis on ozone stressed Arabidopsis using an Affymetrix array. To date, no global gene expression experiments have been performed on ozone stressed trees, and this is to be the focus of my research.

As mentioned, microarray analysis provides a basis for further studies with a more hypothesis driven approach. Analysis of plants with mutations in the genes of interest is likely to provide valuable information concerning their function in the response to ozone. The most widely used method for generating null mutants or "knockouts" in Arabidopsis is insertional mutagenesis. This is achieved through use of the bacterium *Agrobacterium tumefaciens*, which is capable of inserting T-DNA into random locations in the genome. A population of plants can then be screened for insertions in the gene of interest. In contrast to techniques such as antisense mediated silencing, this allows creation of stable knockouts, and can target specific genes within families. Also, transgenic reconstruction can generate plants with variable expression of the knocked-out gene through replacement with a modified promoter. Resources for Arabidopsis with specific T-DNA insertions are currently available and the library is continuing to expand, and a project is also underway to produce poplar knockouts.

Data analysis

Due to the large volume of data produced, extracting meaningful information from microarrays has represented a challenge to the researcher, and numerous statistical techniques have been developed and modified. This section reviews the issues surrounding microarray data analysis.

Data normalisation

Normalisation is the process of removing unwanted non-biological variation from data. This procedure is essential for microarrays for a number of reasons, primarily initial differences in sample amounts, the effect of laser settings on intensity, and differences in incorporation efficiencies for the two fluorophores. This technical variation must first be removed in order to extract the underlying biological information.

Global normalisation

The simplest normalisation is to assume an overall 1:1 ratio for the two channels. This assumption is valid only if the genes on the array represent a random sample of the genome of the organism, or ideally the entire genome. If the genes were not randomly sampled and the average expression ratio is expected to change in one direction, this criterion would not be met. Assuming an overall 1:1 expression ratio of the 2 samples, the technical variation mentioned above can be countered by centring the data to achieve an overall 1:1 ratio.

Intensity dependent normalisation

Although the total intensity normalization mentioned above serves to remove much of the technical variation encountered, numerous articles have reported intensity dependent effects on expression ratios (for example, Yang et al., 2002), the nature of

which can depend on the fluorophore. Such effects can be revealed in ratio-intensity (RI) plots, which are commonly used for quality control. Locally weighted linear regression (Lowess, Cleveland, 1981) has become an accepted method to remove intensity dependence, and is now available in commercial software packages. It functions by calculating intensity dependent deviations in the RI plot, and applying a weighting to the spots which do not match expected values. Intensity dependent effects can also be controlled to an extent at the image analysis stage, prior to data analysis. The detector in the scanner becomes saturated at a certain intensity, and beyond this no more meaningful data can be extracted. White spots indicate that saturation has been reached, and these can be excluded from the analysis.

Other normalisation procedures

Normalisation of array data is an active field, with a number of research groups attempting to tackle the issues associated with global normalisation methods such as Lowess that assume a 1:1 expression ratio for the 2 channels. Such methods include use of internal controls, in which sequences of a gene(s) not present in the target organism are spotted on the array, and the sample RNA is "spiked" with RNA encoded by this gene. If equal quantities of spiking RNA are loaded into the cDNA synthesis, one would expect a 1:1 expression ratio for this gene in the 2 channels, and data can be normalised on the basis of the intensities of these spots. The effectiveness of normalising a very large data set on the basis of a small set of controls is however questionable. Other methods include adaptive identification of housekeeping genes from array data to which results can be normalised (Wang et al., 2002; Wilson et al., 2003; Stoyanova et al., 2004). Implementation of these methods is inhibited by lack of

available software, meaning that Lowess normalisation is still the most popular method. It is likely that, in coming years, commercial software will incorporate improved methods.

Statistical approaches to identifying differentially expressed genes

Fold change

Measuring fold change in expression of each gene and applying a cut-off value is the simplest analysis method for identifying differentially expressed genes and was used in numerous early studies (Schena et al., 1996; DeRisi et al., 1997). Although simple to implement, this method has a number of flaws, not least the arbitrary nature of selecting a cut-off point (Cui and Churchill, 2003), which is often 2 fold up- or down-regulation. The method is also susceptible to variance between samples, as an anomalous sample could artificially distort the fold change. This can to some extent be ameliorated by specifying that the gene must meet the fold change criterion in a certain number of samples. Such tools are available in analysis software such as GeneSpring.

It is these issues that have caused attention to shift towards statistical methods of data analysis. The large amount of data generated has posed problems for traditional statistical procedures. In particular, if the expression of each gene is analysed separately, a percentage of false positive results will occur, which on an array containing many thousands of spots is likely to represent a significant number of genes. New methods and adaptations of existing tests have been developed to tackle these problems.

Analysis of Variance (ANOVA)

ANOVA is an extension of the t-test which allows comparison between 2 or more groups of samples. In a microarray analysis, the expression ratio of each gene is the dependent variable, and the test is conducted on a gene by gene basis. It can immediately be seen that the multiple testing problem detailed above applies here. Traditionally, multiple testing has been accounted for by family-wise error-rate adjustments such as Bonferroni correction. These methods increase the threshold of significance in accordance with the number of tests being performed. In smaller datasets, this may only encompass a few tests, but for microarrays thousands of tests are performed simultaneously. Imposing a Bonferroni correction on such data increases the stringency to such an extent that it can return very few significant results, and may therefore mask useful biological information. Researchers have thus sought a "compromise" to control false positives.

False discovery rate (FDR) control (Storey, 2002) calculates the expected number of true null hypotheses that have erroneously been rejected, thus providing an estimate of the number of genes within a list that are likely to false positives. The researcher can set the desired percentage of false positives that will appear in the list. This procedure is considered more powerful than FWER methods, and more appropriate for microarray analysis (Cui & Churchill, 2003).

Replication of experiments also provides a means to both reduce false positives and identify genes that exhibit consistent expression patterns.

Multivariate approaches

Microarray data contains far more variables (genes) than experimental observations, and is as such amenable to multivariate statistical methods. These techniques identify differentially expressed genes on the basis of their ability to explain the observed data. One such method, Partial Least Squares Discriminant Analysis (PLS-DA), has been used to identify differentially expressed genes in microarray experiments (Nguyen and Rocke, 2002; Street et al., in press). This procedure involves specifying the main groups of interest (for example the control and treated channels, or species), and assigning a score to each gene which corresponds to its ability to explain the separation of the groups. PLS-DA can be performed in the SIMCA P package (Version 10, Umetrics, Sweden), which assigns a variable importance (VIP) score to each gene. Nguyen and Rocke (2002) determined (by bootstrap analysis) a VIP score of 2 to be a suitable significance threshold for an array containing 10,000 elements, whilst other studies have used the technique to produce a list of a predetermined number of genes. For example, Musumarra et al. (2004) produced lists of the 35 genes most diagnostic of various types of cancer. Such multivariate approaches are useful as they do not encounter the same multiple testing issues as ANOVA.

1.10 Aims and objectives

- To construct an ozone enrichment system capable of exposing young poplar trees to an acute ozone treatment.
- To assess whether two poplar species, *P. deltoides* and *P. trichocarpa*, exhibit contrasting sensitivity to an acute ozone treatment, in order to provide a basis for microarray analysis and QTL mapping.
- To produce transcript profiles of the two species using cDNA microarrays in order to identify genes that are upregulated by ozone treatment, and also those which exhibit species specific expression patterns.
- To assess the effect of an acute ozone treatment upon salicylic and jasmonic acid concentrations in the two species.
- To perform a field trial on an F_2 mapping population, Family 331, in open-top chambers, and assess the effect of a chronic ozone treatment on physiological traits.
- To map QTL using the physiological data, thereby identifying genomic regions involved in mediating the response to ozone.
- To identify groups of sensitive and tolerant F_2 genotypes for microarray analysis, providing further information on the genes involved in sensitivity to ozone.
- To use the newly sequenced poplar genome to form a link between the genetic and physical maps.
- To use this information to locate QTL and candidate genes from microarray analysis on the physical sequence, and identify co-located candidate genes and QTL regions.

Chapter 2: Design, construction and testing of an ozone enrichment system

2.1 Introduction

Since the damaging effects of elevated tropospheric ozone have been recognised, there has been a requirement for experimental systems in which the mechanisms underlying ozone sensitivity can be probed under controlled conditions. Researchers have used a variety of approaches depending on the aspect of the response to ozone that is under investigation. Growth chambers have been used to investigate the short term response (Paakkonen et al., 1996; Vahala et al., 2003), and carry the advantage that high ozone concentrations can easily be achieved. As such this method has generally been used to investigate the response to acute ozone treatment. Open-top chambers and free-air enrichment sites (Broadmeadow et al., 2000; Karnosky et al., 2005; Iglesias et al., 2006; Li et al., 2006), allowing growth of even larger trees, have been used to study the response to a chronic ozone treatment, such as effects on growth traits and ozone-induced senescence.

In this study, an ozone system capable of exposing poplar saplings to an acute ozone treatment was constructed. It was intended for the system to be self-regulating, and capable of maintaining a consistent target concentration across enriched chambers, whilst maintaining ambient concentrations in control chambers. As ozone is potentially hazardous and corrosive to many metals and plastics, measures were taken to ensure safety, and these are described.

2.2 Materials and methods

Growth chambers

The wooden growth chambers were built by Dr. K. Warwick at the University of Sussex, and measured 800 mm (length) x 700 mm (width) x 600 mm (height). The roofs of the chambers were constructed from 10 mm heat resistant glass.

An air conditioning unit was installed to allow continuous air flow through the chambers. This delivered external air to a header unit, with 8 x 90 mm pipes delivering air to each chamber. Control of the air flow rate into the chambers was made possible by adjustment of butterfly valves on each of the pipes. Air was pumped out of the chambers through a second set of 90 mm pipes into an exhaust vent.

Lighting

2 Philips PL-90E metal halide lamps (Philips, Croydon, UK) were installed at 30 cm above each chamber. A timer switch was used to control photoperiod.

Measurement of light intensity and airflow

The light intensity was measured at 9 points in each chamber using a LI-COR 1600 photon flux meter (LI-COR, Lincoln, USA). Airflow was measured using a wind vane anemometer. The flow rate in m s^{-1} was measured at the point where the air conditioning pipes entered the chambers. Adjustments were made to the butterfly valves controlling the airflow through each inlet to equalise airflow to each chamber.

Ozone delivery system

An oxygen cylinder with a nominal capacity of 3400 L was used to deliver oxygen to an ozone generator (ECO3, Torino, Italy) through Tygon Ultrasoft R1000 ozone resistant tubing (Tygon, Charny, France). The generator delivered pure ozone to a cylindrical buffer through Tygon Ultrasoft R1000 tubing. Air was pumped into the buffer through Tygon R3603 tubing (3.2 mm internal diameter) from two air pumps. The buffer was connected to a series of 8 solenoid valves by 6 mm PTFE tubing.

The valves, which delivered ozone to the chambers, were linked in series. Delivery of ozone from the valves to the chambers was achieved through 6mm PTFE tubing. These tubes entered the chambers through a 6mm diameter hole in the inlet pipe of the air conditioning system directly adjacent to the chamber. Each tube was labelled with its corresponding chamber number.

Control of ozone concentration

A 6 mm PTFE sample tube was fed from a 6 mm hole in each chamber and connected to 8 solenoid valves connected in series. The valve series was connected to an ozone analyser (Model 8810, Monitor Labs Inc.) through 6 mm PTFE tubing which delivered information on the ozone concentration in each of the chambers to a control unit. The control unit and software were designed and constructed by Franco Miglietta (IBIMET, CNR, Florence), allowing control of flow rate, duration of valve opening, valve aperture and analyser purge time. Readings were uploaded to a computer, and adjustments were made to ensure the desired concentrations were reached.

Safety

As ozone corrodes many metals and plastics, only stainless steel fittings, PTFE or Tygon tubing, and silicon were used. The use of compression fittings ensured a gas tight seal around the tubing. Each fitting was assessed for leaks by applying soapy water to the joints whilst oxygen was pumped round the system. The inlet and sample tubes were secured and sealed to the chambers using silicon sealant. The buffer was fitted with an exhaust valve in case of build up of excess pressure. This was connected to the exhaust running from the room to the outside by PTFE tubing. A purge pump was installed in the room to remove ozone from the room in case of leakage, and connected to the exhaust by PTFE tubing. Two ozone monitors were installed, one of which was linked to the electrical supply of the ozone generator, resulting in cessation of ozone generation in event of leakage. The other (Ecosensor C-30ZX, Dryden Aqua, Edinburgh, UK) was attached to the metal girders supporting the growth chambers. A window was installed in the door of the room so that this was clearly visible from outside. This monitor was tested by placing it inside a chamber and enriching it with a known concentration of ozone. Componets of the system are shown in Figure 2.1. COSHH data for ozone can be found at http://www.ozone-industries.co.uk/coshh.html.

a)

b)

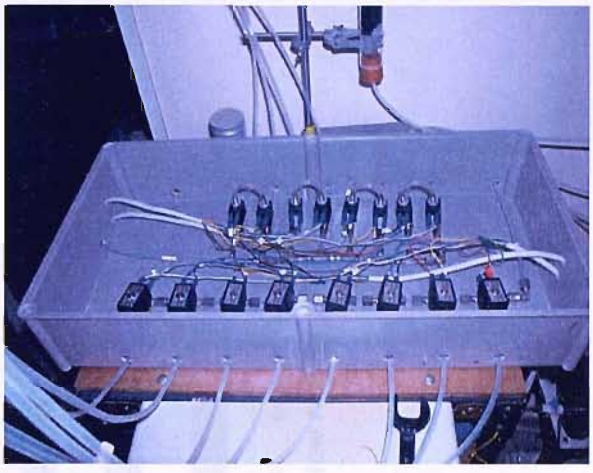

c)

Figure 2.1: Components of the ozone enrichment system showing **a)** growth chambers, **b)** valve system for ozone delivery and monitoring, **c)** ozone control unit.

2.3 Results

Light intensity, air flow, temperature and humidity

Mean photon flux and air flow rate for each chamber are presented in Figure 2.2. Flow rates were approximately 3.2 m s^{-1} in all chambers, and light intensities range from 104 to 134 µmol m^{-2} s^{-1}. Mean relative humidity was 72 %, and mean temperature was 25.1°C, with no significant difference between chambers.

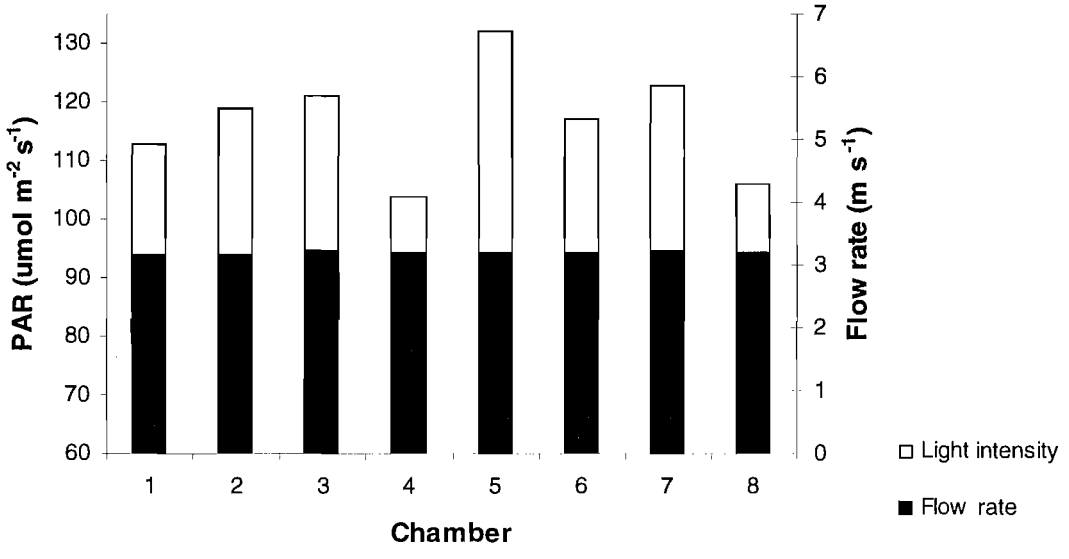

Figure 2.2: Photosynthetic photon fluence rate (PPFR) (black bars) and air flow rates (white bars) through eight growth chambers designed for ozone fumigation.

Unwanted enrichment of ambient chambers

Figure 2.3 a) illustrates some ozone enrichment in the ambient chambers, whilst Figure 2.3 b) shows the result of adjustment of the scanner purge time in the control program, with no enrichment registered in ambient chambers.

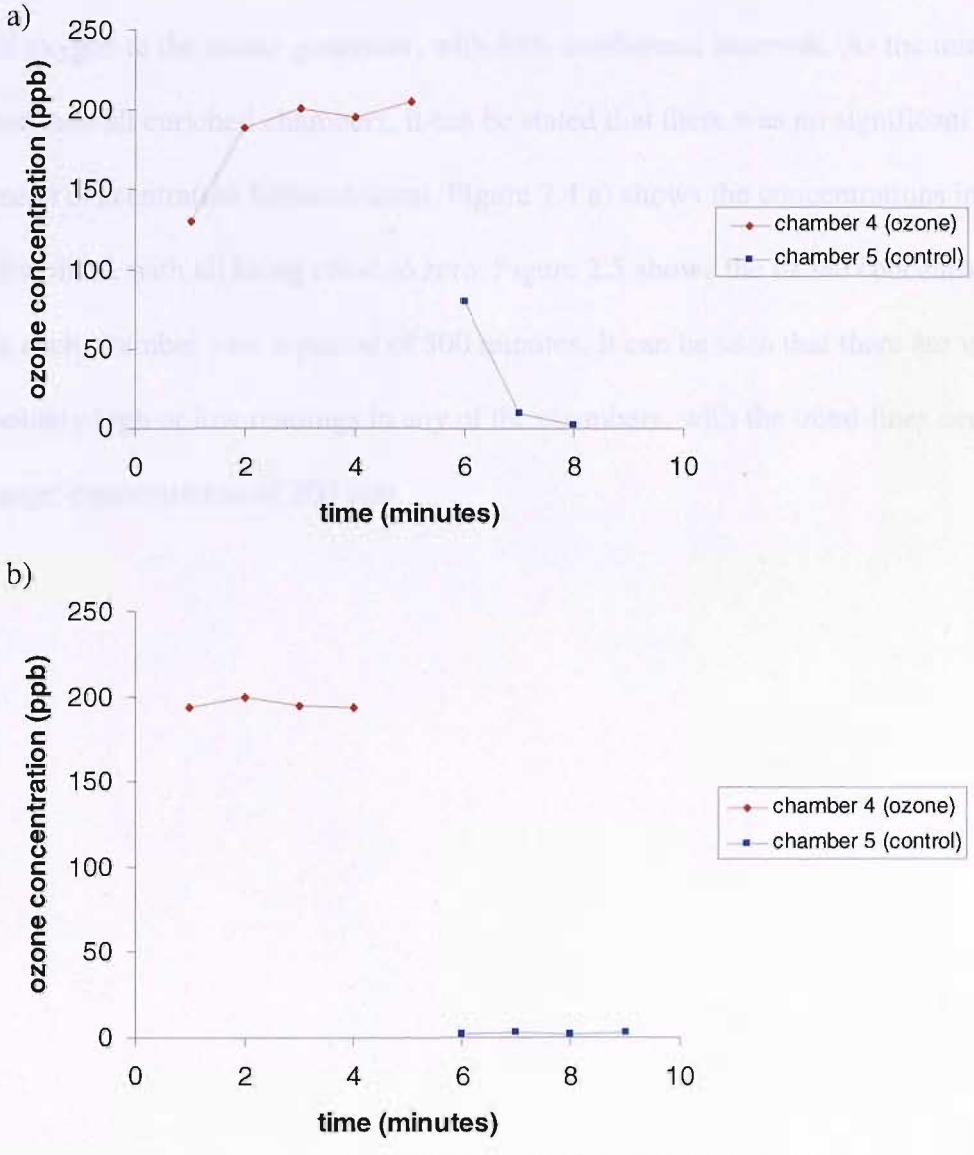

Figure 2.3: Ozone concentrations in chambers 4 (ozone treated) and 5 (ambient) recorded **a)** prior to increasing ozone analyser purge time, and **b)** after purge time had been increased by 1 min, showing removal of apparent ozone enrichment from control chamber. Target concentration was 200 ppb in chamber 4 and 0 ppb in chamber 5.

Achieving a stable target ozone concentration

It can be seen from Figure 2.4 b) that the target concentration of 200 ppb was not initially reached in the enriched chambers, due to deficient ozone production. Figure 2.4 c) shows the correct concentration in all enriched chambers following incremental increase of flow of oxygen to the ozone generator, with 95% confidence intervals. As the intervals overlap between all enriched chambers, it can be stated that there was no significant difference in mean concentration between them. Figure 2.4 a) shows the concentrations in the control chambers, with all being close to zero. Figure 2.5 shows the ozone concentration recorded in each chamber over a period of 500 minutes. It can be seen that there are very few notably high or low readings in any of the chambers, with the trend-lines centred on the target concentration of 200 ppb.

a)

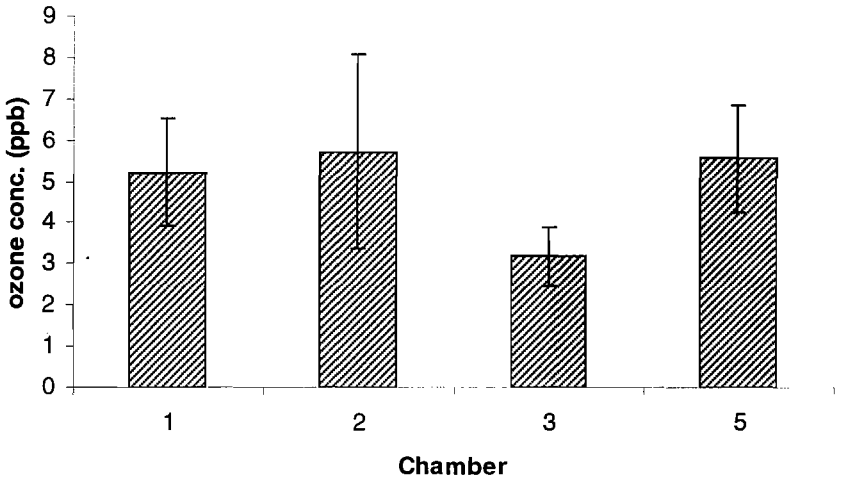

b)

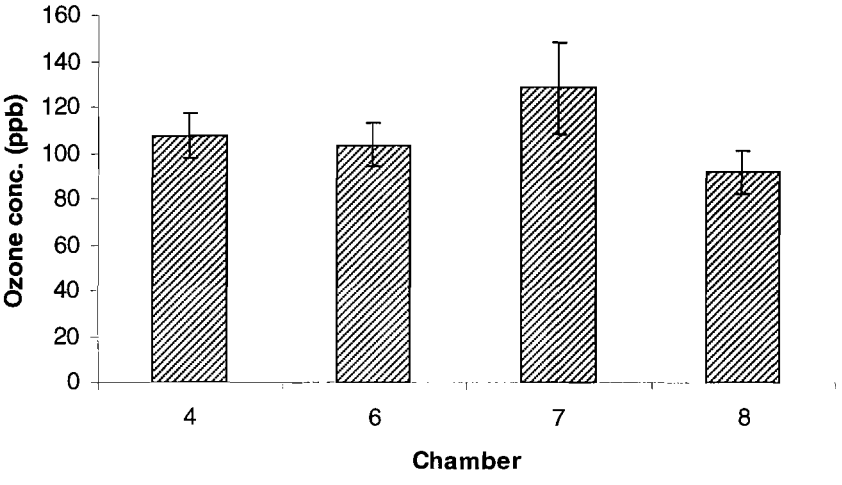

c)

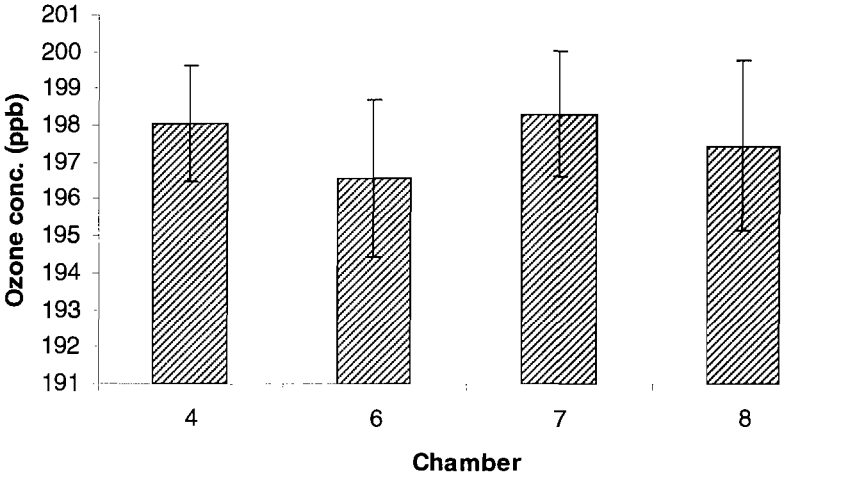

Figure 2.4: Ozone concentrations achieved in **a)** control chambers, **b)** treated chambers before adjustment of ozone delivery, and **c)** treated chambers after adjustment. Target concentration was 200 ppb in treated chambers, and 0 ppb in control. Error bars represent 95 % confidence intervals.

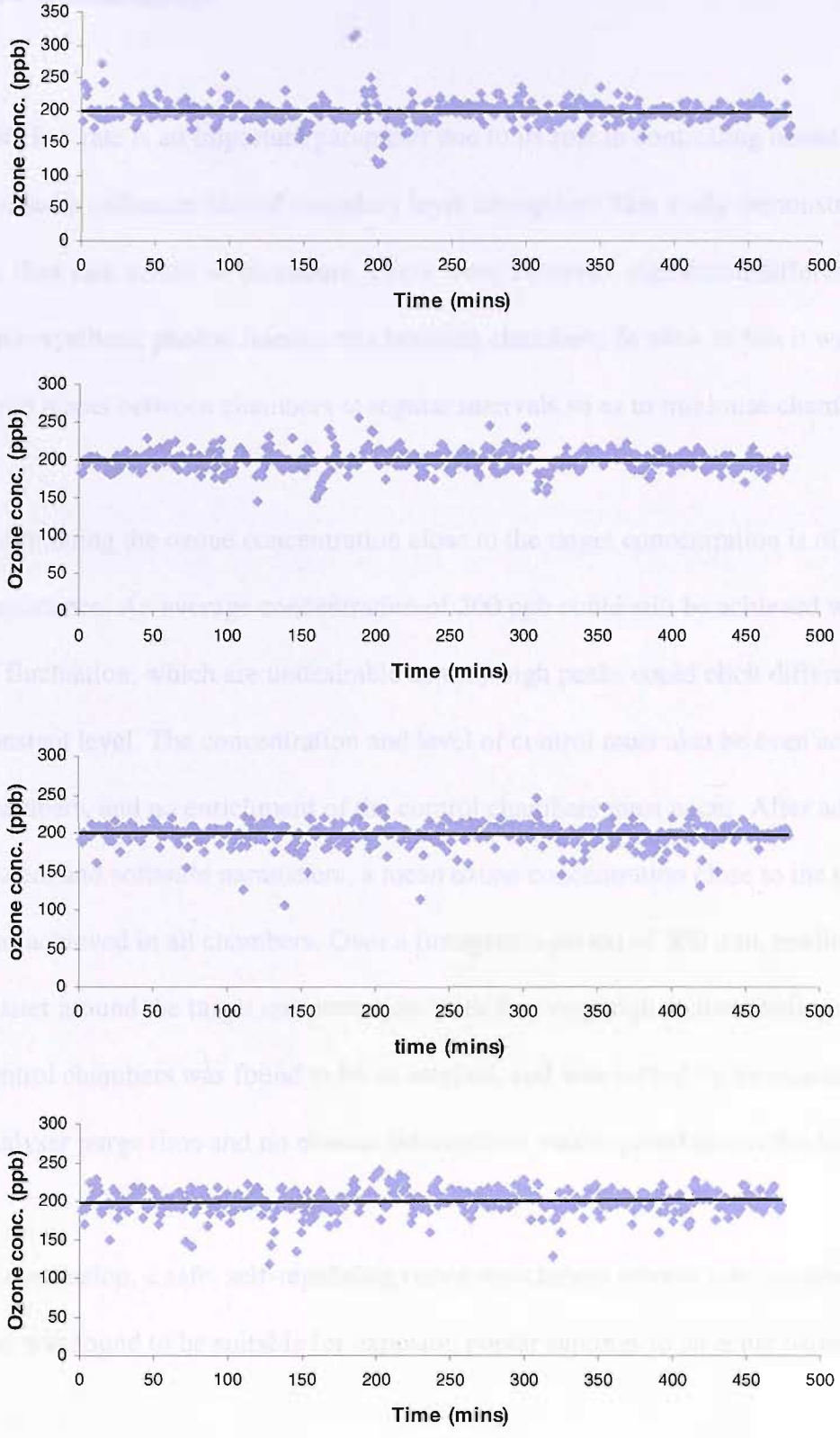

Figure 2.5: Ozone concentrations in four treated chambers measured over a 500 min fumigation period, showing best fit line. The target concentration was 200 ppb for all chambers.

2.4 Discussion

Air flow rate is an important parameter due to its role in controlling ozone flux, and also due to its influence on leaf boundary layer disruption. This study demonstrated a constant air flow rate across all chambers. There were, however, significant differences in photosynthetic photon fluence rate between chambers. In view of this it was decided to swap plants between chambers at regular intervals so as to minimise chamber effects.

Maintaining the ozone concentration close to the target concentration is of paramount importance. An average concentration of 200 ppb could still be achieved with high levels of fluctuation, which are undesirable as very high peaks could elicit different responses to a constant level. The concentration and level of control must also be even across the chambers, and no enrichment of the control chambers must occur. After adjustments to the system and software parameters, a mean ozone concentration close to the target of 200 ppb was achieved in all chambers. Over a fumigation period of 500 min, readings were found to cluster around the target concentration, with few very high or low readings. Enrichment of control chambers was found to be an artefact, and was solved by increasing the ozone analyser purge time and no manual intervention was required across the fumigation period.

In conclusion, a safe, self-regulating ozone enrichment system was constructed and tested, and was found to be suitable for exposing poplar saplings to an acute ozone treatment.

Chapter 3: Physiological analysis of ozone-exposed *P. trichocarpa, P. deltoides*, and genotypes of the mapping population, Family 331

3.1 Introduction

As elevated tropospheric ozone has been shown to have detrimental effects on a variety of plant species, including those of commercial importance, considerable effort has been focussed on cataloguing symptoms and unravelling their underlying causes. Visible damage was the first symptom to be attributed to ozone stress (Heggestad, 1959), and considerable progress has been made into understanding the genetic and biochemical basis of plant response.

Ozone has since been found to have a negative effect on numerous commercially important traits, including photosynthesis and chlorophyll content (Farage et al., 1991; Glick et al., 1995; Farage, 1996; Miller et al., 1999; Iglesias et al., 2006), root (Cooley & Manning, 1987; Shafer & Heagle, 1989; Coleman et al., 1996; Karnosky et al., 1996) and shoot growth (Gunthardt-Goerg, 1993; Karnosky et al., 1996), which have a large impact on productivity. One of the most commonly observed responses is an increase in leaf abscission as a result of premature senescence (Kargiolaki et al., 1991; Coleman et al., 1995; Karnosky et al., 1996, Li et al., 2006), and this has been suggested as an important determinant of sensitivity, resulting in reduced plant productivity.

Contrasting patterns of sensitivity to ozone treatment have been observed between species and ecotypes (Rao and Davis, 1999; Rao et al., 2000; Vahala et al., 2003; Li et al., 2006). If such variation exists between the parents of a mapping population, it can be harnessed to allow genetic dissection of the response to ozone stress through use of QTL analysis. It is a prerequisite for a QTL study that the mapping population possesses continuous variation in the trait under investigation, and this is most often the case if the species used to construct

the pedigree display contrasting phenotypes or responses to a treatment. The first part of this chapter sought to determine whether the grandparents of the *Populus* mapping population, Family 331, exhibited a contrasting response to acute ozone treatment, in order to justify performing experiments using the F_2 individuals.

Following this assessment, 164 genotypes from the F_2 population, along with *P. trichocarpa* and *P. deltoides*, were grown in open-top chambers with a view to characterising the response of this family to a chronic (100 ppb) ozone stress. All individuals were scored for growth traits, senescence, chlorophyll content and visible damage. The frequency distribution of each trait was also assessed, with those exhibiting a quantitative distribution being considered suitable for QTL mapping.

Stomatal conductance has been found to decrease in response to ozone in the majority of species studied (Taylor & Dobson, 1989; Pearson & Mansfield, 1993; Koch et al., 2000). As stomata represent the gas exchange interface between the leaf and the atmosphere, changes in aperture are likely to have an impact on ozone flux to the tissue, and it has previously been found that a tolerant clone of hybrid poplar exhibits a greater decrease in aperture compared to a sensitive clone (Koch et al., 1998) and could therefore be important in determining sensitivity. The stomatal response of *P. deltoides* and *P. trichocarpa* and selected F_2 genotypes exhibiting contrasting sensitivity to chronic ozone stress were investigated, with a view to determining its importance in governing sensitivity.

Analysis of genotypes exhibiting extreme phenotypes may be of use in studying a given trait, as an F_2 population may have greater phenotypic separation than that seen in the parental species, known as transgressive segregation. Selection of genotypes on this basis

may also be useful in removing unwanted variation associated with traits other than that under investigation (Borevitz, 2003). This chapter identified a group of ozone sensitive and ozone tolerant genotypes from the F_2 population exposed to a chronic ozone treatment, on the basis of visible damage to leaves. These data were used to assess the influence of visible leaf damage upon other physiological traits, in particular whether it has deleterious effects on overall productivity.

Also of interest is whether the extent of visible damage seen during a chronic ozone treatment is predictive of symptom formation under an acute exposure. To investigate this, the selected genotypes were exposed to 200 ppb ozone for 9 hrs and scored for visible damage. Genotypes were selected from this for future microarray analysis.

3.2 Materials and methods

Experiment 1- Physiological analysis of P. trichocarpa and P. deltoides exposed to an acute ozone treatment

Growth of experimental material

24 cuttings of *Populus deltoides* Marsh (Clone ILL-129) and 30 of *Populus trichocarpa* T. & G. (Clone 93-968) were obtained from 3 field sites in Hampshire (Headley Nurseries, Chilworth and the University of Southampton). The cuttings were soaked in cold water overnight, and planted in John Innes no. 2 compost (John Innes Manufacturers Association, Harrogate, UK) in 1.75 L pots with two buds left exposed above soil level. The pots were assigned randomly to two controlled environment rooms set at 22 °C, PAR 160 μmol $m^{-2}s^{-1}$ and 16 hr photoperiod, and were watered daily.

Ozone exposure

Thirty three days after planting, the plants were transferred to the ozone enrichment chambers, with 5 *P. trichocarpa* and 4 *P. deltoides* assigned to random positions in each chamber. They were allowed to acclimate for 48 hr under continuous light before the ozone treatment regime, at a mean temperature of 24 °C and PAR 120 μmol $m^{-2}s^{-1}$. Mean airflow through the chambers was 2.5 m s^{-1}.

Ozone was generated using an ECO3 generator (Torino, Italy), and delivered to a cylindrical buffer, which was connected to a series of solenoid valves by PTFE tubing. The buffered ozone was delivered to the chambers through PTFE tubing. Air samples from each

chamber were fed to an ozone monitor (Model 8810, Monitor Labs Inc.), which connected to a feedback system designed by Franco Miglietta (University of Florence) to allow automated control of ozone concentration.

The ozone exposure regime consisted of a 5 day treatment of 200 ppb ozone, and photos were taken of leaf Ln+5 of each plant after 9 hrs, 14 hrs, 24 hrs and 5 days of exposure. Stomatal conductance measurements were taken on young and semi-mature leaves of all plants after 3 hrs, 9 hrs and 24 hrs of exposure using a LI-COR 1600 porometer (LI-COR, Nebraska, USA).

Experiment 2- Further characterisation of the early stomatal response

The above experiment was repeated using 12 replicates of each species for each treatment, and stomatal conductance measurements were taken on all plants after 3 hrs of exposure to 200 ppb ozone.

Experiment 3- Physiological analysis of the F_2 mapping population

Open-top chambers

The experiment was conducted in 16 open top chambers at Headley Nurseries, Hampshire (described in Broadmeadow et al., 1999). Eight chambers were ozone enriched, and eight exposed to ambient air. Prior to planting, dolomitic lime, base dressing and slow release osmocote were applied. The chambers were irrigated daily by overhead sprinklers delivering water at approximately 12 L h^{-1} for 30 min from 07:00-07:30, and for a further 30 min from 19:00-19:30. Airflow was approximately 0.57 $m^3 s^{-1}$ in all chambers, equating to approximately two air changes min^{-1}. This was reduced to approximately 0.28 $m^3 s^{-1}$ between 20:00 and 10:00. Day length was not controlled.

Plant material

Hardwood cuttings were supplied by a DEFRA plantation of Family 331 at Headley Nurseries, Hampshire, UK, taken in December 2003. Cuttings were stored at 4°C until required. Three replicates of 164 genotypes were each assigned a random number between 1 and 492. These were divided between 8 chambers, giving 61 plants in 4 chambers and 62 in the remaining. The pattern was repeated for the ambient and treated groups, and the chambers were paired based on their nearest neighbour. A unique label denoting genotype, position and treatment was attached to each cutting. The cuttings were then soaked in cold water for 24 hours prior to planting. The cuttings were planted on 04/06/2004 in rows 25 cm apart with two viable buds above the soil surface. The plants were sprayed with Ambush on 22/06/2004 to control beetle damage, and with Cypermethrin on 24/09/2004 for spider mite.

Ozone exposure

The ozone enrichment system was maintained by Mark Broadmeadow (Forestry Commission, Alice Holt, UK). Ozone was generated by electrical discharge, using a model B063 Odotrol generator (Wallace & Tiernan, Kent, UK), and the concentration measured optically (model 8810, Monitor Labs, California, USA). Needle valves were used to balance the flow to each chamber. The exposure regime consisted of a square waveform fumigation of mean 93.1 ppb between 11:00 – 18:00 from 14/7/2004 – 20/10/2004. No significant difference between chambers was found. The mean concentration outside the fumigation period was 8.1 ppb. The mean ozone concentration in ambient chambers was 16.7 ppb during the fumigation period, and 7.9 ppb outside, again with no significant difference between chambers.

Measurement of physiological parameters

Tree growth

Total number of leaves included all leaves from the first unfurled leaf and all scars, measured after 30 and 70 days of treatment. Height and basal stem diameter were recorded after 65 days of treatment. Diameter was measured 5 cm above the base of the main stem.

Leaf abscission and visible damage

The percentage of abscised leaves was recorded by counting the number of leaf scars and expressing this as a percentage of total leaf number including scars. This trait was recorded after 30 and 70 days of treatment. Visible damage was also recorded at these time points, and was measured as the percentage of leaves exhibiting ozone induced flecking or necrosis. These values were expressed as a percentage of the remaining leaves (total leaf number – abscised leaves). These measurements were also used to select a group of 5 sensitive and 5 tolerant genotypes for further investigation.

Leaf growth and chlorophyll content

A digital photo of the first fully unfurled leaf on each plant was taken after 46 days of treatment. White paper was used as a background, and the plant label as a scale. The leaf was marked with cotton tied around the petiole. At 50 days of treatment, a second set of photos was taken of the marked leaves. Leaf area was measured for both time points using Image J (http://rsb.info.nih.gov/ij/). Relative leaf area expansion rate ((Area $_{day\ 50}$ – Area $_{day\ 46}$)/ Area $_{day\ 46}$) and absolute expansion rate (Area $_{day\ 50}$ – Area $_{day\ 46}$) were calculated. Chlorophyll content measurements were taken from the second interveinal section of Leaf 9 using a CCM-200 chlorophyll content meter (Opti-Sciences, MA, USA).

Data analysis

Data were recorded in Microsoft Excel. Homogeneity of variance and normality of residuals were checked, and data was normalised using Box-Cox transformation where necessary. Data were analysed using ANOVA in Minitab 14 (Minitab, Coventry, UK).

Stomatal conductance

All stomatal conductance measurements were made using a LI-COR 1600 Porometer (LI-COR, Nebraska, USA).

P. deltoides and *P. trichocarpa.*

The stomatal conductance of a young and semi-mature leaf was recorded at 8 time points from 0300 – 2130 on each replicate of *P. deltoides* and *P. trichocarpa* in the ambient and treated regimes. Due to the amphistomatous nature of *P. deltoides*, for this species measurements were taken from both the upper and lower surfaces of the leaf.

Sensitive and tolerant genotypes

Measurements were taken from the upper and lower surfaces of young and semi-mature leaves of 5 ozone sensitive and 5 tolerant clones (selected on the basis of early season visible damage) between 1100 and 1400. The order of measurements was random to minimise effect of time of day.

Experiment 4- Physiological analysis of sensitive and tolerant genotypes exposed to an acute ozone treatment

Plant material and ozone exposure

5 replicates of 5 sensitive and 5 tolerant genotypes were grown and exposed to the ozone treatment regime described for the grand-parental experiment (Experiment 1). Each genotype was represented in each chamber, with the fifth replicate being randomly assigned. The percentage coverage of ozone-induced necrosis was recorded on each leaf of each plant.

3.3 Results

Contrasting visible symptoms in P. deltoides and P. trichocarpa in response to acute ozone treatment in growth chambers (Experiment 1)

The photographic record revealed a marked difference in damage between the two species after ozone treatment (Figure 3.1). *P. trichocarpa* leaves began to develop lesions within 9 hours of treatment with 200 ppb ozone, manifested as red spots. These spread and blackened with further exposure. After 5 days, the leaves were almost completely black and desiccated. It was of note that symptoms were more severe in older leaves. No such symptoms were observed in *P. deltoides*, with all leaves remaining unblemished for the duration of the treatment.

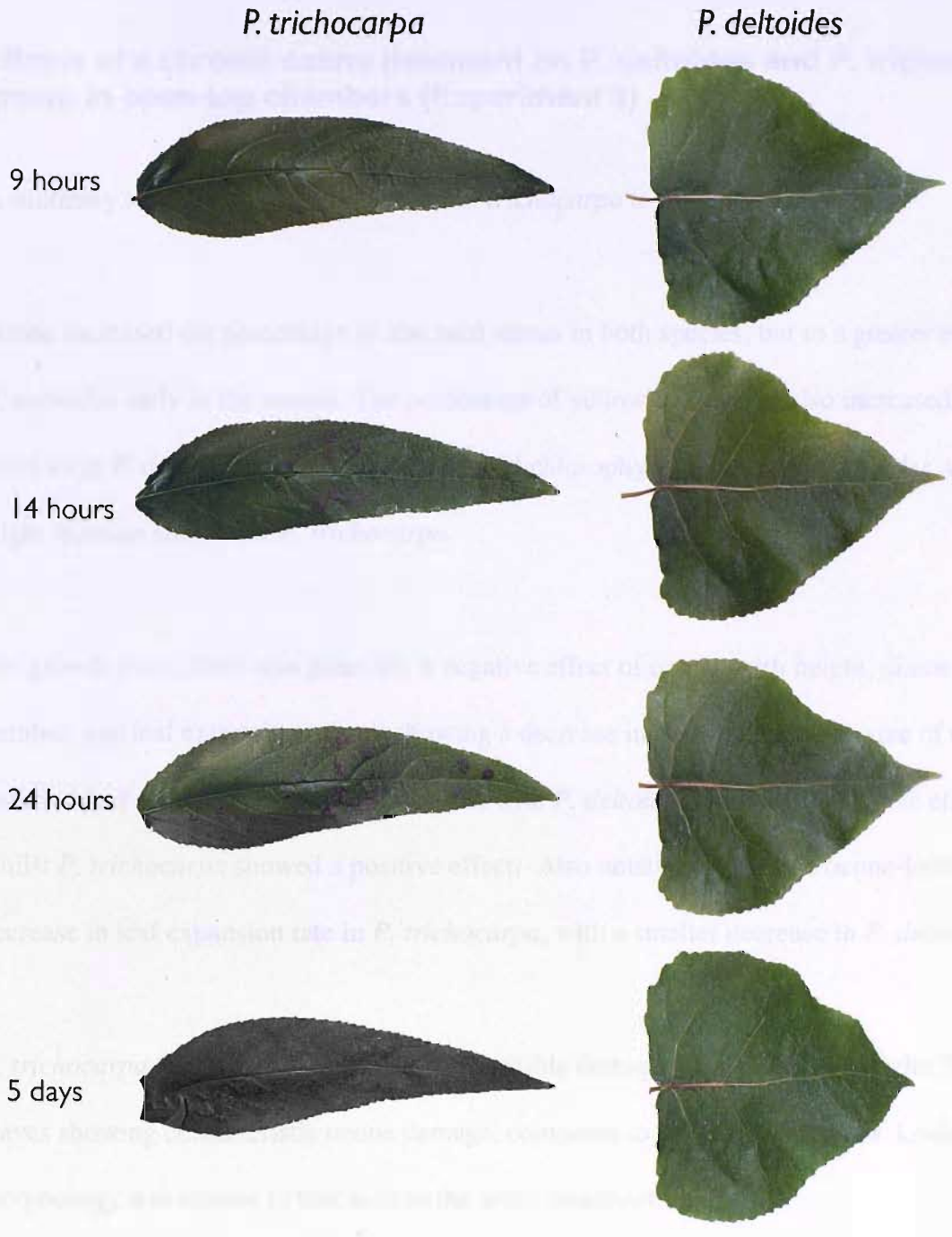

Figure 3.1: The progression of O_3 damage for *P. deltoides* and *P. trichocarpa* exposed to 200 ppb ozone in growth chambers for 5 days, showing necrotic lesion formation in *P. trichocarpa*, with a lack of visible symptoms in *P. deltoides*.

Effects of a chronic ozone treatment on P. deltoides and P. trichocarpa grown in open-top chambers (Experiment 3)

A summary of traits for *P. deltoides* and *P. trichocarpa* is shown in Table 3.1a.

Ozone increased the percentage of abscised leaves in both species, but to a greater extent in *P. deltoides* early in the season. The percentage of yellow leaves was also increased, again more so in *P. deltoides*. Ozone greatly reduced chlorophyll content in *P. deltoides*, with a slight increase shown for *P. trichocarpa*.

For growth traits, there was generally a negative effect of ozone, with height, diameter, leaf number, and leaf expansion rate all showing a decrease in both species. The size of the first unfurled leaf showed contrasting responses, with *P. deltoides* showing a negative effect, whilst *P. trichocarpa* showed a positive effect. Also notable is the large ozone-induced decrease in leaf expansion rate in *P. trichocarpa*, with a smaller decrease in *P. deltoides*.

P. trichocarpa exhibited considerably more visible damage than *P. deltoides*, with 51% of leaves showing characteristic ozone damage, compared to 0% for *P. deltoides*. Lesion morphology was similar to that seen in the acute treatment.

Effects of a chronic ozone exposure on the F_2 population grown in open-top chambers (Experiment 3)

A summary of traits for the F_2 population is shown in table 3.1b.

For all traits, there was a highly significant effect of genotype ($p<0.0001$), confirming the hypothesis that this population was suitable to study the genetic basis of the response to ozone.

No significant ozone effect on height was found. For basal stem diameter a small (-3.2%) but significant negative effect ($F_{1,132}=11.24$, $p<0.001$) of ozone treatment was found. Ozone had a positive influence on the total number of leaves initiated both early ($F_{1,123}=4.62$, $p<0.05$) and late ($F_{1,126}=5.45$, $p<0.05$) in the season.

The effect of ozone fumigation on leaf area and leaf expansion is shown in Figure 3.2. The area of the first unfurled leaf was significantly greater in ozone ($F_{1,93}=6.82$, $p<0.01$), whilst leaf area expansion rate was significantly reduced ($F_{1,93}=7.82$, $p<0.01$). No significant effect on final leaf area was found, although the genotype*treatment interaction was almost significant ($F_{93,274}=1.25$, $p=0.09$).

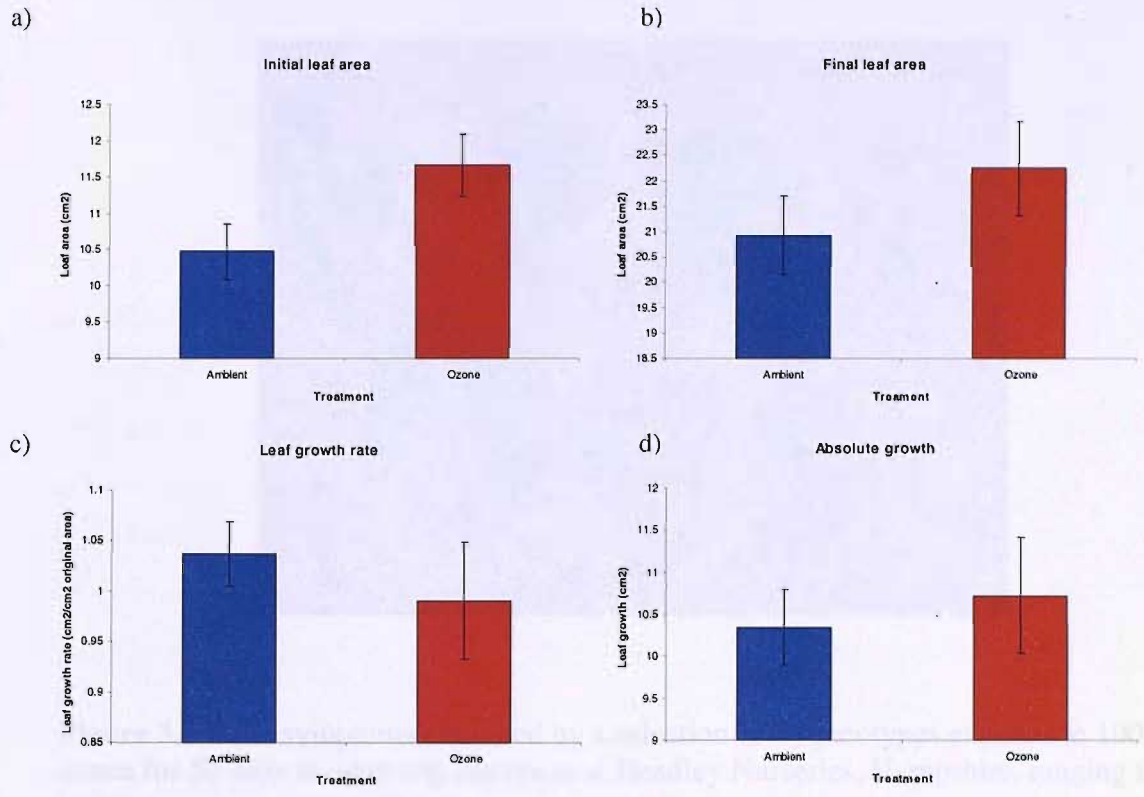

Figure 3.2: The effect of 100 ppb ozone fumigation in open-top chambers on **a**) area of the first unfurled leaf after 46 days of treatment **b**) area of this leaf after 50 days of treatment **c**) relative leaf growth rate, measured as (area on day 50 - area on day 46)/(area on day 46) **d**) absolute leaf growth rate, measured as the increase in leaf area between day 46 and day 50.

There was a highly significant increase in leaf abscission both early and late season ($p<0.001$). Chlorophyll content showed no significant treatment effect, but a significant genotype*treatment interaction ($F_{126,416}=1.27$, $p<0.05$). Some genotypes showed an increase in chlorophyll content in response to ozone, whereas others exhibited a decrease.

The extent of visible damage was highly variable. Figure 3.3 depicts the range of symptoms observed.

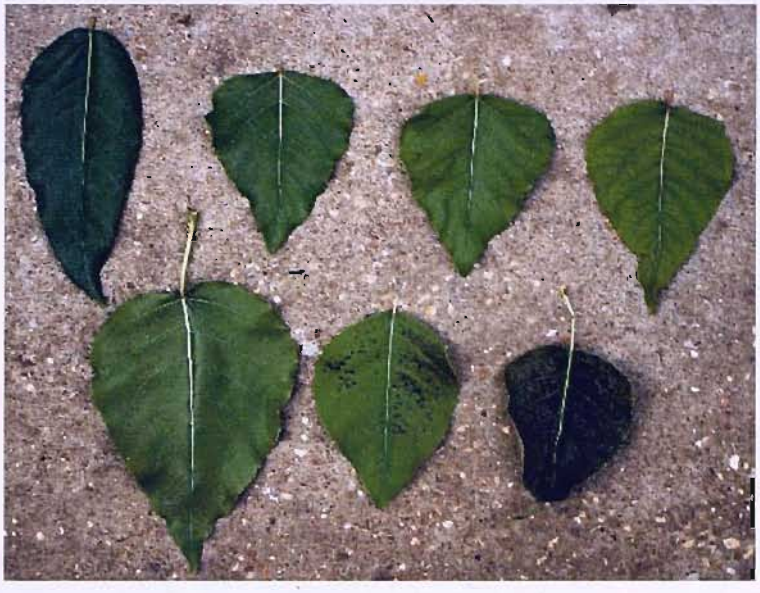

Figure 3.3 : The symptoms exhibited by a selection of F_2 genotypes exposed to 100 ppb ozone for 50 days in open-top chambers at Headley Nurseries, Hampshire, ranging from no visible symptoms (top left) to severe necrosis (bottom right).

a)

	P. deltoides				*P.trichocarpa*			
	Control	Ozone	% effect	Significance	Control	Ozone	% effect	Significance
Height (cm)	55.30	53.00	-4.34	ns	79.30	72.30	-9.68	ns
Diameter (mm)	6.03	5.43	-10.00	ns	6.47	5.17	-20.20	*
Leaf number (30d)	15.70	14.70	-6.80	ns	19.70	15.30	-28.76	ns
Leaf number (70d)	21.30	18.30	-16.39	*	26.70	26.00	-2.69	ns
Chlorophyll content (CCM reading)	15.10	9.53	-58.45	**	20.70	21.90	5.48	ns
% abscised (30d)	7.10	17.60	59.66	***	8.80	10.30	14.56	*
% abscised (70d)	18.50	40.00	53.75	***	22.80	53.90	57.70	***
Area of first unfurled leaf (cm^2)	7.40	6.64	-11.38	*	9.94	12.62	21.20	*
Leaf expansion rate (% area increase)	74.60	68.20	-9.38	ns	87.20	54.40	-60.29	*

b)

	F_2 population					
	Control	Ozone	% effect	Treatment	Genotype	Genotype*treatment
Height (cm)	78.70	79.74	1.30	ns	***	ns
Diameter (mm)	7.09	6.57	-3.20	***	***	ns
Leaf number (30d)	19.60	20.30	3.44	*	***	ns
Leaf number (70d)	26.10	27.15	3.84	**	***	ns
Chlorophyll content (CCM reading)	21.06	21.22	0.78	ns	***	*
% abscised (30d)	2.45	12.77	80.78	***	***	N/A
% abscised (70d)	14.59	33.24	56.11	***	***	*
Area of first unfurled leaf (cm^2)	10.56	11.81	10.60	*	***	ns
Leaf expansion rate (% area increase)	99.80	90.70	-10.03	**	*	ns

Table 3.1: Summary of traits measured in **a**) *P. deltoides* and *P. trichocarpa*; and **b**) the F_2 population in response to a chronic 100 ppb ozone treatment. Where traits were measured on more than one occasion, this is indicated by 30d and 70d (30 or 70 days of exposure). The data represent means for each trait recorded in ambient conditions and elevated ozone, and the percentage effect of ozone upon the trait. A general linear model was used to analyse all data except *% abscised (30d)* where a Kruskal-Wallis test was performed due to a non-normal distribution. Significance levels are indicated by * $p<0.05$, ** $p<0.01$, ***$p<0.001$.

Frequency distributions for all traits are shown in Figures 3.4 and 3.5. For leaf abscission, a skew towards zero is seen for the trees grown in ambient air, with a transition towards a normal distribution later in the season. The highly significant increase in abscission under ozone exposure is reflected in these distributions, which are shifted strongly to the right when compared to the control. This is also true for visible damage early in the season. Chlorophyll content has an approximately normal distribution which is similar for both control and treated plants. An approximately normal distribution is seen for height, leaf number and diameter. There is a slight shift to the left for diameter and to the right for leaf number for ozone treated trees, corroborating the significant ANOVA results. The area of the first unfurled leaf shows a positive shift in ozone, again matching the statistical findings. Leaf area expansion shows a larger number of control trees falling into the higher categories. Both of these traits approach a normal distribution.

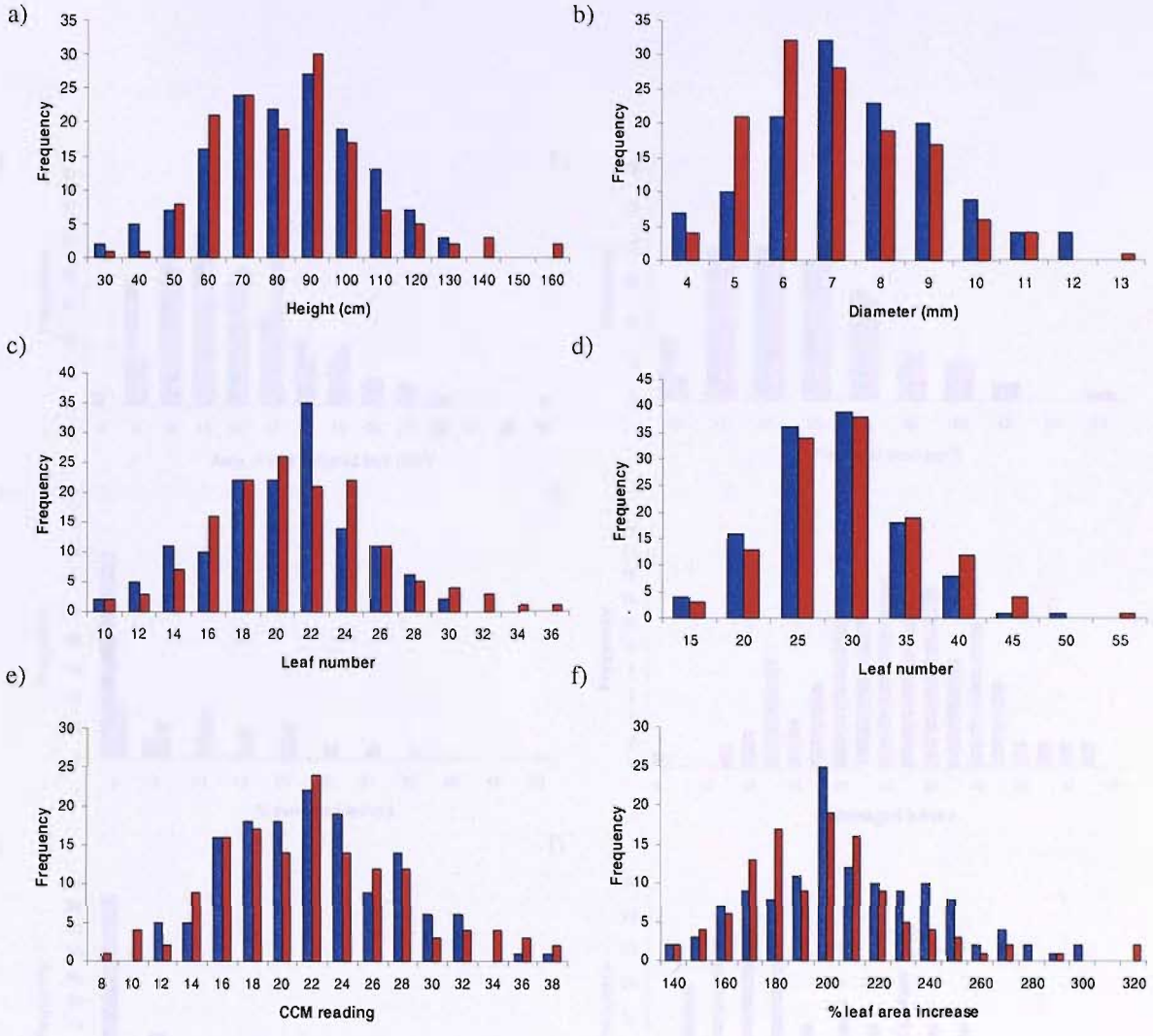

Figure 3.4: Frequency distributions of **a**) height (after 65 days of treatment), **b**) diameter (after 65 days), leaf number (**c**) after 30 days and **d**) after 70 days), **e**) chlorophyll content (after 45 days) and **f**) % leaf area increase (measured as the increase in leaf area between 46 days and 50 days, relative to the area at 46 days) in the F_2 population exposed to 100 ppb ozone.

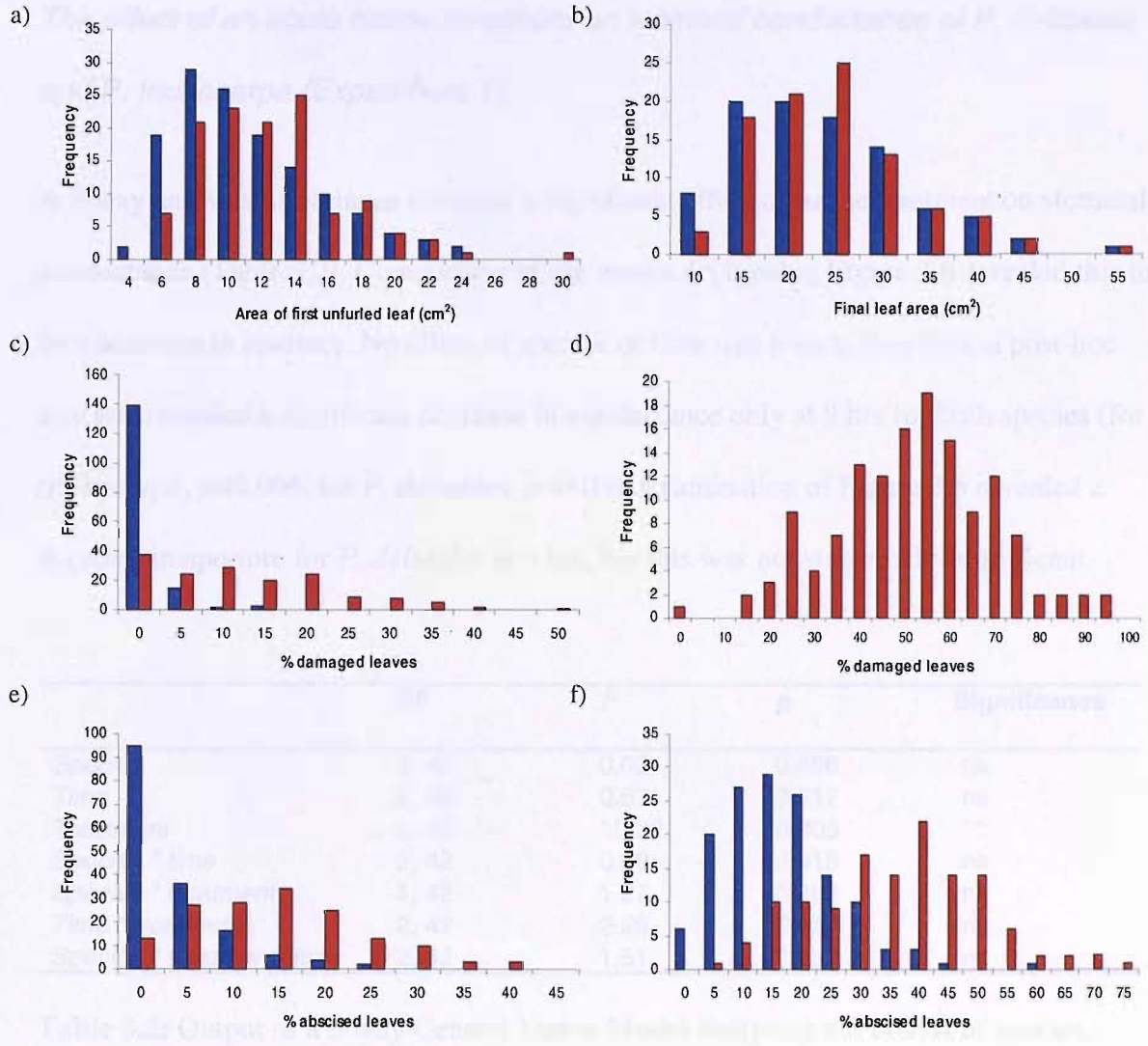

Figure 3.5: Frequency distributions of **a)** area of first unfurled leaf at 46 days of treatment, **b)**area of this leaf at 50 days, **c)** % damaged leaves (after 30 days), **d)** % damaged leaves (after 70 days), **e)** % abscised leaves (after 30 days), **f)** % abscised leaves (after 70 days) in the F_2 population exposed to 100 ppb ozone.

Stomatal conductance

The effect of an acute ozone treatment on stomatal conductance of P. deltoides and P. trichocarpa (Experiment 1).

A 3-way analysis of variance revealed a significant effect of ozone treatment on stomatal conductance (Table 3.2). Comparison of the means depicted in Figure 3.6 revealed this to be a decrease in aperture. No effect of species or time was found. However, a post-hoc analysis revealed a significant decrease in conductance only at 9 hrs for both species (for *P. trichocarpa*, p=0.006, for *P. deltoides*, p=0.03). Examination of Figure 3.6 revealed a decrease in aperture for *P. deltoides* at 3 hrs, but this was not statistically significant.

	DF	*F*	*p*	Significance
Species	1, 42	0.02	0.886	ns
Time	2, 42	0.67	0.517	ns
Treatment	1, 42	10.32	0.003	**
*Species * time*	2, 42	0.09	0.918	ns
*Species * treatment*	1, 42	1.27	0.266	ns
*Time * treatment*	2, 42	2.26	0.117	ns
*Species * treatment *time*	2, 42	1.51	0.233	ns

Table 3.2: Output of a 3-way General Linear Model analysing the effects of species, treatment (control or ozone enriched), time, and all interactions on stomatal conductance of *P. deltoides* and *P. trichocarpa* exposed to 200 ppb for 28 hrs. Measurements were taken at 3, 9 and 28 hrs.

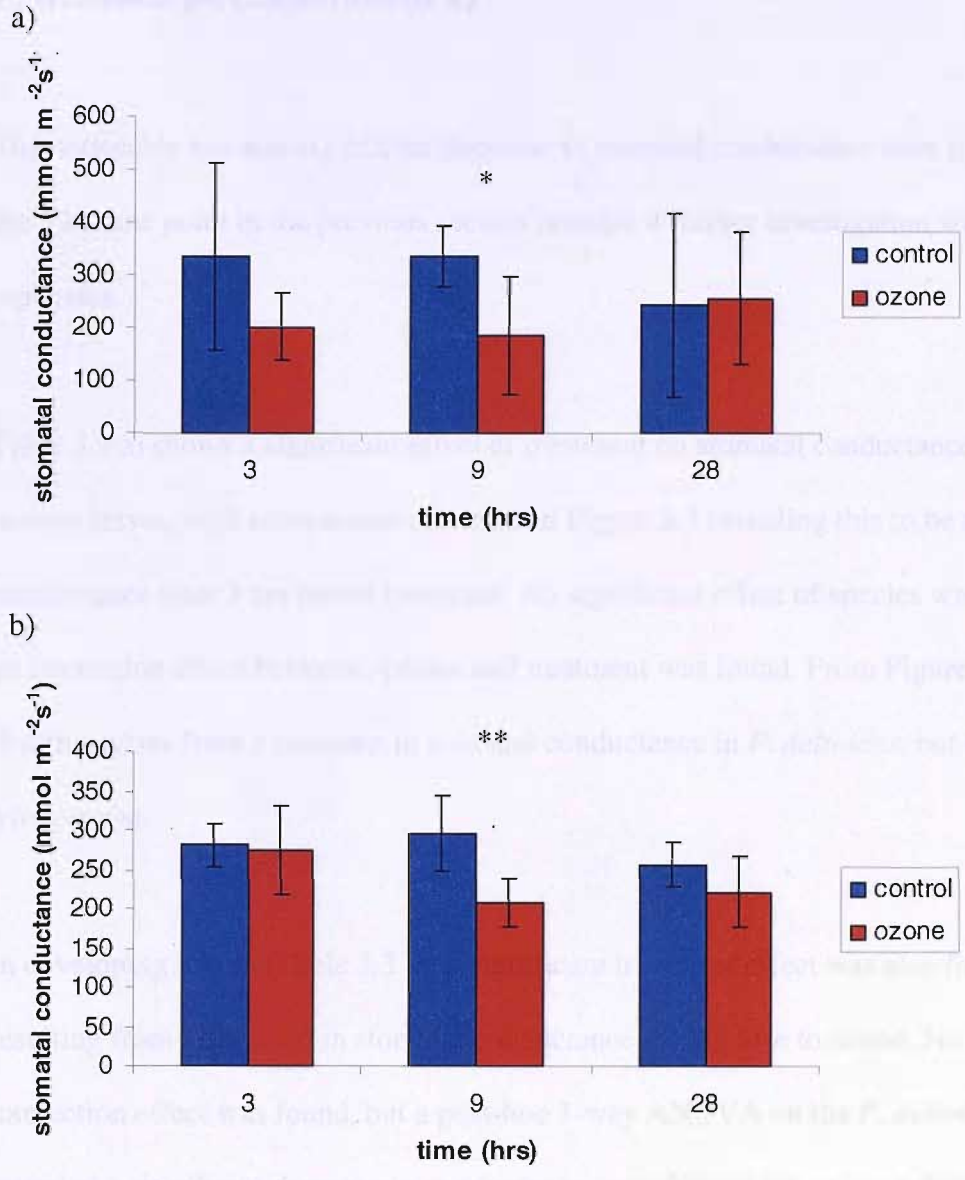

Figure 3.6: The effect of a 28 hr 200 ppb ozone treatment on stomatal conductance (g_s) in **a**) *P. deltoides* and **b**) *P. trichocarpa*. Results of post-hoc 1-way ANOVA show significant decrease in g_s at 9hr for both species (* $p<0.05$, ** $p<0.01$).

Further investigation of the early stomatal response of P. deltoides and P. trichocarpa (Experiment 2)

The noticeable but non-significant decrease in stomatal conductance seen in *P. deltoides* at the 3 hr time point in the previous section prompted further investigation with additional replicates.

Table 3.3 a) shows a significant effect of treatment on stomatal conductance in semi-mature leaves, with comparison of means in Figure 3.7 revealing this to be a decrease in conductance after 3 hrs ozone treatment. No significant effect of species was observed, but an interaction effect between species and treatment was found. From Figure 3.7, it is clear that this arises from a decrease in stomatal conductance in *P. deltoides*, but not in *P. trichocarpa*.

In developing leaves (Table 3.3 b), a significant treatment effect was also found, again resulting from a decrease in stomatal conductance in response to ozone. No significant interaction effect was found, but a post-hoc 1-way ANOVA on the *P. deltoides* data revealed a significant decrease in conductance (p=0.02), whilst no such difference was found in *P. trichocarpa* (p=0.463).

Post-hoc 1-way ANOVA revealed stomatal conductance under ambient conditions to be higher in mature *P. deltoides* leaves than *P. trichocarpa* leaves of a corresponding age (p=0.010), with the reverse being true for developing leaves (p=0.018).

a)

	D.F	*F*	*p*
Species	1, 44	0.05	=0.824
Treatment	1, 44	35.31	<0.0001
Species*treatment	1, 44	22.41	<0.0001

b)

	D.F	*F*	*p*
Species	1, 44	28.26	<0.0001
Treatment	1, 44	4.71	=0.035
Species*treatment	1, 44	1.70	=0.199

Table 3.3: Output of a two-way ANOVA, showing the effect of species (*P. deltoides, P. trichocarpa*) and 3 hr treatment (200 ppb ozone, ambient air) on stomatal conductance for **a**) semi-mature leaves, and **b**) developing leaves.

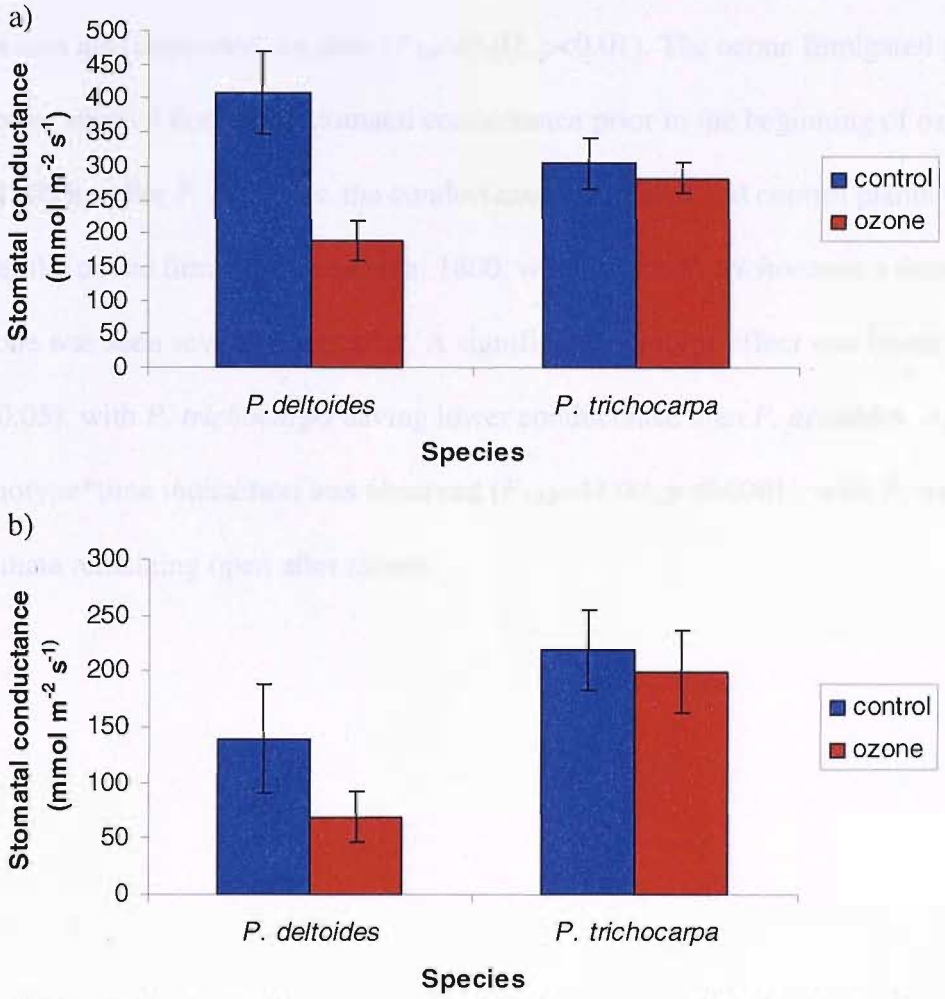

Figure 3.7: The stomatal response of **a**) semi-mature, and **b**) developing leaves of *P. trichocarpa* and *P. deltoides* to 3 hrs treatment with 200 ppb ozone, showing 95% confidence intervals.

The effect of a chronic ozone treatment on stomatal conductance of P. deltoides and P. trichocarpa (Experiment 3)

Ozone treatment had no significant effect on stomatal conductance of young leaves. A significant genotype*time interaction was found ($F_{7,63}$=9.86, p<0.0001). This is reflected in Figure 3.8, which shows that *P. trichocarpa* exhibits delayed stomatal closure. For *P. deltoides,* Figure 3.8 shows a general trend towards an increase in stomatal conductance under ozone treatment, although this is not statistically significant.

For semi-mature leaves, a significant treatment effect was found ($F_{1,7}$=5.64, p<0.05), and this was also dependent on time ($F_{7,62}$=3.07, p<0.01). The ozone fumigated groups of both species showed decreased stomatal conductance prior to the beginning of ozone treatment at 1100 hrs. For *P. deltoides,* the conductance for treated and control plants was similar after the ozone fumigation ceased at 1800, whereas for *P. trichocarpa* a decrease under ozone was seen several hours after. A significant genotype effect was found ($F_{1,7}$=9,58, p<0.05), with *P. trichocarpa* having lower conductance than *P. deltoides*. Again, a genotype*time interaction was observed ($F_{7,62}$=41.07, p<0.0001), with *P. trichocarpa* stomata remaining open after sunset.

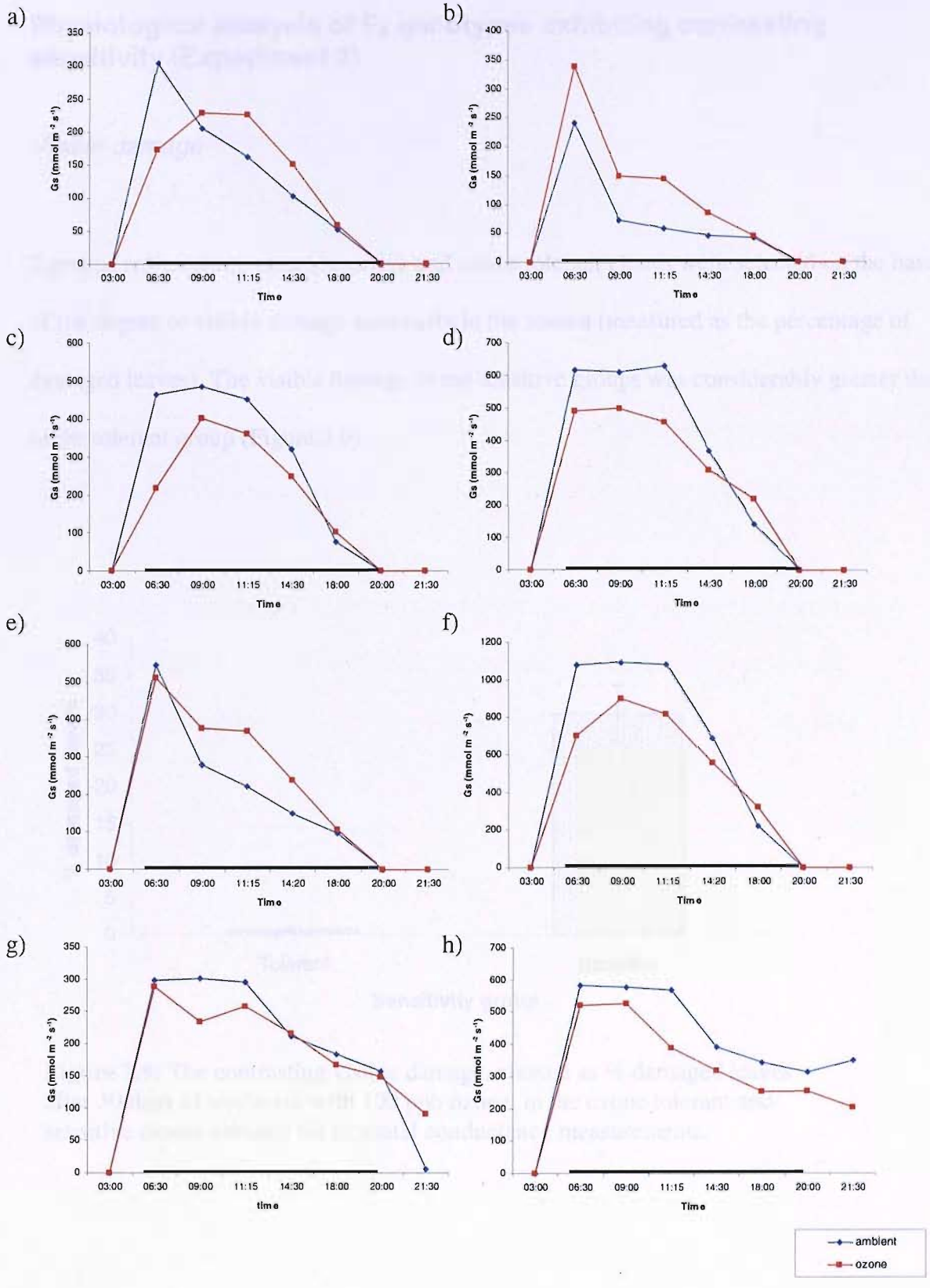

Figure 3.8: Diurnal stomatal conductance pattern for **a**) upper and **b**) lower surface of young *P. deltoides* leaves; **c**) upper and **d**) lower surface of semi-mature *P. deltoides* leaves; total (upper + lower surfaces) conductance for **e**) young and **f**) semi-mature *P. deltoides* leaves; total conductance for **g**) young and **h**) semi-mature *P. trichocarpa* leaves. Measurements were taken after 35 days of treatment with 100 ppb ozone commencing at 1100 and ending 1800 hrs. Photoperiod is indicated as a black bar on the *x* axis.

Physiological analysis of F_2 genotypes exhibiting contrasting sensitivity (Experiment 3)

Visible damage

2 groups representing ozone sensitive and ozone tolerant clones were selected on the basis of the degree of visible damage seen early in the season (measured as the percentage of damaged leaves). The visible damage in the sensitive groups was considerably greater than in the tolerant group (Figure 3.9).

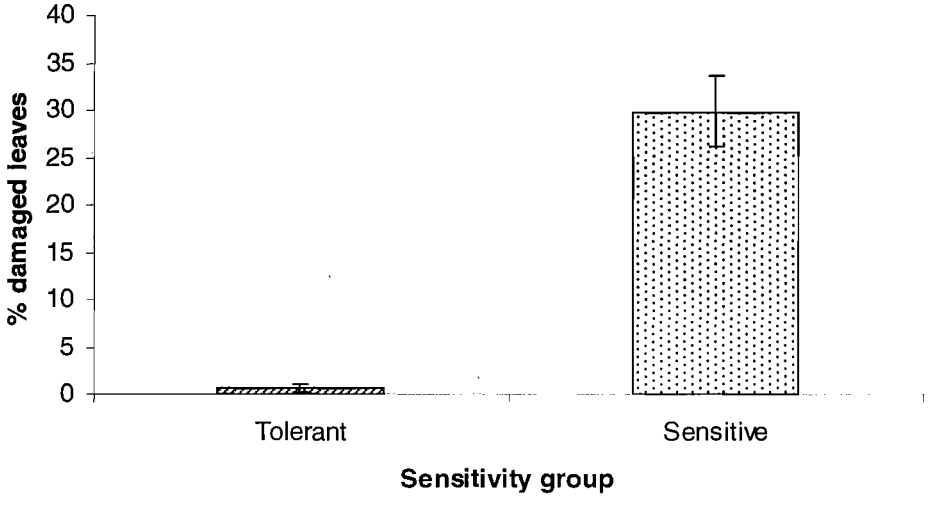

Figure 3.9: The contrasting visible damage, classed as % damaged leaves after 30 days of treatment with 100 ppb ozone, in the ozone tolerant and sensitive clones selected for stomatal conductance measurements.

Stomatal conductance

The effect of ozone treatment on stomatal conductance of the sensitive and tolerant genotypes is shown in Figure 3.10.

A significant treatment effect was found for semi-mature leaves, with ozone reducing conductance ($F_{1,8}$=16.46, p<0.005). Conductance did not depend on sensitivity group, and there was no sensitivity group*treatment interaction. The genotypes differed significantly in their conductance ($F_{8,8}$=5.72, p<0.05), but this was not dependent on treatment.

For young leaves, no terms in the test were significant; indicating that the conductance of young leaves is not dependent on genotype, treatment or sensitivity group, or any interactions thereof.

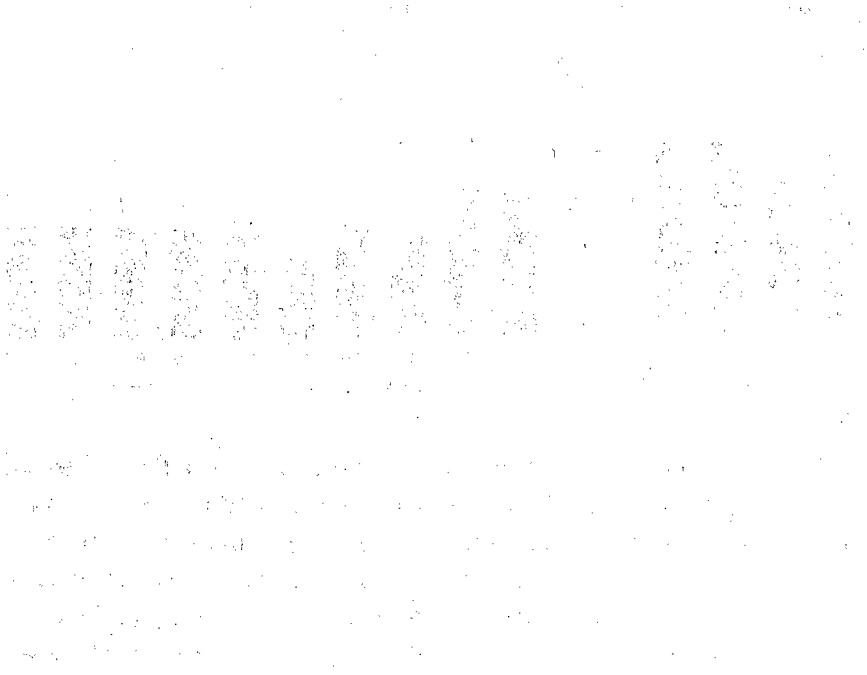

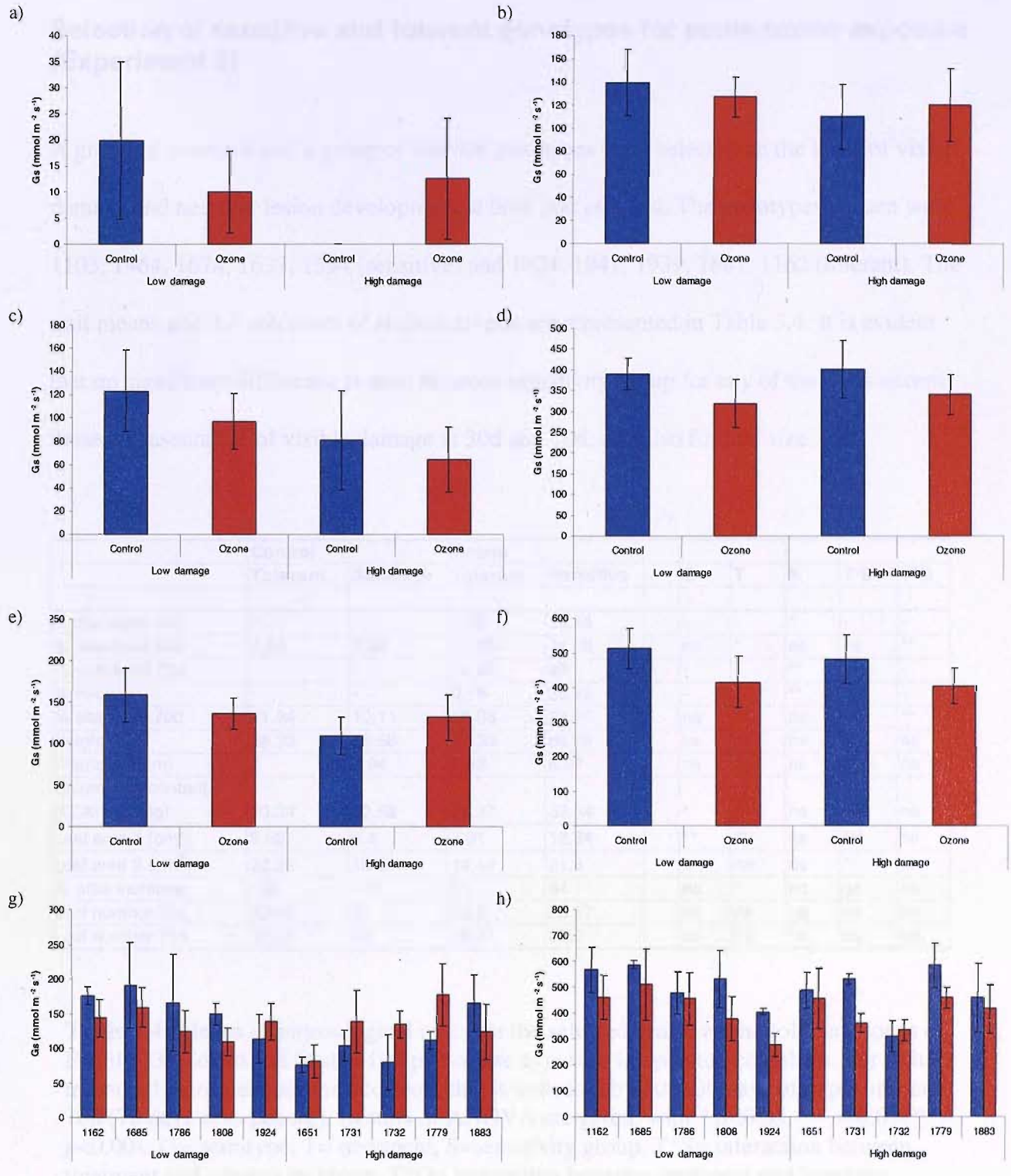

Figure 3.10: The effect of ozone fumigation on stomatal conductance (+/- 1 SE) of **a)** upper surface and **b)** lower surface of young leaves; **c)** upper surface and **d)** lower surface of semi-mature leaves; total conductance (upper + lower surfaces) of **e)** young and **f)** semi-mature leaves; total conductance of **g)** young and h) semi-mature leaves separated by genotype. "Low damage" represents tolerant genotypes, "High damage" represents sensitive genotypes. Measurements were taken between 1100 and 1400 during the fumigation period. Red bars represent ozone treated plants, and blue bars control plants.

Selection of sensitive and tolerant genotypes for acute ozone exposure (Experiment 3)

A group of sensitive and a group of tolerant genotypes were selected on the basis of visible damage and necrotic lesion development at both 30d and 70d. The genotypes chosen were 1103, 1964, 1678, 1637, 1594 (sensitive) and 1924, 1941, 1939, 1881, 1162 (tolerant). The trait means and the outcomes of statistical tests are represented in Table 3.4. It is evident that no significant difference is seen between sensitivity group for any of the traits except those representative of visible damage at 30d and 70d, and also for leaf size.

	Control		Ozone						
	Tolerant	Sensitive	Tolerant	Sensitive	G	T	S	T*S	T*G
% damaged 30d	-	-	1.36	19.54	-	-	*	-	-
% abscised 30d	0.53	2.89	11.26	14.08	ns	*	ns	ns	**
% damaged 70d	-	-	24.05	40	-	-	**	-	-
% necrotic	-	-	0.18	23.23	-	-	**	-	-
% abscised 70d	11.84	10.11	16.08	29.25	ns	ns	ns	ns	**
Height (cm)	88.33	78.58	77.33	88.28	ns	ns	ns	ns	ns
Diameter (mm)	8	6.94	6.53	6.97	ns	ns	ns	ns	ns
Chlorophyll content (CCM reading)	20.34	20.58	24.37	33.34	*	*	ns	ns	ns
Leaf area 1 (cm^2)	9.52	6.4	7.91	12.34	**	**	ns	***	ns
Leaf area 2 (cm^2)	22.21	13.31	14.14	21.8	*	ns	ns	**	ns
% area increase	134	116	81	84	ns	*	ns	ns	ns
Leaf number 30d	23.45	21	20.5	23.87	ns	ns	ns	ns	ns
Leaf number 70d	30.81	28	29.41	32.2	ns	ns	ns	ns	ns

Table 3.4: Means of physiological traits for the selected sensitive and tolerant clones of Family 331, identified from a 100 ppb ozone exposure in open top chambers. For traits measured on more than one occasion, this is indicated by 30d (30 days of exposure) and 70d (70 days of exposure). Results of ANOVA are given, with * $p<0.05$, ** $p<0.01$, *** $p<0.001$. G= genotype, T= treatment, S=sensitivity group, T*S= interaction between treatment and sensitivity group, T*G= interaction between treatment and genotype.

Exposure of sensitive and tolerant genotypes to an acute ozone treatment (Experiment 4)

Table 3.5 depicts the percentage of leaves exhibiting visible damage, and average percentage leaf area covered by damage for each genotype after 9 hrs treatment with 200

ppb ozone. A highly significant effect of sensitivity group and genotype was found for both variables ($p<0.001$), with the sensitive genotypes showing more severe symptoms. The extent of damage seen in these genotypes was considerably greater than in *P. trichocarpa*, and resembled that seen in the chronic exposure. It is of note that 2 tolerant genotypes (1924 and 1162) developed some symptoms, but less severe than all sensitive genotypes except 1637, which showed no visible damage. In order to achieve maximum separation between the groups, the three most tolerant (1881, 1939, 1941) and most sensitive (1964, 1103, 1678) were selected for further analysis (covered in Chapter 4) Figure 3.11 shows the visible symptoms observed on these genotypes.

	Genotype	% damaged leaves	Average coverage
Tolerant	1162	18.10	3.36
	1881	0	0
	1924	9.52	4.73
	1939	0	0
	1941	0	0
Sensitive	1103	27.50	4.17
	1594	19.71	5.14
	1637	0	0
	1678	54.52	14.62
	1964	28.89	8.72

Table 3.5: The percentage of leaves ozone damage, and average leaf area covered by ozone damage for five ozone sensitive and five tolerant genotypes of Family 331 after exposure to 9 hrs 200 ppb ozone in growth chambers.

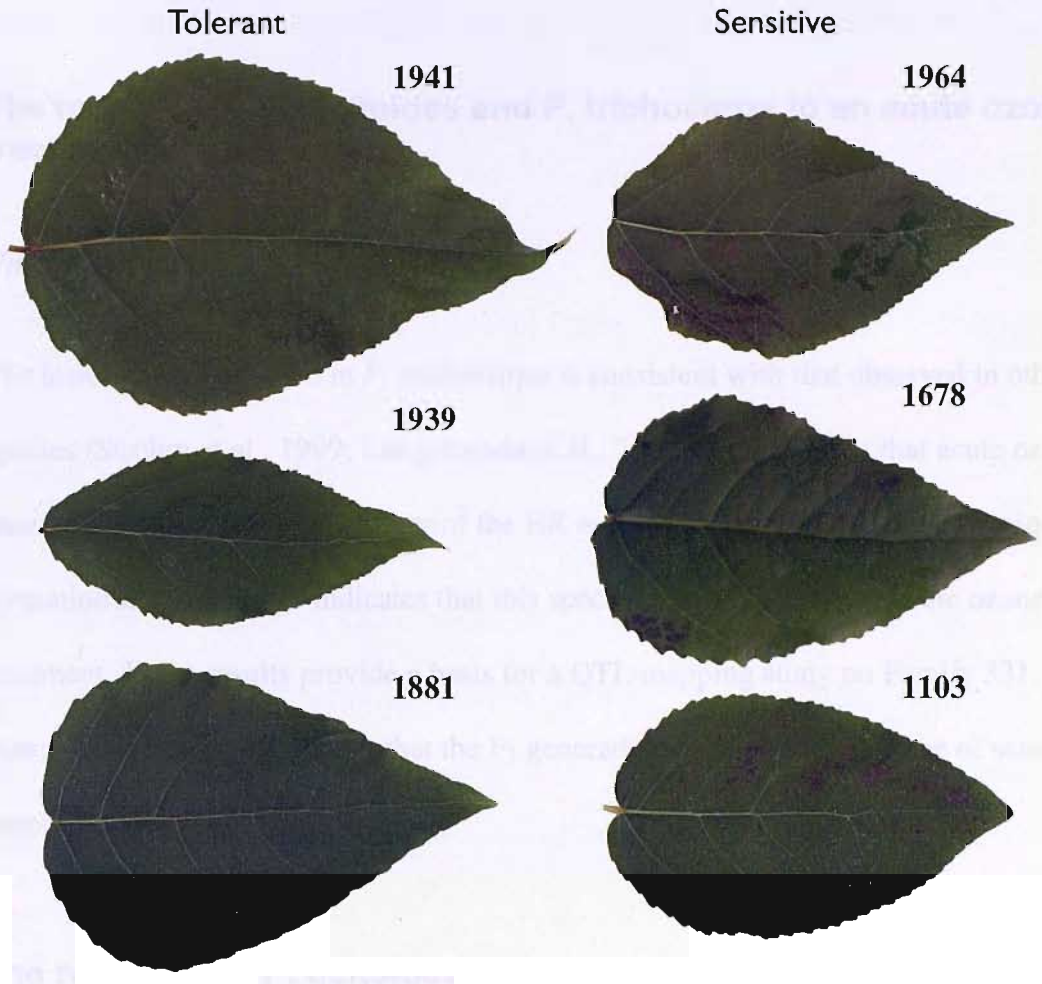

Figure 3.11: The response of three ozone tolerant and three sensitive F_2 genotypes of Family 331 to a 9 hr exposure of 200 ppb ozone in growth chambers, showing necrotic lesions in the sensitive clones.

3.4 Discussion

The response of P. deltoides and P. trichocarpa to an acute ozone treatment

Visible damage

The lesion formation seen in *P. trichocarpa* is consistent with that observed in other species (Strohm et al., 1999; Langebartels et al., 2002), and suggests that acute ozone treatment acts as an abiotic elicitor of the HR in this species. The absence of lesion formation in *P. deltoides* indicates that this species is less sensitive to acute ozone treatment. These results provide a basis for a QTL mapping study on Family 331, with such parental differences indicating that the F_2 generation will exhibit the range of sensitivity required.

The response of P. deltoides, P. trichocarpa and the F_2 mapping population to a chronic ozone treatment

Growth

These results demonstrate the detrimental effect of ozone on stem volume and hence biomass, and are consistent with those from other studies (Karnosky et al., 1996; Reinert et al., 1996), and have previously been found to be related to decreased photosynthetic productivity (Coleman et al., 1995). The shift in height/diameter ratio, indicated by a significant decrease in diameter with no significant change in height, could be considered a compensatory response to the growth inhibiting effect of ozone, as it is likely to be important for the plant to maintain height growth to avoid being out-competed by neighbouring plants. Previous work has demonstrated a decrease in root/shoot ratio, which

may serve a similar purpose (Coleman et al., 1996; Karnosky et al., 1996; Reinert et al., 1996). Such changes in partitioning may have deleterious effects on both the plant and the soil ecosystem. Redistribution of resources from the roots is likely to have a negative impact on nutrient uptake, and may also affect soil micro-organisms that depend on root exudates (Edwards, 1991). Total number of leaves initiated showed a small but significant increase in ozone both early and late in the season. This is an interesting result, as previous studies have demonstrated either a decrease or no effect (Gunthardt-Goerg et al., 1993; Karnosky et al., 1996). It is hypothesised that this is due to re-translocation of resources from leaves undergoing premature senescence to the growing apical meristem. Initiating more leaves in conditions of accelerated senescence is likely to be beneficial to the plant, increasing the amount of absorbed photosynthetically active radiation. It would be interesting to see if a similar response occurred during other treatments that result in senescence, such as rust infection.

Chlorophyll content

The effect of ozone on chlorophyll content was dependent on genotype, with some clones showing a decrease, some an increase, and some no effect. Numerous studies have reported a decrease in chlorophyll content following ozone fumigation, with a smaller number showing an increase (Edwards, 1991). It is however possible that these results reflect differences in developmental stage of the leaf, as Ln+9 is unlikely to represent the same leaf age across all the genotypes, which have been shown to exhibit differing growth rates. In larger individuals, Ln+9 may represent a relatively young leaf, and a relatively old leaf in smaller plants. In light of hypotheses concerning accelerated senescence and resource reallocation, it is plausible that those leaves showing an increase in chlorophyll content

were relatively young and receiving redistributed nitrogen from older, senescing leaves, whilst those showing a decrease were undergoing senescence themselves. An increase in pigment content has previously been demonstrated (Edwards, 1991), and it has been hypothesised that reallocation of nitrogen to the remaining leaves may have a "fertiliser" effect, increasing pigment content and therefore photosynthesis. It is also well established that ozone can result in accelerated senescence and therefore reduced chlorophyll content.

Ideally, plastochron index would be measured on all genotypes to allow an analogous leaf to be selected from each, although this was not feasible in this investigation due to intrinsic variability in height within the population. Alternatively, measurements could have been taken from a number of leaves which would have been more representative of the plant as a whole. Canopy level measurements would serve to provide a more accurate measure of overall ozone effect, although this would also be very difficult in the confines of the chambers.

Leaf expansion

The decrease in relative expansion rate in ozone treated plants is suggestive of a negative impact of ozone on growth of young leaves. It is of note, however, that initial leaf size is higher in the ozone treated group. These results may therefore indicate a positive effect of ozone on growth of young leaves. The lower relative expansion rate seen under ozone treatment may be due to the size of the first unfurled leaf, as expansion rate is related to leaf developmental stage. Those in the ambient group may have been in the phase of maximal expansion rate, whilst the ozone treated group may have attained this stage prior to measurement. Further work could address this hypothesis by measuring leaf expansion rate prior to unfurling. An increase in leaf expansion has been observed previously in

poplar saplings grown in 100 ppb ozone in growth chambers (Mills et al., pers. comm.). Hydroxyl radicals are capable of causing scission of polysaccharide chains (Fry, 1998), and it is possible that ozone-generated hydroxyl radicals may break load-bearing bonds in the cell walls by scission of polysaccharides, causing increased growth in the young leaves of the ozone treated group. An increase in young leaf area would be also consistent with the hypothesis of nutrient reallocation from older, senescing leaves.

Visible damage

Ozone greatly increased the occurrence of visible damage, manifested as small flecks or larger necrotic spots, which has been observed in a range of species (Heggestad, 1959; Berrang et al., 1991; Kargiolaki et al., 1991; Piikki et al., 2004). There was considerable variation in the extent of this damage, with some genotypes showing very little; whilst others had over 90% damaged leaves later in the season. Young leaves typically showed very little damage in comparison to older leaves. This could be a function of the duration of exposure, with young leaves having received a lower dose than older leaves. It has also been demonstrated that the antioxidant status of leaves declines with age, which may have a deleterious effect on ozone detoxification (Guzy & Heath, 1993; Pell et al., 1997; Strohm et al., 1999; Loreto et al., 2001). It is also notable that stomatal conductance was lower in younger leaves, which may limit ozone flux to the underlying tissue.

It is of interest that, although *P. deltoides* had the lowest visible damage scores, 68 genotypes exceeded the visible damage scores of *P. trichocarpa*. This indicates a degree of transgressive segregation for this trait within the population, with accumulation of deleterious alleles from both parents in some genotypes. The variation observed both in the

number of leaves exhibiting damage and also in the size of the lesions renders this population suitable for studying the mechanisms of lesion formation.

A group of plants that formed large necrotic lesions and a group that showed very little visible damage were selected. These were grown in controlled environment chambers and subjected to a 200 ppb acute ozone treatment. This allowed assessment of whether plants resilient or sensitive to chronic ozone show similar patterns under an acute ozone treatment, and provided material for microarray analysis in Chapter 4. It would also be interesting to analyse the concentrations of JA, SA and ethylene in the sensitive and tolerant groups, as these hormones are implicated in mediating the response to ozone.

Leaf abscission

The marked increase in leaf abscission is consistent with previous work (Keller, 1988; Kargiolaki et al., 1991; Karnosky et al., 1996; Piikki et al., 2004; Riikonen et al., 2004), and serves to demonstrate the detrimental effect of ozone on leaf biomass. It is highly likely that such premature leaf fall will result in decreased photosynthetic productivity, and therefore contributes to the decrease in stem diameter. Coleman et al. (1995) commented that ozone sensitivity was directly related to leaf retention and maintenance of photosynthetic productivity. The highly significant genotype and genotype by treatment interaction strongly indicate that the clones are very variable in their abscission rates both in ambient air and in response to ozone. Again, this variation is useful in elucidating the mechanisms of both natural and ozone induced abscission through procedures such as QTL mapping. As ethylene has been shown to regulate the timing of leaf senescence in Arabidopsis (Weaver et al., 1998; Grbic & Bleecker, 1995), differences in ethylene

production may be involved in this case. This could be tested by determining ethylene levels in genotypes with very high and very low abscission.

Stomatal conductance

P. deltoides and *P. trichocarpa* exposed to an acute ozone treatment

The stomatal closure exhibited by both species within 9 hours of treatment is consistent with the decreased stomatal conductance found in numerous other species (Taylor and Dobson, 1989; Pearson and Mansfield, 1993). As the experiment was performed under continuous light, it is likely that stomatal closure was being stimulated by ozone, as light is known to be a major factor in increasing stomatal aperture through both photosynthesis dependent and independent mechanisms (Shimazaki et al., 1986). This is in contrast to data presented by Torsethaugen et al. (1999), who found that ozone specifically inhibited inward-rectifying K^+ channels and therefore stomatal opening. It is therefore likely that the underlying mechanism of decreasing stomatal aperture in response to ozone is interspecifically variable. Three main mechanisms of stomatal closure in response to ozone have been postulated. Decreased photosynthesis caused by ozone treatment could result in an increase in intercellular CO_2. As stomatal aperture has been found to decrease with increasing CO_2 (Broadmeadow et al., 1999; Tricker et al., 2005), this may result in stomatal closure. Alternatively, oxidation of membrane ion channels or damage to the integrity of the membrane could result in leakage of osmotically active solutes, for example K^+ (Dominy and Heath, 1985). This could in turn result in increased guard cell water potential and efflux of water, causing the stomata to close. Third, it has been suggested that ozone-induced stomatal closure shares part of its pathway with the ABA-induced response, both

resulting in increased guard cell calcium and stomatal closure mediated by ROS (Pei et al., 2000). The latter hypothesis suggests that drought and ozone induced stomatal closure may occur through overlapping pathways. It is therefore possible that ozone stress acts as an elicitor of a drought response.

No statistically significant difference in stomatal conductance was found between species in Experiment 1. It is of note, however, that *P. deltoides* has a considerably lower mean stomatal conductance after 3 hours of ozone treatment than *P. trichocarpa*. As the sample size in the first experiment was low, this aspect merited further investigation to decipher whether stomatal sensitivity to ozone does differ between the species. It is clear from the Experiment 2 that *P. deltoides* exhibited a significant decrease in stomatal conductance after a 3 hour treatment with 200 ppb ozone in both mature and developing leaves, whilst *P. trichocarpa* showed no such change. As stomata are known to regulate ozone flux to the mesophyll, it can be hypothesised that *P. trichocarpa* received a higher dose of ozone, resulting in increased sensitivity.

By 24 hours, the stomatal conductance had recovered to near control values in both species. Such acclimation has been observed previously in *Plantago major* (Reiling and Davison, 1995). It is possible that detoxification mechanisms are induced by ozone treatment, and are able to halt oxidation of ion channels and re-establish membrane integrity in the guard cells. Induction of antioxidants has been observed in response to ozone (van Hove et al., 2001), and may therefore be involved in this process. It is also possible that acclimation of photosynthesis occurred, which could result in increased stomatal conductance. Recovery of photosynthesis and stomatal conductance has been observed even with continuing ozone flux in *Plantago major* (Reiling and Davison, 1995) and in radish (Held et al., 1991). Recovery of photosynthesis seems unlikely in this case, particularly for *P. trichocarpa*,

which exhibited increased chlorosis subsequent to the recovery of the stomata, indicating photosynthetic decline. In this species, it also seems unlikely that stomatal recovery is an adaptive response, as the plants continued to sustain damage.

P. deltoides possessed significantly higher stomatal conductance under ambient conditions. It has been found that stomatal density is considerably higher both on the adaxial and abaxial surfaces of *P. deltoides* (Ferris et al., 2002), and it is likely, therefore, that this is a contributing factor. However, differences in stomatal aperture may also be involved. Interestingly, developing leaves of *P. deltoides* had lower stomatal conductance than those of *P. trichocarpa.* This may be due to delayed stomatal initiation in this species, or immaturity of the photosynthetic, signalling or physiological components involved in stomatal opening.

It is of note that developing leaves exhibited considerably lower stomatal conductance than mature leaves in both species, and were also undamaged by ozone treatment. It is possible that lower ozone flux to the tissues contributed to this, although roles for other processes cannot be precluded. For example, developing leaves may possess better antioxidant defences, or may differ in aspects of the signalling pathways leading to cell death.

The stomatal response of *P. deltoides*, *P. trichocarpa* and selected F_2 genotypes to a chronic ozone treatment.

P. deltoides and *P. trichocarpa*

The two parental species exhibited marked differences in both distribution of stomata and in diurnal conductance patterns. *P. deltoides* is an amphistomatous species, whilst *P. trichocarpa* has stomata largely on the abaxial surface, with few on the adaxial surface. It is therefore unsurprising that *P. trichocarpa* showed zero conductance on the adaxial surface. The significant genotype and genotype*time effects are reflective of the finding that *P. trichocarpa* exhibited delayed night-time closure and lower total conductance. It is of note that both species achieved a similar maximum conductance on the lower surface. Delayed night time closure has previously been reported in this species (Snyder et al., 2003), and the underlying mechanisms are currently under investigation (Rodriguez-Acosta, pers. comm.).

For young leaves, no significant effect of ozone on stomatal conductance was found. For *P. deltoides,* there was a trend towards increased stomatal conductance in young leaves under ozone treatment, although this was not statistically significant. Taylor and Dobson (1989) reported a similar result for beech, in which second flush leaves showed an increased conductance. Increased conductance could be explained by reallocation of resources to the young leaves and increased photosynthesis. This may result in decreased C_i and hence stomatal opening. For *P. trichocarpa*, this trend was not seen; rather there is a slight tendency towards stomatal closure.

For semi-mature leaves, ozone significantly decreased stomatal aperture in both species, which is consistent with results from other research (Olsyk & Tibbits, 1981; Ashmore & Onal, 1984; Chevone & Yang, 1985; Taylor & Dobson, 1989; Pearson & Mansfield, 1993; Lethiec et al., 1994; McAinsh et al., 1996; Torsethaugen et al., 1999). This may be due to inhibition of photosynthesis resulting in high C_i and therefore stomatal closure, or due to direct effects on the guard cells as proposed by Toresthaugen et al. (1999). It is interesting to note that there was a negative effect on stomatal conductance outside the hours of ozone fumigation. This could be due to impaired stomatal opening due to inhibition of inward rectifying K+ channels (Torsethaugen et al., 1999), or impaired photosynthesis. It is also possible that the guard cell membranes were damaged by ozone, resulting in perturbation of ion fluxes. For total conductance, there was a significant genotype*treatment*time interaction. This was not a surprising result, as *P. deltoides* closes its stomata at night, and therefore will not exhibit an ozone effect, whilst the effect of ozone continued to be manifested in *P. trichocarpa* after sunset. A decrease in stomatal conductance is likely to have profound implications for CO_2 uptake and therefore carbon gain and productivity.

Sensitive and tolerant F_2 genotypes

Total stomatal conductance in semi-mature leaves was decreased significantly by ozone treatment. Corroborating the results found in *P. deltoides* and *P. trichocarpa*. The absence of a significant effect for sensitivity group or group*treatment interaction indicates that the stomatal conductance of semi-mature leaves showed a similar response to ozone for both groups. The significant genotype effect indicates that the clones had different stomatal conductance values regardless of treatment. The same trend was shown for the abaxial stomatal conductance. For young leaves, there was no significant treatment effect, which

was also similar to the results found for the parental genotypes. It is clear that there are a range of values for the adaxial surfaces, with some genotypes showing zero conductance. This indicates that some individuals have inherited the *P. deltoides*- like amphistomatous phenotype. It would be interesting to measure this in the whole F_2 population to discover whether the trait was quantitatively distributed and under control of a number of genes.

The lack of significant differences between the sensitivity groups gives a good indication that stomatal conductance is not the primary basis of sensitivity determination in these genotypes. Further time points could be included to detect possible effects of time of day, which would be missed by measurements at a single time point. As the leaves of the sensitive group were exhibiting visible damage at the time of measurement, it is possible that conductance differences earlier in the growing season and prior to damage may have had an influence. It would therefore be useful to measure conductance as several points during the ozone treatment.

Selection of sensitive and tolerant genotypes for acute ozone exposure and subsequent microarray analysis

It is evident from the trait data for the sensitive and tolerant genotypes that the selection process successfully reduced the complexity of studying visible damage when compared to *P. deltoides* and *P. trichocarpa*, with no significant difference between sensitivity group observed for any traits except measurements pertaining to visible damage, except for leaf size. This is in contrast to *P. deltoides* and *P. trichocarpa*, which exhibit differences for numerous traits besides visible damage. Removing the influence of other traits is likely to be desirable when studying a single trait, in this case visible damage (Borevitz et al., 2003).

It is of interest that sensitivity group influences the leaf area measurements, with ozone treatment resulting in greater leaf area at both time points in the sensitive group, with the opposite response in the tolerant group. This may indicate that ozone induced damage results in a compensatory response in younger leaves to counter the effects of decreased photosynthetic productivity in the damaged leaves. This result corroborates that for the F_2 population, in which ozone also induced a significant increase in size of the first unfurled leaf.

It is of note that visible damage had no significant influence on stem height and basal diameter, which are important for biomass production. This may indicate that visible damage is not a good marker for overall productivity, although it would be useful to assess this in future seasons or in larger trees. If visible damage had a negative influence on root biomass, productivity in future seasons may be affected.

The significantly greater visible damage seen in the selected sensitive genotypes in response to 9 hr of 200 ppb ozone indicates that amount of visible damage in a chronic treatment is a good indication of sensitivity to an acute treatment. The fact that damage in the sensitive genotypes was generally greater than that seen in *P. trichocarpa* demonstrates transgressive segregation for the response to acute ozone in the F_2 population, and indicates that that the experiment has been successful in identifying genotypes exhibiting a more divergent response to acute ozone treatment than *P. deltoides* and *P. trichocarpa*. This is likely to be of use for further characterising the gene expression profiles pertaining to ozone sensitivity, and is studied in Chapter 4. It is of note that three genotypes exhibited unexpected behaviour, with two tolerant clones showing some visible symptoms (although generally less severe than the sensitive genotypes), and one sensitive clone showing no

symptoms. It is possible that the ozone concentration required to induce visible damage in the tolerant clones was not reached during the chronic exposure, but was exceeded in the acute treatment. This could be of importance when considering selection of a poplar 'ideotype', as trees in a plantation may be exposed to chronic low level exposure with episodic acute exposures. Ideally trees showing resistance to both types of stress should be selected. In the interest of achieving maximum separation between sensitivity groups for transcript profiling, the three most sensitive and three most tolerant genotypes were selected for microarray analysis in Chapter 4.

3.5 Conclusions

The first part of this chapter successfully identified two poplar species, *P. trichocarpa* and *P. deltoides,* with contrasting sensitivity to an acute ozone treatment. This provided a basis for further study on the F_2 mapping population bred from these species, Family 331. The F_2 population were exposed to 100 ppb ozone for 3 months in open-top chambers, and profound effects on numerous physiological traits were identified, including leaf abscission, leaf number and expansion, stem diameter and visible damage. These traits were quantitatively distributed, rendering them amenable to QTL mapping techniques. *P. deltoides* and *P. trichocarpa* were found to differ in their stomatal response to ozone. In particular, *P. deltoides* closed its stomata more rapidly in response to an acute treatment, which may be considered as a determinant of the tolerance seen in this species. Conversely, groups of ozone sensitive and tolerant genotypes of the F_2 population did not show a contrasting stomatal response to chronic ozone fumigation, indicating that it may not be the primary determinant of sensitivity. The chronic exposure identified groups of sensitive and tolerant genotypes, which showed contrasting visible damage symptoms but with little

difference in other traits. In general, these were found to behave in a similar fashion when exposed to an acute ozone treatment, and three sensitive and three tolerant genotypes were selected for future microarray analysis.

Chapter 4: Gene expression analysis of *P. deltoides, P. trichocarpa* and ozone sensitive and tolerant genotypes of Family 331

4.1 Introduction

Ozone enters the leaf through stomata, resulting in production of toxic reactive oxygen species (ROS) (Wohlgemuth et al., 2002). Responses range from accelerated senescence (Kargiolaki et al., 1991; Coleman et al., 1995; Karnosky et al., 1996) and a decrease in growth rate (Karnosky et al., 1996; Reinert et al., 1996; Karnosky et al., 2005), to foliar injury manifested as necrotic lesions analogous to those formed during the hypersensitive response (HR) (Strohm et al., 1999; Langebartels et al., 2002; Wohlgemuth et al., 2002). Concomitant with these symptoms is an up-regulation of defence and stress related genes and compounds (Eckey-Kaltenbach et al., 1994; Conklin and Last, 1995; Matsuyama et al., 2002; Ludwikow et al., 2004), and a down-regulation of photosynthetic components (Conklin and Last, 1995; Glick et al., 1995).

Microarrays provide a high-throughput technique to monitor the expression of many thousands of genes in parallel. They have provided an insight into the genetic basis of diverse processes, such as human disease (Golub et al., 1999; Bittner et al., 2000; Perou et al., 2000) and cell cycle progression (Cho et al., 1998; Spellman et al., 1998; Breyne & Zabeau, 2001). The plant science community has also embraced the technology, and arrays are now available for a number of species, including *Populus*.

Transcript profiles have been produced for plants exposed to a number of biotic and abiotic stresses, including insect damage (Reymond et al., 2000), drought (Seki et al., 2002), and ozone (Matsuyama et al., 2002; Ludvikow et al., 2004; Li et al., 2006). Such studies allow large scale identification of stress responsive genes, and provide a basis for more targeted

analysis. For example, a recent study by Li et al. (2006) identified ozone responsive genes in Arabidopsis ecotypes, and related these to the differences in sensitivity seen between them.

To date, the only study to have produced a transcript profile of ozone stressed trees used a small scale 4600 EST macroarray from adventitious root and leaf libraries, and found a large number of genes to be up- or down-regulated by treatment with ozone alone or in combination with CO_2 (Gupta et al., 2005) These included those involved in cell death, defence and senescence, such as transcripts encoding ACC oxidase and senescence-associated genes.

Poplar is now established as a model tree, and has an expanding array of genomic and genetic resources, including cDNA microarrays from the University of Umeå, the University of Helsinki and recently from the commercial resources, Picme (www.picme.at) and NimbleGen Systems (www.nimblegen.com). A number of mapping populations are also available, four of which are being grown as part of the Popyomics project.

The investigation in Chapter 3 demonstrated highly divergent symptoms in two *Populus* species. *P. trichocarpa* developed necrotic lesions within 9 hours of an acute ozone treatment, while *P. deltoides* remained free of visual symptoms. These phenotypic differences indicate that this is a good model system in which to study the genetic basis of the sensitivity of trees to ozone stress. This experiment sought to provide a transcript profile of ozone stressed trees, with an over-arching aim to provide a list of genes that are differentially expressed between the two species in response to ozone. A recent study by Lee et al. (2006) used microarrays to reveal 120 differentially expressed genes between two

pepper cultivars showing a contrasting response to ozone. Such differentially expressed genes can be considered candidates for causing differential sensitivity. The first part of this chapter focused on the use of a targeted "stress" microarray from the University of Helsinki to probe the response of *P. deltoides* and *P. trichocarpa* to an acute ozone treatment.

Analysis of genotypes exhibiting extreme phenotypes for a trait has been suggested as a method for understanding the genetic basis of the trait in question (Borevitz, 2003). It has been proposed that F_2 genotypes at the extreme tails of a distribution for a particular trait will exhibit greater phenotypic separation than the parents due to transgressive segregation (depicted in Figure 4.1). Also, selecting genotypes on this basis may aid in removal of unwanted variation not specifically associated with the trait. This investigation used microarrays to probe the transcriptional response of two groups of three genotypes of Family 331 exhibiting contrasting sensitivity to acute and chronic ozone stress (identified in Chapter 3) in an effort to decipher further the patterns of gene expression associated with ozone sensitivity or tolerance.

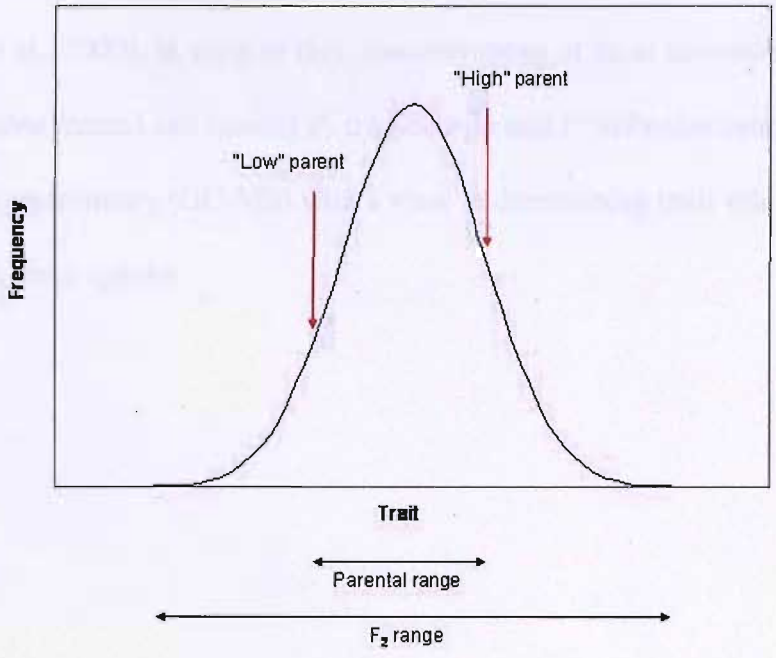

Figure 4.1: Frequency distribution of a normally distributed trait, showing transgressive segregation in an F_2 population. The phenotypic range of the population can be seen to extend beyond that of the parental genotypes.

The transcriptional data generated can also be used in conjunction with QTL mapping with a view to identifying the genes underlying QTL, with genes that are differentially expressed between the grand-parents or sensitivity groups that colocalise to QTL representing candidates for being important in mediating the response. This is covered in Chapter 5.

As transcription represents just one point of regulation in the synthesis of proteins or compounds, direct confirmation of the levels of end-products of a pathway is required before firm conclusions can be drawn concerning their abundance. The phytohormones salicylic acid and jasmonic acid have received considerable attention concerning their role in the response to ozone treatment, with salicylic acid believed to act as a positive regulator of cell death, and jasmonic acid as a negative regulator (Orvar et al., 1997; Rao et al., 2000;

Rao & Davis, 2001). Induction of defence pathways through the action of these hormones has also been proposed to be an important determinant of ozone sensitivity in hybrid poplar (Koch et al., 2000). In view of this, concentrations of these hormones were measured in acute ozone treated and control *P. trichocarpa* and *P. deltoides* using gas chromatography – mass spectrometry (GC-MS) with a view to determining their role in the response to ozone in these species.

4.2 Materials and methods

Experiment 5- Microarray analysis of *P. deltoides* and *P. trichocarpa* exposed to an acute ozone treatment

See Materials and methods in Chapter 3, Experiments 1 and 2 for details of growth of experimental material and ozone exposure

Sampling

One plant of each species was sampled from each chamber, with an additional *P. trichocarpa* sample taken from a randomly chosen chamber, giving a total of 5 replicates for *P. trichocarpa* and 4 for *P. deltoides* for both treated and control. A whole leaf sample of Ln+5 and additional leaves were taken and frozen in liquid N.

RNA extraction and quantification

Total RNA was extracted from Ln+5 of each plant using a modified version of the method described in Chang et al (1993). Spermidine was omitted from the extraction buffer, and 2.67 % β-mercaptoethanol was added. After precipitation, two additional CHISAM extractions were performed. RNA concentration was determined using an Eppendorf Biophotometer (Eppendorf, Hamburg, Germany), and quality was assessed using a 1 % (w/v) agarose gel.

Array design and construction

17 cDNA libraries, with a total of 13838 ESTs, were produced by Brosché et al. (2005) from *P. euphratica* grown in Ein Advat Valley, Israel, and also control and stress exposed trees. The ozone subtractive library is of particular relevance to this investigation, details of which can be found in Brosché et al. (2005).

From these libraries, 8153 ESTs were spotted on poly-lysine slides. It is estimated that there are at least 6340 distinct genes on the array. Spiking and negative controls were sourced and amplified from the Arabidopsis functional genomics control set (http://arabidopsis.info/), and further *C. elegans* controls were also spotted. Further details concerning array production can be found in Brosché et al. (2005), and the EST database and annotation is located at http://sputnik.btk.fi.

Microarray hybridisation

The following steps were performed at the University of Helsinki.

cDNA synthesis

1 µl oligo dT (Invitrogen, Paisley, UK) was added to 25 µg total RNA in 15.5 µl RNase free water. The sample was heated at 65 °C in a heating block for 10 min. The sample was placed on ice for 1 min. A reverse transcription mastermix was prepared, consisting of 6 µl

5X first strand buffer, 3 µl DTT, 3 µl 10X amino-allyl dNTP mix, 0.5 µl Super RNase inhibitor and 1 µl SuperScript III per reaction (all from Invitrogen, Paisley, UK). 13.5 µl mastermix was then added to each sample, and the preparation incubated at 46 °C for 1 hr. 1 µl MMLV-RT RNase H point mutant (Promega, Southampton, UK) was added to each sample, and further incubated for 1 hr. 2 µl fresh 5M NaOH and 8 µl 0.5M EDTA were added and the samples incubated for 15 min at 65 °C to stop the reverse transcription and degrade remaining RNA. The reaction was neutralised with 20 µl 1M HEPES (pH 7.5).

cDNA clean-up using Qiagen PCR purification kit (Qiagen, Crawley, UK)

40 µl water and 500 µl PB were added to each sample and mixed thoroughly using a pipette. The sample was transferred to a QiaQuick column, and centrifuged at maximum speed for 1 min. The flow-through was discarded and 750 µl fresh phosphate –ethanol wash buffer added to the column. The column was centrifuged for 1 min and the flow through discarded. The column was then centrifuged for 1 min and transferred to a labelled 1.5 ml microfuge tube. 30 µl H_2O was added to the column, incubated at room temperature for 1 min and centrifuged for 1 min. A further 20 µl H_2O was added and the column centrifuged for 1 min. The sample was dried in a speed vac (Savant, Minnesota, USA) to 27 µl.

Coupling of Cy dyes to cDNA

A tube of dye ester was resuspended in 73 µl water-free DMSO, and 4.5 µl aliquots made, which were stored at -80°C. 3 µl 1M $NaHCO_3$ (pH 9.3) were added to the cDNA sample. From this point onwards all steps are carried out in minimal light. 4.5 µl Cy-dye

(Amersham, Buckinghamshire, UK) were added to the sample and incubated at room temperature for 1 hr. 4.5 µl 4M hydroxylamine were added to stop the reaction.

Clean-up of labelled cDNA using Qiagen PCR purification kit

The Cy3 and Cy5 reactions were mixed and 22 µl H_2O added. Clean-up was performed according to the manufacturer's protocol. The reaction was then dried in a speed-vac.

Prehybridisation of slides

This was begun during the cDNA synthesis. 1 L prehybridisation solution (5X SSC, 0.1% SDS, 2% BSA) was heated for 30 min at 50 °C in an oven. The position of the spotted area of the slide was marked on the reverse using a diamond pen. The slide was placed in a UV cross-linker (Stratagene, California, USA) set at 90 mJ. The slide was washed for 30 s in 0.1% SDS, 30 s in MQ water and incubated for 3 min in near boiling water. The slide was washed in 95% EtOH for 90 s, and centrifuged for 5 min at 50 g in a bench-top centrifuge. The slide was immediately transferred to a staining dish containing pre-heated prehybridisation solution. The preparation was transferred to an oven and incubated at 50 °C.

Hybridisation

The slide was removed from the prehybridisation solution and washed for 30 s in MQ H_2O and 30 s in 95% EtOH. The slide was centrifuged for 5 min at 50 g in a bench-top

centrifuge. A lifter slip (Erie Scientific, Portsmouth, USA) (pre-washed in 0.1% SDS, MQ H_2O, and EtOH) was placed on the marked area of the slide.

2 µl poly-A, and 48 µl hybridisation buffer 3 (Ambion, Cambridgeshire, UK) were added to the probe and mixed. The probe was denatured by incubation at 96 °C for 2 min, and centrifuged at 15,700 g for 30 s. The probe was then added to the slide adjacent to the lifter slip. Approximately 50 µl MQ H_2O were added to each well in the 10 -capacity hybridisation chamber (Genetix, Hampshire, UK) to maintain humidity, and the slide inserted. The chamber was incubated at 50 °C for 16-18 hr in an oven.

Post-hybridisation washing

All washing steps were performed in coplin staining jars. The slide was gently agitated in wash buffer1 (2X SSC, 0.5% SDS) to remove the lifter slip and transferred to fresh wash buffer 1. The jar was covered with aluminium foil and incubated in an oven for 15 min at 50 °C. The slide was then transferred successively to wash buffer 2 (0.5X SSC, 0.5% SDS) for 15 min at 50 °C, wash buffer 3 (0.5X SSC) at room temperature for 5 min, WB4 (0.2X SSC) at room temperature for 1 min and WB5 (0.06X SSC) at room temperature for 1 min. The slide was transferred immediately to a bench-top centrifuge and centrifuged for 5 min at 50 g.

Array scanning

Arrays were scanned using a ScanArray500 (PerkinElmer Life and Analytical Sciences, Boston, MA). Initially, a line scan was performed on a row of spots at 90 % laser power,

and the Cy3 and Cy5 laser intensities were equalised on the basis of this. The final scan was performed at 5 μm resolution, and the data saved in TIFF format.

Experiment 6- Microarray analysis of sensitive and tolerant genotypes

See Materials and methods in Chapter 3, Experiment 5 for details of growth of experimental material and ozone exposure.

Sampling

Ln+5 of each plant was sampled into liquid nitrogen after 9 hr ozone exposure. The percentage coverage of ozone-induced necrosis was also recorded on each leaf of each plant.

RNA extraction and pooling strategy

RNA extraction was performed using the method described for the grand-parental experiment on 3 tolerant and 3 sensitive clones which were identified as having the most divergent sensitivity. Equal amounts of RNA from the five replicates of each clone for each treatment were pooled to give 100 μg RNA per treatment per clone to be used for cDNA synthesis. The procedure is summarised in Figure 4.2.

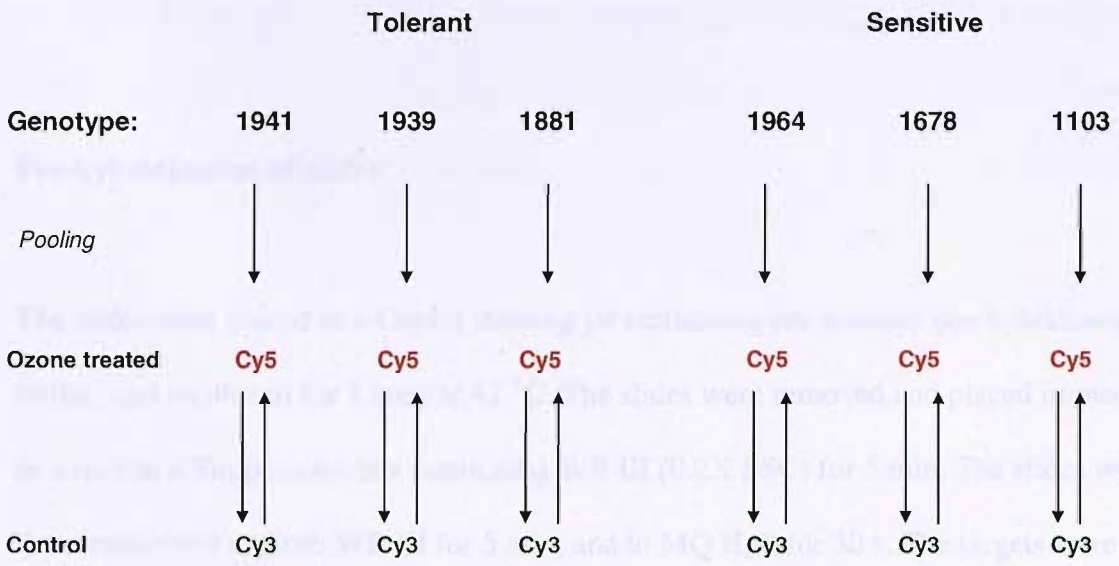

Figure 4.2: A summary of the experimental design for microarray analysis of the response of groups of tolerant and sensitive genotypes to an acute ozone treatment, showing pooling and dye-swap strategies. 5 replicates of each genotype were pooled for each treatment, with the pool constituting a biological replicate.

Microarray production

Microarrays were purchased from Picme (www.picme.at) and consisted of 26915 ESTs spotted on glass slides. The ESTs printed on the PICME poplar arrays were produced by INRA-Nancy (Martin et al.), INRA-Orleans (Leple et al.), and University of Helsinki (Kangasjarvi et al.) within the framework of the LIGNOME and ESTABLISH programme respectively. Further details of array content and production can be found at www.picme.at.

Microarray hybridisation

Preparation of labelled cDNA

This was performed as described in Experiment 5, except 100 μg total RNA were used for each channel.

Pre-hybridisation of slides

The slides were placed in a Coplin staining jar containing pre-warmed pre-hybridisation buffer, and incubated for 1 hour at 42 °C. The slides were removed and placed immediately in a rack in a Tupperware box containing WB III (0.2X SSC) for 5 min. The slides were then transferred to fresh WB III for 5 min, and to MQ H_2O for 30 s. The targets were denatured by placing the slides in boiling water for 1 min, and then transferred to 4 °C ethanol. The slides were then transferred to 50 ml Falcon tubes and immediately centrifuged at 3000 g for 1 min.

Probe preparation

The sample containing the Cy3 labelled sample was dissolved in 25 µl MQ H_2O and 50 µl formamide. The sample was then transferred to the corresponding Cy5 sample and 25 µl Amersham hybridisation buffer added. The combined samples were then vortexed and centrifuged at 15700 g for 1 min. The probe was denatured at 95 °C on a heating block for 1 min. The sample was then placed on ice for 30 s and centrifuged.

Hybridisation and washing

Hybridisation was performed in an HS400 hybridisation station (Tecan, Reading, UK). The slides were washed for 1 min in pre-hybridisation buffer. The prepared probe was then added, and the slides hybridised for 16 hr at 42 °C with low agitation frequency. The slides

were then washed 5 times for 1 min in each of WBI (1X SSC, 0.2% SDS), WBII (0.1X SSC, 0.1% SDS) and WBIII, and then for 1 min in MQ H_2O, and 1 min in 100% EtOH. The slides were dried with nitrogen gas.

Slide scanning

The slides were scanned on a Genetix Aquire scanner (Genetix, Hampshire, UK) at 5 μm resolution. PMT settings were adjusted to equalise the channel intensities.

Microarray data analysis

The following procedures were common to both microarray experiments unless otherwise stated

Spot-finding

The TIFF images were analysed using GenePixPro 5.1 (Axon Instruments, Union City, California). Spots were flagged as "bad" if the median signal intensity was less than 500 or equal to 65535. For the grand-parental experiment, spots were also flagged if less than 150 μm in diameter. Images were also checked manually.

Expression analysis

The data were imported into GeneSpring 7 (Silicon Genetics, Redwood City, CA), with the signal value for each channel corresponding to the median intensity – background intensity for each spot. The results were Lowess normalised, and MA plots were produce in the R

statistical package (http://www.r-project.org/) to check for removal of intensity dependent artefacts. All spots flagged as "bad" were excluded from the analysis. A dye-swap normalisation was applied to the slides in which the dye orientation was reversed.

Partial least squares discriminant analysis (PLS-DA) was performed in the software package SIMCA P (Umetrics Ltd, Windsor, UK). The normalised data were imported and scaled by mean centring. A Variable Importance (VIP) score was generated for each EST on its ability to explain the separation between groups (treatment and species/sensitivity group). The top 50 genes for each experiment were taken to be differentially expressed, and all exceeded a VIP score of 2, as used by Nguyen and Rocke (2002).

Experiment 7- Real-time PCR confirmation of microarray results

Plant material

Real-time PCR was performed on *P. deltoides* and *P. trichocarpa* exposed to 9 hours of 200 ppb ozone or ambient air, as described in Chapter 3, Experiment 1. Four biological replicates were used for each species in each condition. Four technical replicates were performed for each biological sample.

RNA extraction and cDNA synthesis

RNA extraction and cDNA synthesis were performed as described in Experiment 5. Genomic DNA was removed from RNA using the Turbo DNAFree kit (Ambion, Cambridgeshire, UK) according to the manufacturer's protocol.

Primer design and synthesis

Primers were designed from EST sequences represented on the *Populus euphratica* microarray that demonstrated a range of expression patterns in the parental microarray experiment. EST P0000200001G2 (unknown protein) was used as a reference gene as it exhibited consistent expression across all arrays. Beacon Designer (Premier Biosoft, CA, USA) and the Sigma-Genosys Custom Oligo service (Sigma Aldrich, Dorset, UK) were used for primer design and synthesis.

The sequences of forward and reverse primers are shown in Table 4.1.

Gene identifier	Annotation	Primer sequence (5' to 3') *Forward*	*Reverse*
P0000200003B10	Carbonic anhydrase	ACCCTAAGGCATTCGAACCT	GGCAAGCTCGGAGTACAGTC
P0000200006C6	Chlorophyll A/B binding protein	AGGCTGAGCTTGTGAATGGT	CCACTGAGGAGCATTGATGA
P0000200001G2	Unknown protein	GTCAACCTACAACTGTGATTGC	TGCCACAAATGCTCAGACC
P0000400008B9	Peroxidase	ATTTCCACGACTGCTTTGTTC	CAAGGTCAGGTTGGGAAGG
P0000800008B6	SAG-like	CAGTGGGAAGAATTGGAACAAG	GCCTGAAGAGCAGATAGATGG

Table 4.1: The primer sequences (forward and reverse) used for RT-qPCR analysis of four genes showing expression changes in response to 200 ppb ozone treatment. P0000200001G2 (unknown protein) was used as a reference gene. Primers were designed using Beacon Designer from EST sequences present on an 8,000 element *Populus euphratica* microarray.

Real-time PCR

The DyNAmo SYBR Green qRT-PCR kit (Finnzymes, Espoo, Finland) using 96-well polypropylene microplates (MJ Research Inc., MA, USA) was used according to the manufacturer's protocol. 1 µl cDNA was used in a 20 µl reaction volume.

RT-qPCR was performed in a DNA Engine Opticon 2 (GRI, Essex, United Kingdom) using the following protocol.

The plate was first denatured at 95 °C for 30 s. 35 cycles of the following steps were then performed: a denaturation step at 95 °C for 30 s, an annealing step at the temperature appropriate for the primers for 30 s, and an elongation step at 72 °C for 30 s.

Data Analysis

PCR efficiencies and initial transcript abundance were calculated per well for the four biological and four technical repeats using the software LinReg PCR and the method described in Ramakers (2003). Reactions with efficiencies of below 1.8 were removed. The mean of the technical replicates for each biological repeat was calculated and normalised against that of the reference gene, and the expression ratio for the control and ozone treated groups was calculated.

Experiment 8- Quantification of JA and SA concentrations

12 replicates of *P. deltoides* and 12 of *P. trichocarpa* were exposed to 200 ppb ozone or ambient air for 24 hrs. The growth conditions were as described in the Materials and methods section of Chapter 3, Experiment 1. Ln+5 of 4 treated and 4 control plants was sampled at each of 3 time points (3, 9 and 24 hrs). Approximately 0.1 g ground leaf tissue from each sample was transferred to a 2 ml labelled microfuge tube for use in subsequent steps.

The following steps were performed by Matthieu Pinel at the University of Helsinki.

1 ml dichloromethane was added to an aliquot of the ground leaf tissue and mixed for 5 s. 100 ng/µl [^{13}C]SA or 25 ng/µl [1,2^{13}C]JA were added as standards. The preparation was centrifuged at 15,700 g for 5 min in a microcentrifuge. The lower phase was removed from each tube and transferred to 2 ml glass vials. The separation stage was repeated if required. 2 µl 2M trimethylsilyldiazomethane were added, and the sample incubated at room temperature for 30 min.

A 10 µl glass pipette was inserted into a hole in the lid of the glass vial, and a pin connected to a nitrogen cylinder inserted into a second hole. The pressure from the cylinder was slowly increased to 2 bar. The sample was placed in a heating block and heated to 70 °C and left to evaporate completely, then transferred to a 200 °C heating block for 2 min. The preparation was then eluted from the pipette into 1 ml glass vials using 200 µl dichloromethane. This step was repeated for a total of four elutions.The sample was transferred to a speedvac and dried to 100 µl at 37 °C.

Separation was performed on a gas chromatograph (HP 6890, Agilent Technologies, Avondale, PA) on an Rtx-5MS column (Restek Corp., Bellefonte, PA) with a helium flow rate of 1 ml min^{-1}. Detection of SA and JA and the standards was performed by mass spectrometry (HP 5973, Agilent Technologies, Avondale, PA). Data were analysed in Xcalibur 2.0 (Thermo Electron, USA), and the concentration of SA or JA per g fresh tissue calculated.

4.3 Results

Microarray analysis of P. deltoides and P. trichocarpa exposed to an acute ozone treatment (Experiment 5)

Of the 32 arrays hybridised, 19 passed the quality control criteria. Chips were discarded due to having very high background, or absent or very low signal in one or both channels. Examples are shown in Figure 4.3 a and b.

Examination of the example MA plots (Figure 4.3 c and d) shows that Lowess normalised data forms a straight line (4.3 d), indicating no intensity dependence, with an approximately equal number of spots either side of the 1:1 intensity line, indicating that the intensity ratios have been normalised. In contrast, non-normalised data shows both intensity dependence and uneven ratios from the two channels (Figure 4.3 c).

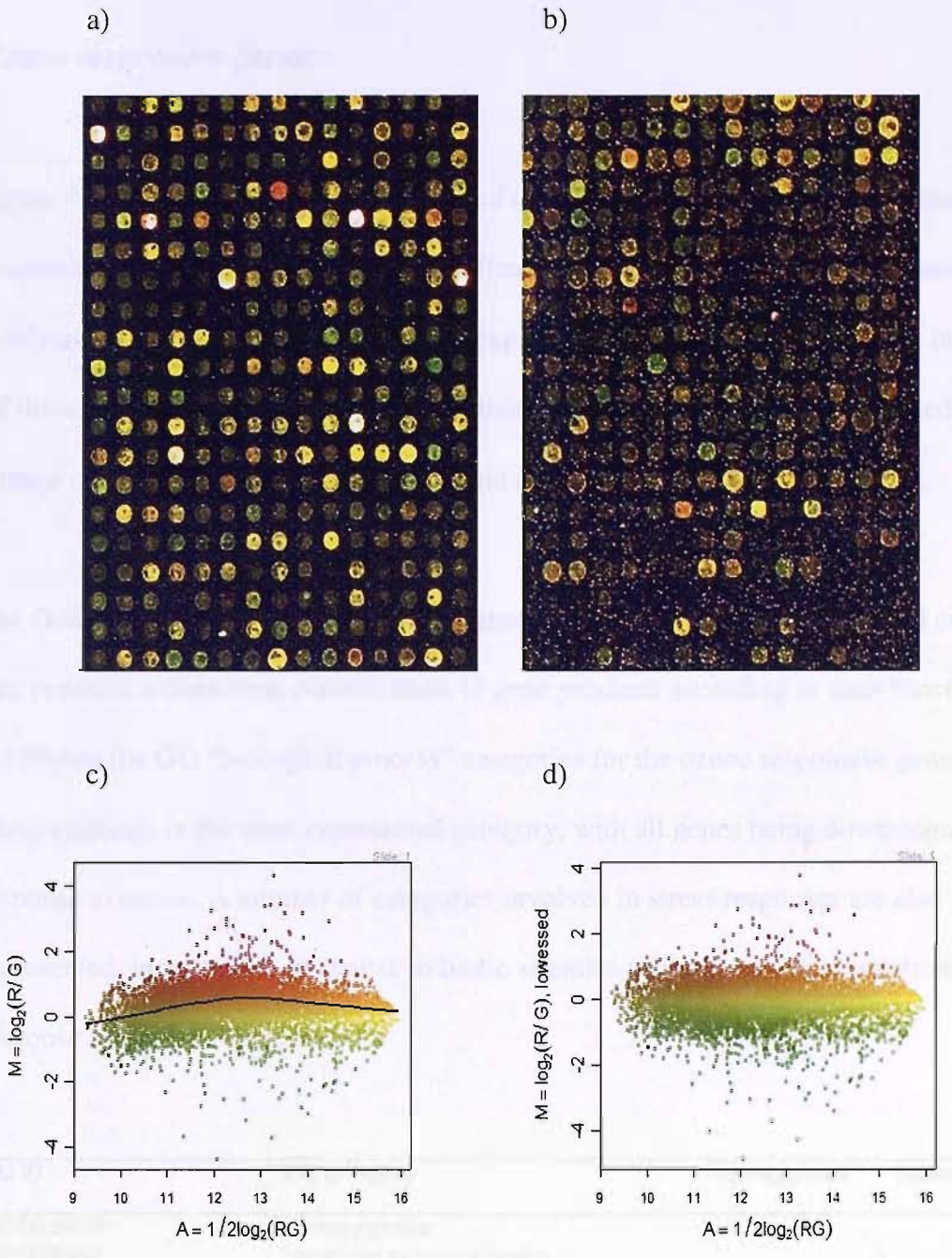

Figure 4.3: A section of an array image with **a**) low background and **b**) high background fluorescence; MA plots showing **c**) pre-normailised data with intensity dependent artefacts and **d**) normalised data.

Ozone responsive genes

Figure 4.8 shows the expression patterns of the 50 genes most influenced by ozone treatment irrespective of species, as identified by Partial Least Squares Discriminant Analysis (PLS-DA). The annotation and expression ratios for these are shown in Table 4.3. Of these, 25 were up-regulated by ozone treatment, and 25 were down-regulated. The fold-change of expression ranged from a 10-fold decrease to 15-fold increase.

The Gene Ontology (GO) project (www.geneontology.org) is an international consortium that provides a consistent classification of gene products according to their functions. Table 4.2 Shows the GO "biological process" categories for the ozone responsive genes. Photosynthesis is the most represented category, with all genes being down-regulated in response to ozone. A number of categories involved in stress responses are also represented; in particular, response to biotic stimulus (all showing up-regulation) and response to oxidative stress.

GO ID	GO category	Up-regulated	Down-regulated
GO:0015979	Photosynthesis		9
GO:0009607	Response to biotic stimulus	5	
GO:0005975	Carbohydrate metabolism	3	2
GO:0006118	Electron transport	3	
GO:0006979	Response to oxidative stress	1	2
GO:0016051	Carbohydrate biosynthesis		2
GO:0015976	Carbon utilisation		2
GO:00096009	Phenylpropanoid metabolism	2	
GO:0009835	Ripening	1	
GO:0006032	Chitin catabolism	1	
GO:0030244	Cellulose biosynthesis	1	
GO:0006006	Glucose metabolism	1	
GO:0006412	Protein biosynthesis	1	
GO:0006950	Response to stress	1	

Table 4.2: Gene Ontology (GO) biological process categories influenced by 9 hrs 200 ppb ozone treatment in *P. deltoides* and *P. trichocarpa*. The species are combined, as the direction of expression change was the same in each.

Gene identifier	Expression ratio		Annotation
	P. deltoides	*P. trichocarpa*	
P0000200005A8	8.268765	4.1723547	glucan endo-1,3-beta-D-glucosidase-like protein
P0000300022A10	8.061784	6.0654716	acidic endochitinase (dbj|BAA21861.1)
P0001000011B7	7.812547	8.150574	dirigent protein, putative
P0000300004G5	5.861146	15.2788315	1,4-benzoquinone reductase-like; Trp repressor binding protein-like
P0000400007F5	5.8605833	11.342267	unknown protein
P0001100010F1	5.653957	13.129352	formate dehydrogenase (FDH)
P0000300003C2	5.2463803	0.8159555	
P0001100012C7	4.868381	4.774026	
P0001100016D5	4.8121896	11.392736	1,4-benzoquinone reductase-like
P0001600003C8	4.755196	3.704584	unknown protein
P0000900011B3	4.597043	2.3544228	ribosomal protein L17 -like protein
P0001100016D4	4.584001	11.502679	
P0000400006B1	4.276353	2.979176	peroxidase
P0001000001H2	4.1972265	3.415427	photoassimilate-responsive protein PAR-1b -like protein
P0000300028G3	3.8119495	3.099152	reversibly glycosylated polypeptide-1
P0001600012E4	3.6947646	6.2310376	unknown protein
P0000400009F11	3.6839018	3.6932113	ABC-type transport protein-like protein
P0001000008H8	3.6315398	4.5403466	cinnamyl-alcohol dehydrogenase ELI3-1
P0001000008C1	3.607712	4.59591	ABC-type transport protein-like protein
P0001000009C2	3.5814638	4.34453	12-oxophytodienoate reductase OPR1 - like protein
P0000300014F6	3.4811344	3.786988	cinnamate-4-hydroxylase
P0001600012C7	3.4454896	4.140734	laccase-like protein
P0000800004H9	3.342137	4.167065	basic chitinase chiB
P0000200001H9	3.2968974	2.371308	putative glutathione S-transferase
P0000400028B2	3.263602	5.661003	6-phosphogluconate dehydrogenase, putative
P0001700001F7	0.2847292	0.8125389	Putative receptor-like serine/threonine kinase
P0000300023C9	0.2823733	0.31479847	Lhca2 protein
P0000100018G12	0.2757348	0.30238062	photosystem II reaction center 6.1KD protein
P0000900013E12	0.2730551	0.35788202	Rubisco activase
P0000100026H10	0.2641881	0.32846394	unknown protein
P0000300023F1	0.258118	0.35121444	Rubisco activase
P0001100015H1	0.2576401	1.0048476	unknown protein
P0000400007G10	0.2539083	0.47941032	peroxidase prxr1
P0000200008C3	0.2430787	0.2852548	Lhcb3 chlorophyll a/b binding protein
P0000200006C6	0.2430655	0.3061822	light-harvesting chlorophyll a/b-binding protein (Cab4)
P0000400040E5	0.2401531	0.33136046	Oxygen-evolving enhancer protein 3 precursor - like protein
P0000300026H8	0.2358436	0.30195463	
P0000400036F12	0.2245901	0.29523084	putative protein 1 photosystem II oxygen-evolving complex
P0001200001G4	0.2061522	0.2784308	chlorophyll a/b-binding protein
P0001100001G4	0.2041947	0.45980567	metallothionein-like protein (AtMT-K)
P0000300021E5	0.1866446	0.21585718	unknown protein
P0000200003B10	0.1588919	0.35827637	carbonic anhydrase, chloroplast precursor
P0001100013F3	0.1541484	0.5249241	unknown protein
P0000300015F1	0.1398324	0.5721612	xyloglucan endo-transglycosylase-like protein
P0000200005H7	0.1387739	0.6951684	xyloglucan endo-transglycosylase-like protein
P0000300025D5	0.1344984	0.6133054	major latex homologue type2
P0000100026G2	0.123462	0.32543984	
P0000900011G3	0.1136813	0.45324314	unknown protein
P0000100025C5	0.1078163	0.30611327	
P0000300033D1	0.1060199	0.4669386	peroxidase prxr1

Table 4.3: 50 ESTs identified as being the most influenced by exposure to 9 hrs 200 ppb ozone by PLS-DA. Blank annotation fields indicate that annotation is currently unavailable. Figures represent the log of the expression ratio (ozone treated : control), and are shown for *P. deltoides* and *P. trichocarpa* separately.

Analysis of biochemical pathways

Following PLS-DA analysis, an overall view of a selection of biochemical pathways in which differentially expressed genes are involved was produced. Figure 4.3 represents the expression patterns of genes involved in photosynthesis. There is a strong overall down-regulation of this category, also with no striking species differences. A large number of genes involved in the phenylpropanoid pathway are represented on the array, with Figure 4.5 depicting their expression patterns. It is clear that the majority of genes involved in this pathway show an up-regulation, with no striking difference between species.

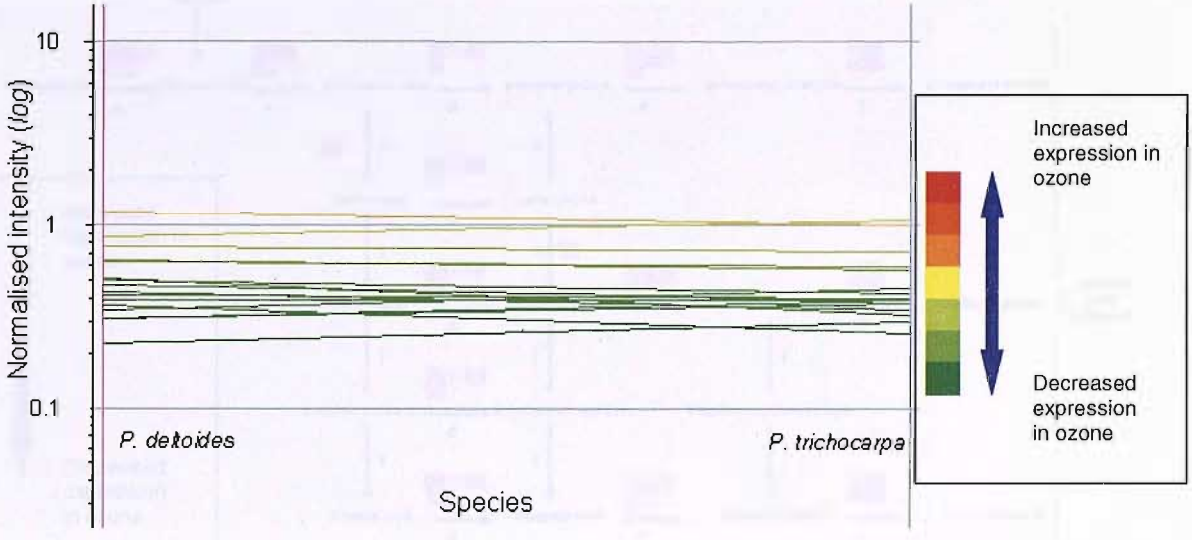

Figure 4.4: The expression ratios (ozone treated/control) of ESTs involved in photosynthesis in *P. deltoides* (d) and *P. trichocarpa* (t) exposed to 200 ppb ozone for 9 hr. Green coloration indicates downregulation in response to ozone, and yellow indicates no change. The results for each species represent an average of replicates from both repeats of the treatment.

P. trichocarpa

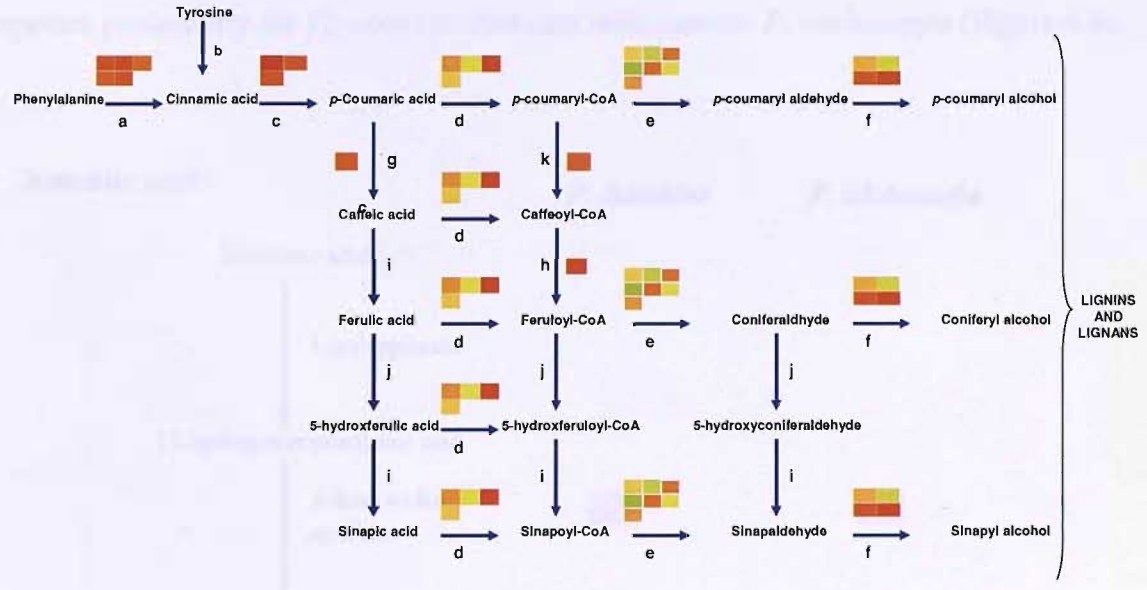

P. deltoides

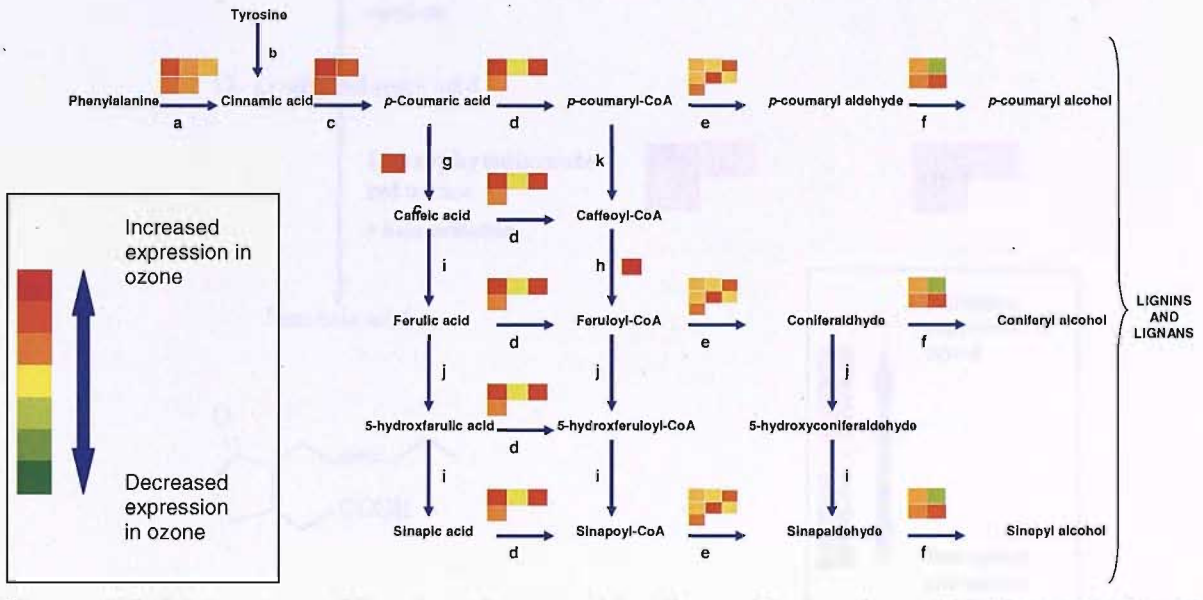

Figure 4.5: Major steps of the phenylpropanoid pathway. Each coloured block represents an EST for a gene encoding an enzyme in the pathway, with red coloration indicating increased expression after 9 hrs 200 ppb ozone treatment, yellow no change, and green decreased expression. **a** Phenylalanine ammonia lyase, **b** Tyrosine ammonia-lyase, **c** Cinnamate-4-hydroxylase, **d** 4-coumarate coA ligase, **e** Cinnamoyl-coA reductase, **f** Cinnamyl alcohol dehydrogenase, **g** *p*-coumarate 3-hydroxylase, **h** caffeoyl-coA *O*-methyltransferase, **i** caffeate *O*-methyltransferase, **j** ferulate 5-hydroxylase, **k** *p*-coumaroyl CoA 3-hydroxlase.

Genes encoding enzymes involved in jasmonic acid synthesis show up-regulation for both species particularly for 12-oxophytodienoate reductase for *P. trichocarpa* (Figure 4.6).

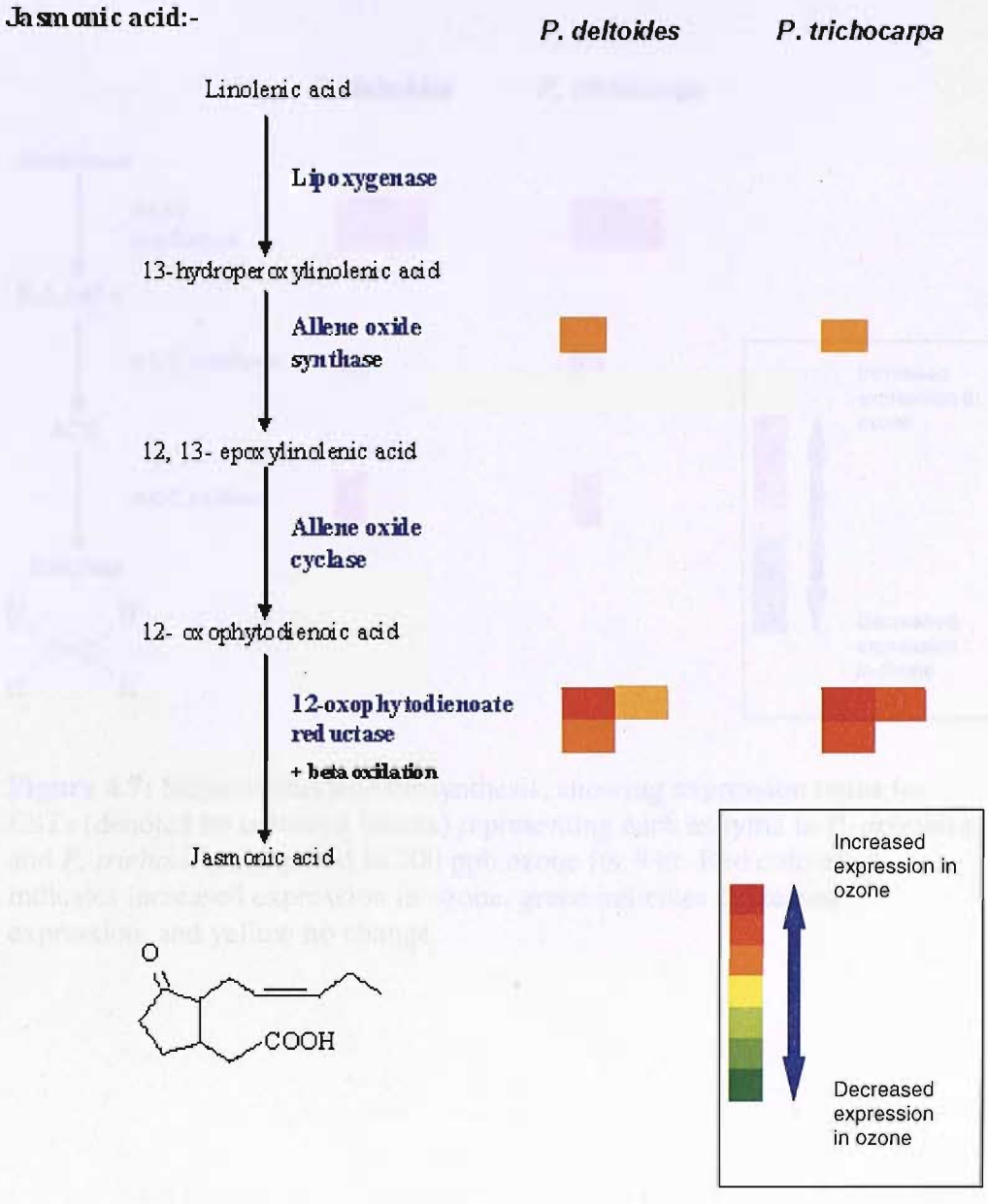

Figure 4.6: Steps of jasmonic acid biosynthesis, showing the expression patterns of ESTs (denoted by coloured blocks) encoding enzymes for *P. deltoides* and *P. trichocarpa* exposed to 200 ppb ozone for 9 hr. Red coloration indicates increased expression in ozone., with yellow indicating no change.

For ethylene biosynthesis (Figure 4.7), *SAM synthetase* shows strong up-regulation for both species. It is notable that the two ESTs for *ACC oxidase* show a very strong increase in expression for *P. trichocarpa*, and less so for *P. deltoides*.

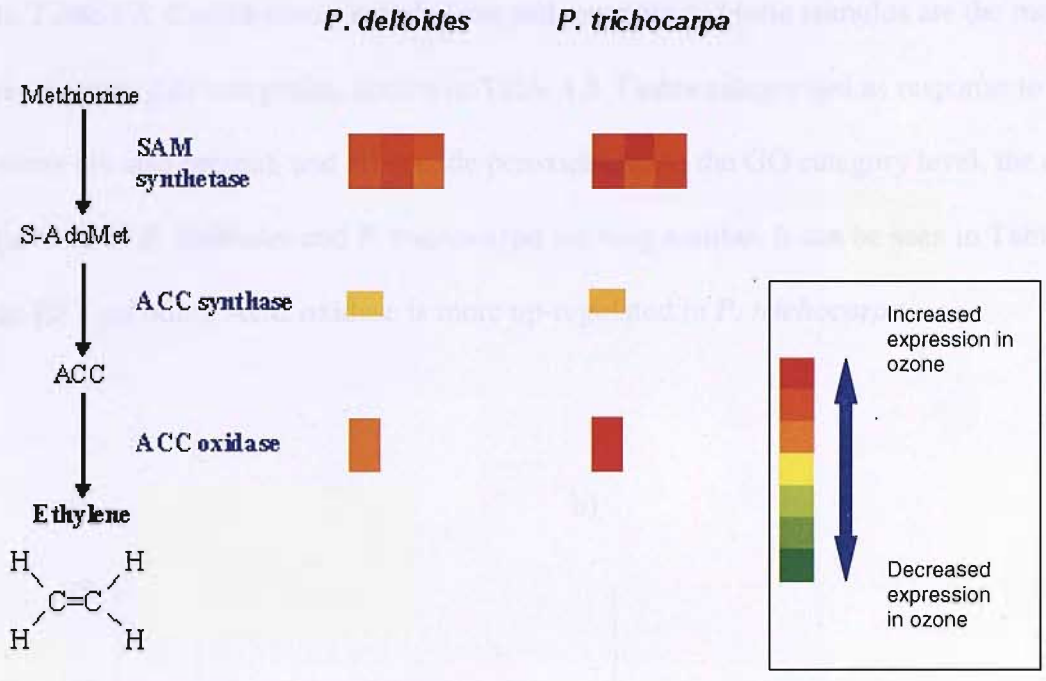

Figure 4.7: Steps of ethylene biosynthesis, showing expression ratios for ESTs (denoted by coloured blocks) representing each enzyme in *P. deltoides* and *P. trichocarpa* exposed to 200 ppb ozone for 9 hr. Red coloration indicates increased expression in ozone, green indicates decreased expression, and yellow no change.

The 50 genes exhibiting the greatest difference in expression patterns between the two species are shown in Figure 4.8, with annotation and expression ratios for each gene shown in Table 4.4. Carbohydrate metabolism and response to biotic stimulus are the most represented GO categories, shown in Table 4.5. Genes categorised as response to oxidative stress are also present, and all encode peroxidases. At the GO category level, the expression patterns of *P. deltoides* and *P. trichocarpa* are very similar. It can be seen in Table 4.4 that an EST encoding ACC oxidase is more up-regulated in *P. trichocarpa.*

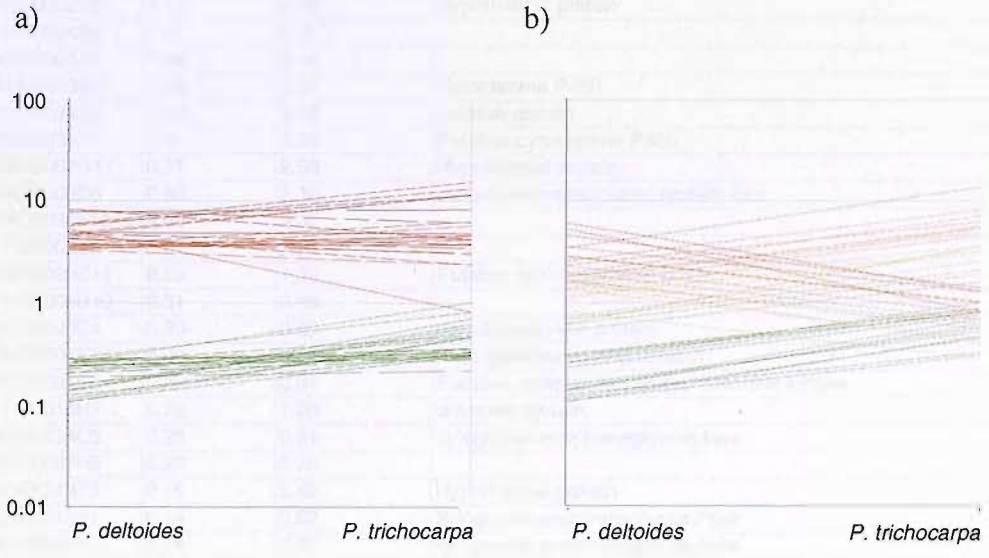

Figure 4.8: Gene expression patterns in *P. deltoides* and *P. trichocarpa* exposed to 200 ppb ozone for 9 hrs in growth chambers. Red coloration indicates up-regulation in elevated ozone, yellow no change, and green down-regulation. The mean expression ratios for *P. deltoides* are shown on the left of each figure and *P. trichocarpa* on the right, with a line joining corresponding genes. a) The 50 genes most influenced by ozone treatment irrespective of sensitivity group; b) the 50 genes showing the greatest differential expression between species. All analysis was performed using PLS-DA on normalised data.

Gene identifier	Expression ratio *P. deltoides*	*P. trichocarpa*	Annotation
P0000400008D12	6.01	1.29	Hypothetical protein
P0000300003C2	5.25	0.82	
P0000900014C3	4.55	1.40	Sinapyl alcohol dehydrogenase
P0001000001B3	3.52	1.29	Pathogenesis-related protein (Fragment)
P0000400005A7	3.45	13.70	probable embryo-abundant protein
P0000800011G8	2.86	1.02	hypothetical protein F19C14.10
P0000900013H6	2.82	1.00	Sinapyl alcohol dehydrogenase
P0000800002F11	2.55	8.16	Kunitz trypsin inhibitor TI3
P0000200004F3	2.32	6.24	NAC domain protein, putative
P0000100020G7	2.28	0.79	light induced protein like
P0000400025G5	2.22	5.87	
P0000300001F12	1.95	0.68	Pollen allergen-like protein
P0000400017F2	1.91	7.13	peroxidase ATP4a
P0001000011E2	1.80	5.35	probable acetone-cyanohydrin lyase
P0000300026C5	1.79	4.89	1-aminocyclopropane-1-carboxylate oxidase
P0000400033B5	1.66	0.55	P0456B03.2 protein
P0000100030C8	1.62	0.61	hypothetical protein
P0000400029A8	1.61	5.72	Peroxidase
P0000200008H5	1.58	0.40	ADR11-2 protein
P0000100014C9	1.55	4.45	Arginine decarboxylase
P0000800005H6	1.39	5.52	hexose transporter - like protein
P0000300022C8	1.36	0.44	Anthocyanin 5-aromatic acyltransferase/benzoyltransferase-like protein
P0001600002H3	1.32	3.65	wound-inducible chitinase homolog win8 precursor
P0000400028H8	1.19	4.68	Hexose transporter
P0001500001B4	1.15	3.14	Jasmonic acid 2
P0001600002H5	1.12	3.40	Hypothetical protein
P0001500004B2	1.07	5.61	
P0000300001A1	1.04	3.02	
P0000300013G1	0.98	0.37	Cytochrome P450
P0001100004G7	0.89	3.26	putative protein
P0000300008F1	0.81	0.28	Putative cytochrome P450
P0000600007G11	0.71	2.53	Hypothetical protein
P0000800008B6	0.68	2.10	senescence-associated protein -like
P0000400036F11	0.62	3.60	
P0001100006E2	0.61	1.91	
P0000400032C11	0.53	1.60	Putative ripening-related protein
P0001100005B10	0.31	0.86	
P0001500003C4	0.30	0.80	polyubiquitin-like protein
P0000400007E10	0.30	0.89	Beta-galactosidase (Lactase)
P0001700001F7	0.28	0.81	Putative receptor-like serine/threonine kinase
P0001100015H1	0.26	1.00	unknown protein
P0000900014C5	0.25	0.81	Xyloglucan endotransglycosylase
P0001100007H8	0.23	0.76	
P0001100013F3	0.15	0.52	Hypothetical protein
P0000300015F1	0.14	0.57	Xyloglucan endotransglycosylase
P0000200005H7	0.14	0.70	Xyloglucan endotransglycosylase
P0000300025D5	0.13	0.61	Putative ripening-related protein
P0000900011G3	0.11	0.45	Hypothetical protein
P0000100025C5	0.11	0.31	Galactinol synthase, isoform GolS-1
P0000300033D1	0.11	0.47	Peroxidase

Table 4.4: The 50 genes identified by PLS-DA as being most differentially expressed between *P. deltoides* and *P. trichocarpa* in response to 9 hrs 200 ppb ozone. Figures represent expression ratio (ozone treated : control), and are sorted by descending expression in *P. deltoides*. Blank annotation fields indicate that annotation is currently unavailable. Expression ratio is on a *log* scale.

GO ID	GO biological process	*P. deltoides* Up-regulated	*P. deltoides* Down-regulated	*P. trichocarpa* Up-regulated	*P. trichocarpa* Down-regulated
GO:0005975	carbohydrate metabolism		4		4
GO:0009607	response to biotic stimulus	4		3	1
GO:0006979	response to oxidative stress	2	1	2	1
GO:0006527	arginine catabolism	1		1	
GO:0015979	photosynthesis	1			1
GO:0016051	carbohydrate biosynthesis		1		1
GO:0005199	structural constituent of cell wall	1			1
GO:0006118	electron transport		1		1
GO:0009813	flavonoid biosynthesis		1		1
GO:0009693	ethylene biosynthesis	1		1	
GO:0008643	carbohydrate transport	1		1	
GO:0006952	defense response	1			1
GO:0006464	protein modification		1		1

Table 4.5: Gene Ontology (GO) categories exhibiting differential expression between *P. deltoides* and *P. trichocarpa* in response to 9 hrs 200 ppb ozone treatment. Figures represent the number of ESTs showing species specific expression patterns in each category, and the number up- and down-regulated in response to ozone.

RT-qPCR confirmation of array results (Experiment 7)

The results presented in Figure 4.9 depict a comparison of the expression ratios from the two replicate array experiments and from RT-qPCR for four genes showing a variety of expression patterns. Congruence between RT-qPCR results is seen for *P. trichocarpa* with qualitative similarity seen in *P. deltoides*, particularly for the genes encoding peroxidase and SAG-like protein. Array results for carbonic anhydrase and chlorophyll A/B binding protein showed distinct variability between array experiments.

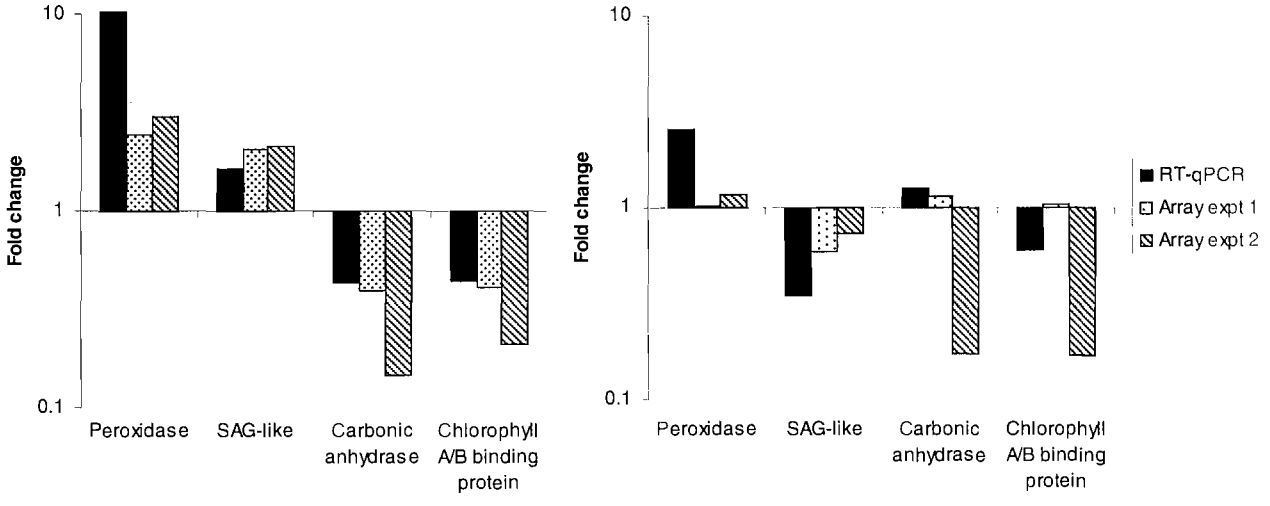

Figure 4.9: Comparison of the expression patterns of 4 genes in two replicate array experiments and RT-qPCR for **a**) *P. trichocarpa* and **b**) *P. deltoides*. Plants were exposed to 200 ppb ozone for 9 hours in all experiments, and LPI 5 was used for analysis. The bars represent a mean of expression ratios (ozone : control) for each species in each experiment. Results were normalised using P0000200001G2 (unknown protein) as a reference gene.

The effect of an acute ozone treatment on levels of JA and SA in P. trichocarpa and P. deltoides (Experiment 8)

Figure 4.10 depicts concentrations of SA and JA achieved in *P. deltoides* and *P. trichocarpa* across 24 hrs exposure to ambient air or 200 ppb ozone. A significant effect of time point was found for SA ($p<0.05$) and this was dependent on treatment ($p<0.05$), with higher concentrations in ozone exposed *P. trichocarpa* at 3 hrs and 24 hrs. Higher concentrations were present in ozone exposed *P. deltoides* at 24 hrs, but also at 9 hrs in those grown in ambient air. A near-significant result for species was found ($p=0.09$), with *P. trichocarpa* containing more SA.

For JA, a significant effect of treatment was found, with an up-regulation seen in elevated ozone. This was also dependent on time-point, and examination of an interaction plot revealed higher concentrations at 24 hrs in particular. No significant effect of species was found, but it is noticeable that ozone treated *P. deltoides* have higher JA levels at all time points, while this is only the case for *P. trichocarpa* at 24 hrs.

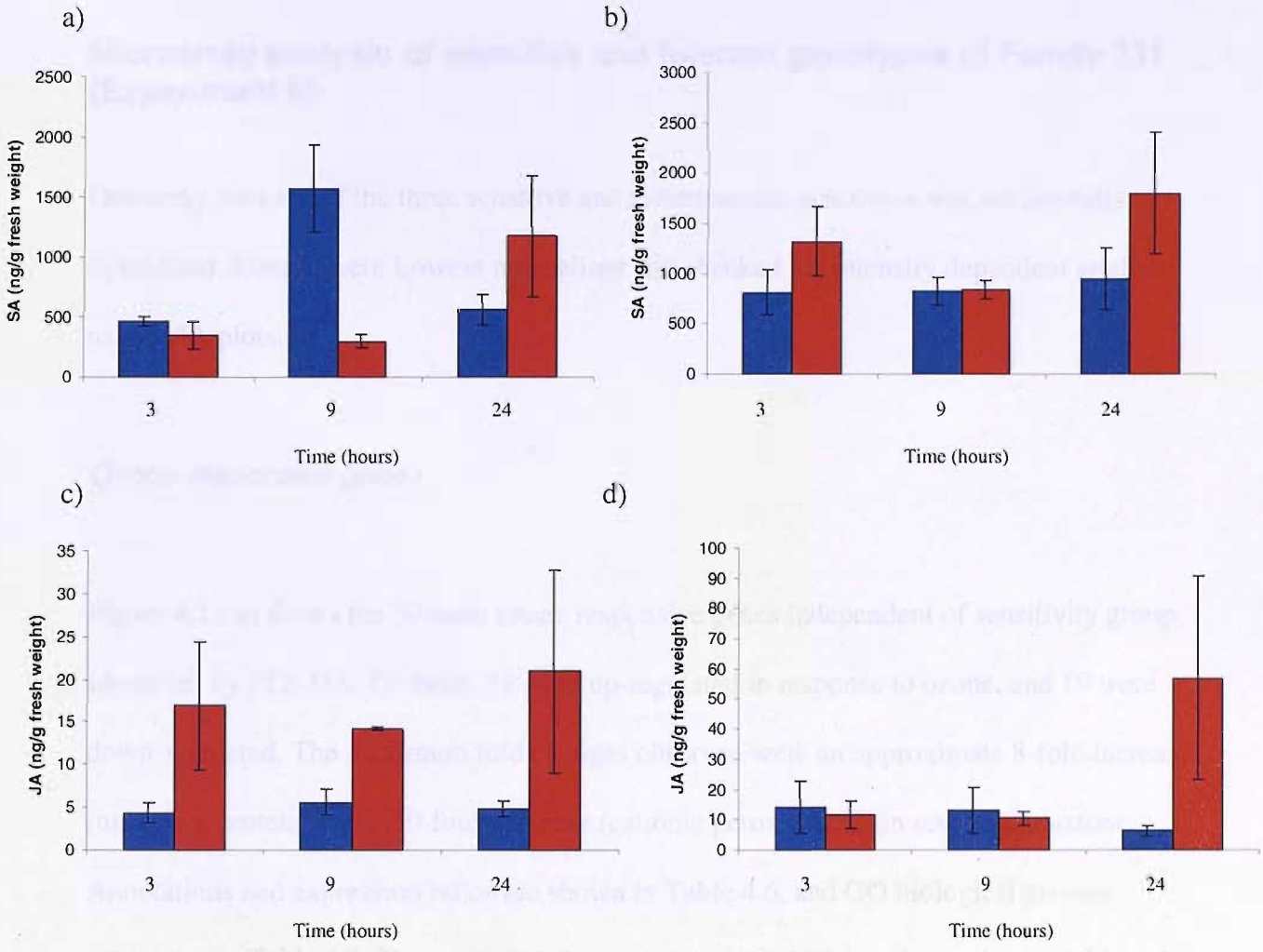

	Species	Treatment	Time point	Species * treatment	Species * time point	Treatment * time point	3-way interaction
Salicylic acid	ns	ns	*	ns	ns	*	ns
Jasmonic acid	ns	*	ns	ns	ns	*	ns

Figure 4.10: Concentrations of salicylic acid (SA) and jasmonic acid (JA) per gram fresh weight of leaf tissue in *P. deltoides* (**a** and **c**) and *P. trichocarpa* (**b** and **d**) exposed to 200 ppb ozone (red) or ambient air (blue) for 24 hours. Sampling points were 3, 9 and 24 hrs. Error bars represent 1 SE. Results of a 3-way general linear model are shown, where **ns** non-significant and * $p<0.05$.

Microarray analysis of sensitive and tolerant genotypes of Family 331 (Experiment 6)

One array for each of the three sensitive and three tolerant genotypes was successfully hybridised. Results were Lowess normalised and checked for intensity dependent artefacts using MA plots.

Ozone responsive genes

Figure 4.11 a) shows the 50 most ozone responsive genes independent of sensitivity group, identified by PLS-DA. Of these, 31 were up-regulated in response to ozone, and 19 were down-regulated. The maximum fold changes observed were an approximate 8-fold increase (unknown protein) and a 10-fold decrease (cationic peroxidase 2) in response to ozone. Annotations and expression ratios are shown in Table 4.6, and GO biological process categories in Table 4.7. The most abundant category is that of protein synthesis and largely consists of ribosomal proteins that are up-regulated. ESTs involved in transport are also well represented, all encoding up-regulated plasma membrane intrinsic proteins. A number of stress-related categories are present in the list, including response to abiotic stimulus, biotic stimulus and oxidative stress. Notably, there are four ESTs encoding metallothionein and all are down-regulated.

Identifier	Expression ratio		Annotation
	Sensitive	Tolerant	
P0000400012B5	8.34	3.06	unknown
P0000800010G1	5.79	2.04	ubiquitin-conjugating enzyme E2 -like protein
R29H08	5.46	2.61	quinone-oxidoreductase QR2
PtaJXT0028C1C0105	5.36	6.56	glyceraldehyde 3-phosphate dehydrogenase, cytosolic
RA01C07	5.29	5.00	osmotin
R55A10	5.06	1.50	glyceraldehyde 3-phosphate dehydrogenase
R76G08	4.89	1.87	60S ribosomal protein L7A
R53G03	4.70	1.75	40S ribosomal protein
R73C03	4.67	1.16	elongation factor-1 alpha 3
R71A10	4.31	1.68	40S ribosomal protein S5
R48B05	4.31	2.03	60S ribosomal protein L10
R70B08	3.79	2.42	glycolytic glyceraldehyde 3-phosphate dehydrogenase
R46D07	3.45	1.51	Kunitz trypsin inhibitor 3
R67B06	3.41	1.78	unknown protein
R13G02	3.31	1.47	plasma membrane intrinsic protein
RSH03E03	3.27	3.20	glutathione S-transferase T3
R68D10	3.18	1.37	40S ribosomal protein S19
R59B05	3.17	1.68	plasma membrane intrinsic protein
R64B05	3.12	2.64	glutathione S-transferase F1
R35C10	3.08	1.68	Kunitz trypsin inhibitor 3
RSH03D09	3.02	1.20	phytosulfokine peptide precursor
RSH01B01	2.96	1.79	40S ribosomal S4 protein
R56F09	2.96	1.64	acidic ribosomal protein P1a
R74D01	2.90	1.77	unknown
RSH03H11	2.63	1.54	ubiquitin extension protein
R50B03	2.62	1.58	ribosomal protein
PtaJXO0019H7H0715	2.58	1.58	plasma membrane intrinsic protein
F11C02	2.48	1.70	60s acidic ribosomal protein P1
R35B07	2.28	4.02	plasma membrane intrinsic protein
RSH11A07	2.04	2.00	unknown protein
RSH14F01	1.98	1.99	60s acidic ribosomal protein P1
P0000100013H11	0.50	0.65	DNA helicase-like
P0001600002D11	0.47	0.27	unknown
P0000100014H7	0.45	0.20	putative GDP-mannose pyrophosphorylase
RSH07A08	0.43	0.52	ribosomal protein S19
R54C11	0.35	0.52	hypothetical protein
P0000300008F11	0.35	1.19	unknown
F03E06	0.30	0.75	hypothetical protein
R50D08	0.28	0.69	hypothetical protein
P0000100023A9	0.26	0.78	unknown
P0001000001H2	0.26	0.49	photoassimilate-responsive protein PAR-1b -like protein
P0000100017A3	0.24	0.70	FRO2-like protein; NADPH oxidase-like
R51F11	0.23	0.61	metallothionein 1a
P0001600002D6	0.22	0.41	unknown
R72D05	0.22	0.58	metallothionein 1a
P0000300006G2	0.21	0.80	unknown
R68G01	0.20	0.32	metallothionein 1a
RA01A11	0.20	0.76	metallothionein 3b
F09C08	0.18	0.35	elicitor-inducible cytochrome P450
R22C10	0.08	0.31	cationic peroxidase 2

Table 4.6: 50 ESTs identified as being the most influenced by exposure to 9 hrs 200 ppb ozone by PLS-DA in two groups of three genotypes showing contrasting sensitivity Figures represent the mean expression ratio (ozone treated : control), and are shown for the sensitive and tolerant groups

GO ID	GO category (biological process)	Up-regulated	Down-regulated
GO:0006412	Protein synthesis	10	1
GO:0009628	Response to abiotic stimulus	2	4
GO:0006810	Transport	4	
GO:0006464	Protein modification	2	
GO:0006979	Response to biotic stimulus	2	
GO:0006118	Electron transport		1
GO:0009058	Biosynthesis		1
GO:0006979	Response to oxidative stress		1
GO:0006006	Glucose metabolism	1	
GO:0008283	Cell proliferation	1	

Table 4.7: Gene Ontology (GO) categories influenced by 9 hrs 200 ppb ozone treatment in two groups of three sensitive and three tolerant F_2 genotypes of family 331. The sensitivity groups are combined, as the direction of expression change was the same in both.

Differential gene expression between sensitivity group

Figure 4.11 shows the 50 genes found to be most differentially expressed between sensitivity group by PLS-DA analysis, with the annotation and expression ratios shown in Table 4.8 It is evident from Figure 4.11 that, in general, greater expression changes were seen in the sensitive group. Table 4.9 shows the GO categories that exhibit differences between sensitivity group, with response to biotic and abiotic stimulus and to oxidative stress being well represented. 8 ESTs annotated as metallothionein show differences, all being more down-regulated in the sensitive group.

Gene identifier	Expression ratio		Annotation
	Sensitive	Tolerant	
P0000400012B5	8.34	3.06	Unknown protein
P0000900010A8	6.73	2.42	Unknown protein
P0000200004C6	5.16	1.88	Unknown protein
R48E11	4.05	1.44	Kunitz trypsin inhibitor 3
P0000600010G11	3.65	0.92	Ripening regulated protein DDTFR18
RSH03H10	3.61	1.54	chalcone synthase
P0001100012D2	3.38	1.55	protein T23E18.4
P0000100018A4	3.32	1.22	Poly(A)-binding protein
R13G02	3.31	1.47	plasma membrane intrinsic protein
P0000400012E5	3.28	1.36	Defender against apoptotic death 1 homolog
R67E04	3.23	1.33	kunitz trypsin inhibitor TI3
R67B05	3.14	1.44	Kunitz trypsin inhibitor 3
R15E12	3.07	1.30	Kunitz trypsin inhibitor 3
P0000300015H1	3.03	1.35	Hypothetical protein
P0001100011G11	3.00	1.23	Unknown protein
Ptajxojxo1E8E0810	2.71	1.24	Adenosylhomocysteinase
P0000200005C5	2.58	0.89	P0005A05.10 protein
R73D10	2.55	1.16	plasma membrane intrinsic protein
PtaJXT0014C11C1105	2.29	1.06	Hypothetical protein
P0000800003F6	2.13	0.89	Skp1
R73G08	2.00	0.52	Lea5 protein
R71B03	1.78	0.57	Lea5 protein
P0000200002D12	0.86	2.02	protein F21J9.28
P0000900008E9	0.42	0.92	Hypothetical protein
Ptac0008D5D0507	0.39	0.85	proline-rich protein
P0001600001C5	0.33	0.81	60S ribosomal protein L30
P0001600002A6	0.33	1.08	Hypothetical protein
P0001100010B9	0.33	0.71	
P0000900008H11	0.33	0.77	Hypothetical protein
PtaJXO0023G2G0214	0.32	0.81	S-adenosylmethionine synthetase
P0001600002G6	0.31	0.80	Similarity to ATP/GTP nucleotide-binding protein
R41G02	0.31	0.73	metallothionein 1a
P0000300023E7	0.30	0.71	
F03A04	0.30	0.70	ribulose-bisphosphate carboxylase small chain
PtaJXT0022E9E0909	0.29	0.62	Tubulin alpha chain
P0001500006H4	0.28	0.63	P0431G06.23 protein
R58G02	0.28	0.74	metallothionein 1a
P0000400021H6	0.28	1.05	Glyceraldehyde 3-phosphate dehydrogenase
P0000900009C7	0.27	0.84	P0677H08.7 protein
R52E11	0.26	0.65	metallothionein 1a
R60G03	0.25	0.60	metallothionein 1a
PtaJXT0025G9G0913	0.25	0.65	Bacterioferritin comigratory protein.
R76G04	0.25	0.62	metallothionein 1a
R41A10	0.25	0.71	hypothetical protein
R51F11	0.23	0.61	metallothionein 1a
R72D05	0.22	0.58	metallothionein 1a
R39A11	0.21	0.47	
PtaXM0026C8C0806	0.19	0.60	Metallothionein-like protein
R06G05	0.18	0.50	peroxidase
PtaC0015E10E1010	0.16	0.46	Similar to peroxidase

Table 4.8: The 50 genes identified by PLS-DA as being most differentially expressed between groups of three sensitive and three tolerant genotypes in response to 9 hrs 200 ppb ozone. Figures represent expression ratio (ozone treated : control), and are sorted by descending expression in the sensitive group.

GO ID	GO biol process	Sensitive		Tolerant	
		Up-regulated	Down-regulated	Up-regulated	Down-regulated
GO:0009628	Response to abiotic stimulus		8		8
GO:0009607	Response to biotic stimulus	4		4	
GO:0006412	protein biosynthesis	1	1	1	1
GO:0006979	Response to oxidative stress		2		2
GO:0006520	Amino acid metabolism		1		1
GO:0006915	apoptosis	1		1	
GO:0009058	Biosynthesis	1		1	
GO:0007010	Cytoskeleton organisation		1		1
GO:0009813	flavonoid biosynthesis	1			1
GO:0000086	G2/M transition of mitotic cell cycle	1			1
GO:0006006	glucose metabolism		1	1	
GO:0015979	photosynthesis		1		1
GO:0006810	Transport	1		1	

Table 4.9: Gene Ontology (GO) categories exhibiting differential expression between groups of three sensitive and three tolerant genotypes of Family 331 in response to 9 hrs 200 ppb ozone treatment. Figures represent the number of ESTs showing species specific expression patterns in each category, and the number up- and down-regulated in response to ozone.

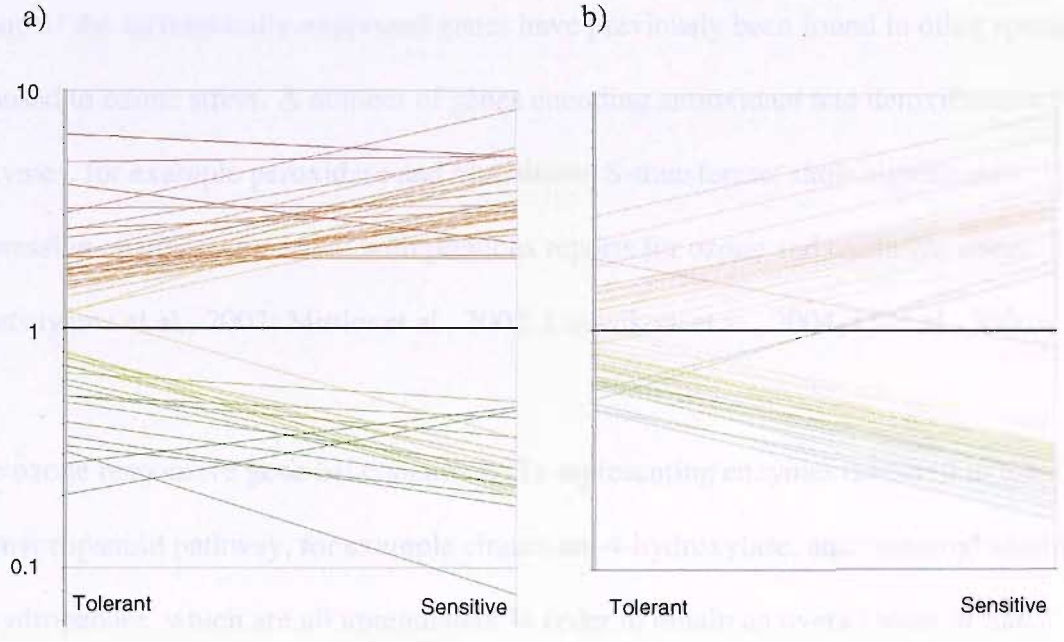

Figure 4.11: Gene expression patterns in groups of three sensitive and three tolerant genotypes of Family 331 exposed to 200 ppb ozone for 9 hrs in growth chambers. Red coloration indicates up-regulation in elevated ozone, yellow no change, and green down-regulation. The mean expression ratios for tolerant genotypes are shown on the left of each figure and sensitive on the right, with a line joining corresponding genes. **a)** The 50 genes most influenced by ozone treatment irrespective of sensitivity group; **b)** The 50 genes showing the greatest differential expression between sensitivity group, as defined by Variable Importance (VIP) score. All analysis was performed using PLS-DA on normalised data.

4.4 Discussion

Ozone responsive genes of P. deltoides and P. trichocarpa

Examination of Figure 4.8 a) and 4.11 a) shows an absence of genes with low fold-changes. This indicates that PLS-DA is effective in identifying treatment responsive genes, and provides a sound alternative to fold change analysis without the associated multiple testing problems of ANOVA. The VIP scores for these genes were all above the cut-off of 2 used by a number of researchers to indicate differential expression (Nguyen & Rocke, 2002; Pérez-Enciso & Tenenhaus, 2003).

Many of the differentially-expressed genes have previously been found in other species exposed to ozone stress. A number of genes encoding antioxidant and detoxification enzymes, for example peroxidase and glutathione S-transferase, show significant expression changes, consistent with previous reports for ozone and oxidative stress (Matsuyama et al., 2002; Mittler et al., 2002; Ludwikow et al., 2004; Li et al., 2006).

The ozone responsive gene list contains ESTs representing enzymes involved in the phenypropanoid pathway, for example cinnamate-4-hydroxylase, and cinnamyl alcohol dehydrogenase, which are all upregulated. In order to obtain an overall view of the pathway, the relevant ESTs, including those not present in the list of differentially expressed genes, were used to annotate the major steps of the pathway. It is clear that there is an overall up-regulation in both species. This is consistent with previous results for ozone stressed plants (Eckey-Kaltenbach et al., 1994; Conklin & Last, 1995; Koch et al., 1998; Paakkonen et al., 1998; Matsuyama et al., 2002; Ludwikow et al., 2004), and has also been found to be a generalised response to abiotic and biotic stress (Dixon and Paiva,

1995). Upon examination of the annotated pathways for the 2 species, it is interesting to note that both exhibit very similar patterns of up-regulation, despite showing great differences in their sensitivity. This indicates that *P. deltoides* was indeed mounting a defence response even though it exhibited no visual symptoms.

The pathway also shows upregulation of cinnamyl alcohol dehydrogenase (*CAD*), which is involved in the synthesis of monolignols (Galliano et al., 1993, Eckey-Kaltenbach et al., 1994). There are conflicting responses in the literature as to whether this leads to increased lignin deposition in ozone stressed plants, with some authors reporting no effect (Bonello et al., 1993; Booker et al., 1996). However, Cabané et al. (2004) reported an increase in the synthesis of condensed lignin in ozone stressed poplar. This has been postulated as a defence mechanism against ozone stress through increase resistance of cells to ROS by thickening of the cell wall. Inspection of the *CAD* ESTs on the pathway indicates *P. deltoides* to have a slightly higher up-regulation than *P. trichocarpa*. This may be a mechanism for increased resistance of *P. deltoides*, although further investigation into lignin content is required to confirm whether such synthesis could take place in the time scale of this experiment.

Previous research has shown a down-regulation of photosynthetic transcripts in response to ozone (Conklin and Last, 1995; Bahl & Kahl, 1995; Glick et al., 1995), leading to a reduction in photosynthetic capacity and premature senescence (Pell & Pearson, 1983; Held et al., 1991; Nie et al., 1993). Genes involved in photosynthesis are well represented on this microarray, encompassing chlorophyll synthesis and the complexes of photosystem I and II. A number of such genes appear in the list of ozone responsive genes, and almost

all show a strong down-regulation, supporting previous findings. Again, these patterns are remarkably consistent between the two species in spite of their contrasting sensitivity.

Hormone biosynthetic genes

Ethylene

Ethylene is recognised as an important mediator of responses to biotic and abiotic stresses (Kende, 1993), and has been found to be induced under ozone treatment (Kangasjärvi et al., 1994; Sandermann, 1996). S-adenosyl-methionine (S-AdoMet) provides the initial substrate for ethylene synthesis, although it is also used in many other biochemical pathways, such as synthesis of polyamines and other stress compounds, and lipid modification (Ravanel et al., 1998). As such, it is believed that conversion of S-AdoMet to 1-aminocyclopropane-1-carboxylic acid represents the first committed step to ethylene biosynthesis (reviewed in Kende, 1993). This investigation demonstrated an up-regulation of *SAM synthetase*, possibly indicating an increase in S-AdoMet synthesis to provide a substrate for synthesis of stress related compounds. *ACC synthase* exhibits a more modest up-regulation in both species, whilst 2 ESTs annotated as *ACC oxidase* show a strong up-regulation in *P. trichocarpa*, but less so in *P. deltoides*. One of these ESTs is present in the list of genes differentially expressed between the species. The strong up-regulation of *ACC oxidase* transcripts may indicate increased ethylene synthesis in *P. trichocarpa*. It is of note, however, that the timing of expression changes in genes involved in ethylene biosynthesis has been found to be temporally variable (Moeder et al., 2002), meaning that *P. deltoides* may have seen a similar up-regulation but at a different point in time. Moeder et al. (2002) also demonstrated a biphasic up-regulation of ACC synthase and ACC oxidase. It is therefore possible that *ACC synthase* may have been strongly up-regulated at

a different time point. This could be resolved by performing RT-qPCR analysis for genes encoding these enzymes on a time-course experiment. As Moeder et al. (2002) demonstrated a necessity for a biphasic induction of ACC oxidase and ACC synthase enzymes for H_2O_2 accumulation and cell death in tomato plants exposed to ozone, these patterns of regulation represent a possible mechanism for the increased cell death seen in *P. trichocarpa*. Further work is required to investigate the temporal differences in expression patterns of the biosynthetic genes for the 2 species, as well as assessing the abundance of the hormone itself. It is also highly likely that there are a number of genes encoding for each enzyme, and Moeder et al. (2002) found that these are differentially regulated during the ozone response in tomato.

Jasmonic acid

Jasmonic acid is involved in induction of stress-related genes, and has been found to be induced in ozone stressed plants, including hybrid poplar (Koch et al., 2000). It has been proposed that JA acts to modulate ozone induced cell death thereby acting antagonistically to SA. These results show an overall up-regulation of genes involved in JA synthesis, particularly for *P. trichocarpa*, which may indicate an increase in JA levels. If *P. trichocarpa* does indeed synthesise more JA, one would expect an attenuation of lesion formation in this species. However, Koch et al. (2000) showed that a sensitive and tolerant clone of hybrid poplar synthesised similar amounts of JA, with the tolerant clone showing insensitivity, as assessed by markers of the JA signalling pathway. This emphasises the importance of hormone perception as well as synthesis. JA sensitivity could be probed in *P. trichocarpa* and *P. deltoides* by analysing the abundance of transcripts specifically induced by JA. Again, it must be noted that a transcriptional up-regulation of biosynthetic enzymes

does not necessarily translate to increased levels of the hormone, and this must be assessed separately.

Salicylic acid

Salicylic acid is also involved in initiating stress gene expression, and is thought to act as a positive regulator of cell death. No ESTs on the Helsinki microarray were found to represent genes involved in its biosynthesis. Due to its potential importance in regulating the ozone response, its levels must be assessed by other means.

Species specific expression patterns between *P. deltoides* and *P. trichocarpa*

An aim of this study was to provide a transcript level comparison between the 2 species, in order to identify candidate genes involved in governing sensitivity. The ozone-responsive pathways detailed above are overall remarkably consistent between the 2 species, which is perhaps surprising considering their highly contrasting response. Similarly, ozone treatment has a very similar effect upon the two species when viewed as up- and down-regulation of GO categories. However, other research has shown such patterns, with only a small subset of genes exhibiting species specific transcript abundance in response to drought stress (Street, pers. comm.).

This study identified the 50 most differentially expressed genes, using PLS-DA. A number of ESTs associated with stress responses were more up-regulated in *P. trichocarpa*, for example those annotated as peroxidase, kunitz trypsin inhibitor, senescence associated

protein and ACC oxidase. This is perhaps unsurprising in view of the greater ozone sensitivity of this species. A notable species specific expression pattern is for *xyloglucan endotransglycosylase (XET)*, with three ESTs that are strongly down-regulated in *P. deltoides*, but only moderately so in *P. trichocarpa*. XETs have been shown to cleave cross-linking glycans in cell walls, and are involved in cell expansion (Fry et al., 1992). A species difference in XET protein levels in response to ozone could be indicative of a differing response of cell expansion and therefore leaf growth. This can be considered in the context of the leaf area measurements discussed in Chapter 3, in which *P. trichocarpa* and the sensitive clones exhibited an increase in area of the first unfurled leaf in response to a chronic ozone treatment, with the opposite response for *P. deltoides* and the tolerant clones. It was hypothesised that damage to semi-mature and mature leaves results in a compensatory response in younger leaves in the sensitive clones, and differences in *XET* expression between the species in this experiment could be an early indication of a difference in the response of leaf growth.

Arginine decarboxylase (ADC) is involved in polyamine biosynthesis, and has been proposed to play a role in tolerance to a number of abiotic stresses, such as salt and chilling (Hao et al., 2005; Legocka & Kluk, 2005). Rowland-Bamford et al. (1989) also found an ADC inhibitor to increase ozone sensitivity in barley. In view of this, it is interesting that *P. trichocarpa* shows greater up-regulation of *ADC2*, but is more sensitive to ozone than *P. deltoides*. However, polyamine synthesis is likely not the only determinant of sensitivity, and it is possible that a sensitive species may possess favourable alleles for genes involved in some pathways governing sensitivity, and deleterious alleles for others. This concept is discussed further in Chapter 5.

Real-time PCR confirmation of array results

For *P. trichocarpa*, the RT-qPCR results strongly corroborate the results for the microarray experiments. This correlation is not as striking for *P. deltoides*. However, the results for the RT-qPCR and microarray experiments are qualitatively similar, and reflect the species specific expression patterns for these genes that were revealed in the analysis of the microarray data.

It is of note that the material used for RT-qPCR was collected from a separate experiment to that used for microarray analysis, and variations between experiments is likely to contribute to anomalous results. In particular, it is noticeable that for ESTs encoding carbonic anhydrase and chlorophyll A/B binding protein, the expression ratios differ considerably between the two microarray experiments themselves.

In conclusion, the results provide support for the microarray data, and confirm the ability of these microarrays to detect species specific expression patterns. The results also indicate that RT-qPCR is an effective means of confirming the validity of microarray data.

Assessment of hormone levels by gas chromatography – mass spectrometry

Jasmonic acid

The gas chromatography mass spectrometry results provided a means to quantify jasmonic acid concentration, and showed a statistically significant increase in JA in ozone stressed

plants, with the increase being dependent on time point. Interestingly, *P. deltoides* showed a considerable increase in JA concentration within 3 hrs, remaining roughly constant for the duration of the experiment. In contrast, *P. trichocarpa* exhibited delayed JA accumulation, and only after 24 hrs do the treated plants show levels above that of controls. Pretreatment with JA has been found to attenuate ozone induced cell death (Orvar et al, 1997), and it has been proposed that JA acts as a negative regulator of lesion formation in a number of species (Orvar et al., 1997; Rao & Davis, 2001). It is therefore possible that the absence of visible symptoms in *P. deltoides* is due to an early increase in JA levels, serving a protective role against ozone. It is of note that *P. trichocarpa* achieved a considerably higher maximum concentration of JA than *P. deltoides*, after 24 hrs of exposure. However, this induction is coincident with lesion formation, and may be the result of a defence response elicited by ozone damage.

These results highlight the potential importance of the temporal dimension of the response to ozone, as the timing of JA accumulation could significantly change its effect. Transient changes in gene expression have also been reported in response to ozone, such as *PAL* and *OMT* (Koch et al, 2000), and it would therefore be of interest to probe the transcriptional response across a time series in *P. deltoides* and *P. trichocarpa*.

Salicylic acid

Salicylic acid is an important compound in the plant defence response, with deficient production resulting in impaired pathogen containment and defence gene induction (Delaney et al., 1994; Sharma and Davis, 1996). It is also believed to act as a positive regulator of ozone induced cell death (Rao and Davis, 2001). This investigation showed a

significant effect of time point on SA levels, which is also dependent on treatment. The highest concentrations in the treated group were found at 24 hrs in both species. It is also of note that high concentrations were also seen at 9 hrs in *P. deltoides*. This is likely to be reflective of the fact that two of the samples were unusable resulting in low replication and high variance.

No significant difference between species was found, indicating that they do not differ in their salicylic acid concentrations when treated with either ozone or ambient air. Therefore, these results do not provide evidence for a role of SA in mediating the contrasting sensitivity of the two species. Nevertheless, this near-significant result, with *P. trichocarpa* containing on average more SA, could merit further investigation, with additional replication, as a potential mechanism for the sensitivity differences seen.

Analysis of F_2 genotypes exhibiting contrasting sensitivity

The work presented in Chapter 3 successfully identified a group of ozone sensitive and a group of tolerant genotypes with greater separation than the grand-parents for ozone-induced visible damage, which were considered as a potential model system for further understanding the genetic mechanisms of lesion formation.

Of the 50 most ozone responsive genes, 11 belong to the protein synthesis GO category. These mainly consist of ribosomal proteins and are generally up-regulated, particularly in the sensitive group. This may be indicative of an increase in overall protein synthesis in response to ozone stress, and could be due to an increased demand for stress-related proteins, and also in order to counter ozone induced protein degradation. Changes in expression of stress-responsive categories (response to abiotic stimulus, biotic stimulus and

oxidative stress) were to be expected, and is consistent with results literature describing similarity between the response to ozone and to pathogens.

It is of note that a number of ESTs of similar annotation are present in the list, in particular those encoding metallothionein and plasma membrane intrinsic proteins. It is possible that there is particularly good coverage of genes encoding these proteins on the array, but it is perhaps more likely that they are ESTs from the same gene, as the collections have not yet been organised into a unigene set. It is probable that this results in over-representation of GO categories with multiple ESTs representing the same gene. Projects are currently underway to organise the EST collections into a unigene set. It is however encouraging that there is consistency between these ESTs in their expression patterns; for example, all those encoding metallothionein are down-regulated. Duplicate ESTs could therefore be considered as technical repeats, and as adding support to the result.

When compared to the results for *P. trichocarpa* and *P. deltoides*, there are some similarities, with representation of genes from stress-related categories appearing in both lists. ESTs encoding peroxidase and kunitz trypsin inhibitor appear in both lists, lending support to their involvement in the response to ozone. Kunitz trypsin inhibitors are protease inhibitors that have previously been found to be induced in heat and drought stress (Ilami et al., 1997; Annamalai et al., 1999), and it seems likely, therefore, that they play a role in the generalised stress response through inhibiting protein degradation. Protein synthesis, the most abundant category in the extreme genotype list, is not represented in the grand-parental list. This may indicate that protein synthesis is more significantly changed in the extreme genotypes, but may also be reflective of the different EST content of the arrays used. The Helsinki array is enriched in stress-related genes, whilst the PICME slides,

although containing the "stress" library, also contain root and shoot libraries. Drawing direct comparisons between the two lists must therefore be treated with caution, and it would be interesting to repeat the grand-parental experiment on the PICME arrays, allowing more effective comparisons to be drawn.

PLS-DA successfully identified a group of 50 genes that were differentially expressed between sensitivity groups. Examination of the expression patterns of these genes reveals that there are larger changes in gene expression in the sensitive group. This may be interpreted as the genotypes in tolerant group not perceiving the ozone treatment as a stress, whilst the sensitive group undergo transcriptional changes associated with a defence response. It is possible that the tolerant species are able to scavenge ROS in the apoplast, and it would be of interest to measure basal levels of antioxidants in each group. As expression changes of a number of genes in response to ozone have been found to be transient, it would be useful to examine gene expression across a time course, as important responses may have been missed by sampling a single time point.

A gene encoding a ripening regulated protein is up-regulated in the sensitive group, but unchanged in the tolerant group. A number of these proteins have been found to be ethylene regulated (Hadfield et al., 2000), raising the possibility that the sensitive group are undergoing an ethylene induced response.

Of interest are two ESTs annotated as Lea5 (late embryogenesis abundant 5), which both show up-regulation in the sensitive group and down-regulation in the tolerant group. This protein has previously been found to be elevated during other abiotic stresses such as salt,

drought, heat and cold stress (Naot et al., 1995; Hwang et al., 2005), and the results presented here provide support for a role in the stress response initiated by ozone.

The plasma membrane intrinsic proteins are a subset of aquaporins that are involved in water transport. More recently, Pastori and Foyer (2002) found that they are able to transport H_2O_2 across the plasma membrane, and may therefore represent an interface between ozone induced ROS production in the apoplast and cytosolic ROS levels. The greater up-regulation for these ESTs in the sensitive group could therefore allow for an increased flux of H_2O_2 into the cytosol and trigger downstream signal transduction pathways.

Examination of the individual genotypes revealed clone 1881, a tolerant genotype, to exhibit greater changes in gene expression than the other tolerant clones. This highlights a disadvantage of using multiple genotypes to form sensitive and tolerant groups, as variability between genotypes is likely to exceed that seen between individuals of the same genotype, which may reduce the likelihood of a statistically significant result. In contrast, the replicates of the grand-parental species used were clonal, and therefore more likely to exhibit a similar response to other individuals of the same genotype. This problem could be circumvented by increasing the size of the sensitive and tolerant groups by identifying additional genotypes, or using several pools of multiple genotypes. However, there is a trade-off between the amount of replication and the degree of separation between the groups. If a larger population was used to screen for ozone sensitivity it would be possible to select additional genotypes and increase the power of the analysis.

4.5 Conclusions

This is the first investigation to use microarray analysis to probe the response of trees to elevated ozone. It has served to demonstrate that similarity exists in the transcriptional response of species exhibiting contrasting sensitivity, but has also successfully identified genes showing differential responses between *P. trichocarpa* and *P.* deltoids, and between groups of tolerant and sensitive F_2 genotypes.

At present, interpretation of the importance and function of these species differences is speculative, and the approach must be combined with other techniques to elucidate this further. A divergent phenotype of parental species is likely to indicate that the mapping population itself will exhibit quantitative variation for the trait, and will thus be suitable for QTL mapping. This technique identifies chromosomal regions important in governing a trait, but these are typically large, often containing hundreds of genes. Alleles at a QTL have previously been found to be differentially expressed (Doebley et al., 1997; Michaels and Amasino, 1999; Cong et al., 2002), and differentially expressed genes which co-locate to QTL can therefore be considered encouraging candidates for being important in mediating the response. The combination of these techniques would therefore serve to identify candidate genes from the transcriptional data, and aid in identification of those genes that play a causative role in the response (Borevitz, 2002). This is the subject of Chapter 5.

Microarrays serve to provide a snap-shot of gene expression at a particular time, and future work could focus on the temporal expression patterns of candidate genes, either through further microarray experiments or RT-qPCR. In order to relate transcript abundance to

levels of proteins and compounds, genomics must be used in conjunction with other techniques, and the growing field of proteomics will aid in elucidating the responses at the protein level. It must also be considered that a candidate gene need not be differentially expressed, and may have alterations in the coding and protein sequence, as has been found for *PHYA* (Maloof et al., 2001).

Chapter 5: QTL mapping and integration of transcriptomic and genetic data

5.1 Introduction

The majority of trait variation in a population is quantitative. Such traits are likely to be under the control of more than one or a few loci, resulting in a complex relationship between genotype and phenotype. QTL mapping is a technique that allows dissection of such quantitative traits, and is capable of identifying multiple loci with a role in trait expression. The technique has been applied to numerous traits and also responses to environmental stresses, for example drought, salinity, ozone and cold stress in rice (Price et al., 1999; Koyama et al., 2001; Andaya et al., 2003, Kim et al., 2004). QTL have also been successfully mapped in *Populus* for growth traits such as stem volume and basal area (Bradshaw et al, 1994) and the response to elevated atmospheric CO_2 (Ferris et al., 2002; Rae et al., in press). The latter studies used a mapping population, Family 331 (Bradshaw et al., 1994), an F_2 pedigree of *P. trichocarpa* clone 93-968 and *P. deltoides* clone ILL 129. These species contrast in their habitat and physiology. This has been a key feature in the success of Family 331 as a mapping population, as for QTL mapping to be possible the trait must segregate in the F_2 population, and this is most likely to occur if the parents exhibit contrasting phenotypes or responses to a treatment. The results presented in Chapter 3, Experiment 1 showed *P. deltoides* and *P. trichocarpa* to exhibit contrasting visible symptoms in response to an acute ozone treatment. On this basis, 164 genotypes of the F_2 population were exposed to a chronic ozone treatment in open-top chambers (detailed in Chapter 3, Experiment 3). Segregation for numerous traits, including those related to growth, senescence, and visible damage, was observed. This chapter has used these data to identify the regions of the genome involved in governing these traits and their response to ozone treatment using QTL mapping.

Although QTL mapping can effectively localise areas of the genome involved in trait expression, these regions are typically large, particularly in trees where production of a very high resolution map, for example through the use of recombinant inbred lines (RILs), is not possible. The confidence interval span of a QTL mapped in Family 331 is typically around 20 cM (Ferris et al., 2002; Street et al., submitted) and will therefore contain many genes. It is clear from this that additional approaches are required to complement these data in an effort to identify the genes underlying the QTL regions. The transcriptional data presented in Chapter 4 provided a list of genes that are differentially-expressed between the grandparents of Family 331, *P. trichocarpa* and *P. deltoides*, and also groups of sensitive and tolerant F_2 genotypes of the population. Such differential-expression may simply be correlated to, rather than causative of, the phenotypic differences, and in isolation microarray analysis is not capable of distinguishing between these possibilities. The power of the above techniques is greatly increased when used in combination, and illustrates the importance of combining genetic and genomic techniques, termed "genetical genomics" (Jansen & Nap, 2001) Alleles underlying QTL have previously been found to exhibit differential expression (Doebley et al., 1997; Cong et al., 2002), and it therefore follows that a gene exhibiting differential expression that also lies within a QTL region represents an encouraging candidate as a gene underlying the QTL region (Borevitz, 2002). It can therefore be seen how microarray profiling could be used to complement QTL mapping to further decipher the genomic elements underlying the response to ozone.

The advent of the genome sequence for *P. trichocarpa* greatly facilitates this approach (http://www.jgi.doe.gov/poplar/), as it allows for alignment of the genetic and physical maps based on genetic markers of known sequence, and therefore the location of the QTL regions on the physical sequence can be found. As the sequences of the ESTs present on

the microarrays used in Chapter 4 are known, those exhibiting species specific expression differences can also be located on the physical sequence and examined for co-location to QTL. This has recently been achieved in a study by Street et al. (in press), which identified candidate genes for drought stress in Family 331 through a combined QTL and microarray approach. Once candidate genes have been identified, their products can be studied in more detail through methods such as knockout studies.

This investigation therefore also seeks to integrate the QTL mapping and transcriptional data to identify specific candidate genes for further investigation. The SSR markers of Family 331 were used to align the physical and genetic maps in order to position QTL on the genome, and assess for co-location to differentially expressed genes identified through microarray analysis.

5.2 Materials and methods

See Materials and methods in Chapters 3 and 4 for details on growth of plant material, trait measurement, and microarray analysis.

QTL mapping

QTL were mapped using a genetic linkage map for Family 331 provided by Tuskan et al. (pers. comm.). The map consisted of 91 SSR markers (genotyped on 350 clones) and 92 AFLP markers (genotyped on 165 clones). Data were first checked for normality using the Anderson-Darling statistic. Non-normal data was transformed using a Box-Cox transformation in Minitab 14. QTL mapping was performed using the out-breeding module of QTL Express (http://qtl.cap.ed.ac.uk, Seaton et al., 2002) with 1000 permutations, and

p=0.05 as the significance threshold. Confidence intervals were calculated as the centimorgan (cM) distance covered by two F values below the maximum F value.

Alignment of the genetic and physical maps and co-location of differentially expressed genes with QTL

The primer sequences for the SSRs on the map (publicly available at http://www.ornl.gov/sci/ipgc/ssr_resource.htm) were located on the physical sequence using the BLAST facility at http://genome.jgi-psf.org. The positions of the SSRs on the genetic and physical maps were converted to ratios, and the linkage groups and chromosomes aligned on the basis of the position of the first and last SSR on each. The 50 most differentially-expressed genes between *P. deltoides* and *P. trichocarpa,* and between the sensitive and tolerant genotypes, were located on the physical sequence using BLAST.

5.3 Results

In total, 58 QTL were identified for 11 traits and were found on all linkage groups except VII and XVI. The individual QTL explained between 1.5 and 16.3 % of phenotypic variance, with the lowest being for basal stem diameter in ozone on LG V(II), and the highest for visible damage in ozone (late season) on linkage group X. The average confidence interval span was 30 cM, with the smallest being 14 cM for visible damage in ozone (late season). All information relating to QTL position and statistics can be found in Table 5.1 and are represented graphically in Figure 5.1.

Trait	C/T/R	LG	Position (cM)	Marker interval	*p* value	PEV
Area of first unfurled leaf	C	VIII(1)	0	p_2607 - o_381a	0.006	12.36
	C	XV	44.2	p_520 - p_2585	0.029	10.15
	R	XIX	13.7	o_277 - AGCGA-19	0.024	9.19
Basal stem diameter	C	X	0.2	p_2571 - CACTG-38	0.004	11.4
	T	III	67.2	o_203 - CACAC-26	0.018	2.32
	T	IV	84.8	p_2826 - CACTG-5	0.003	3.02
	T	V(2)	0	CCCCT-19 - p_2675	0.044	1.51
	T	X	33.2	o_149 - p_2786b	0.038	7.9
	T	XII	23	p_2885 - AGCGA-N3	0.003	2.8
Chlorophyll content	C	I	82	p_93 - p_2889b	0.0011	15
	C	VI	7.2	CTCAG-2 - CCCAT-4	0.004	12.75
	C	VIII(2)	14	CCCCT-N1 - o_202	0.001	11.56
	C	XIV	0.6	CACTG-25 - CCCTC-4	0.019	7.73
	R	V(2)	0	CCCCT-19 - p_2675	0.026	6.81
	R	XI	55	p_2531 - p_204.06	0.042	7.3
	R	XII	0	w_03 - p_495	0.001	12.88
	R	XVII	53	p_2889a - p_2030ab	0.017	9.3
	T	VI	139.2	CCCCT-N11 - o_279	0.043	9.1
	T	VIII(2)	3	CTCAG-N7 - CTCAG-N9	0.004	11.13
	T	X	29.2	p_2887 - o_149	0.03	8.57
	T	XI	36	o_029 - p_2531	0.048	7.45
Height	C	X	0.2	p_2571 - CACTG-39	0.004	11.3
	C	XV	40.2	CACAC-48 - p_520	0.005	10.95
	R	VI	95.2	w_07 - ACCGA-N1	0.003	12.6
	T	X	0.2	p_2571 - CACTG-40	0.043	7.23
	T	XII	24	p_2885 - AGCGA-N4	0.05	6.48
	T	XV	49.2	p_520 - p_2586	0.044	7
Leaf abscission (30d)	C	II	82	p_2797 - p_2766	0.032	8.7
	T	VI	101.2	w_07 - ACCGA-N1	0.013	10.78
	T	X	52.2	o_149 - p_2786b	0.03	8.68
Leaf abscission (70d)	C	X	38.2	o_149 - p_2786b	0.011	11.24
	C	XIX	1.7	CACTG-14 - o_276b	0.007	11.77
	R	IV	6.8	o_349 - t_AG1	0.016	11.12
	T	X	62.2	o_149 - p_2786b	0.021	9.74
	T	XIII	72	CCCTT-N2 - p_2277b	0.05	9.11
Leaf expansion rate	C	XVII	38	p_2889a - p_2030ab	0.014	11.95
	R	XVII	47	p_2889a - p_2030ab	0.02	11.18
	T	XV	40.2	CACAC-48 - p_521	0.02	9.48
Leaf number (30d)	C	X	3.2	p_2571 - CACTG-42	0.032	9.33
	R	VI	95.2	w_07 - ACCGA-N1	0.043	9.27
	T	X	7.2	p_2571 - CACTG-43	0.019	9.48
Leaf number (70d)	C	X	0.2	p_2571 - CACTG-41	0.004	11.64
	R	VI	95.2	w_07 - ACCGA-N1	0.012	13.15
	R	VIII(2)	18	o_127.2 - TCCGT-N14	0.027	5.66
	R	XI	52	p_2531 - p_204.05	0.005	9.56
	T	III	69.2	o_203 - CACAC-26	0.016	9.73
	T	V(1)	48	p_2156 - p_28402	0.01	10.4
	T	VI	109.2	w_07 - ACCGA-N1	0.029	10.71
	T	X	8.2	p_2571 - CACTG-44	0.015	10.05
Visible damage (30d)	T	II	112	o_260 - p_2418	0.036	7.9
	T	XVIII	61.7	o_028a - AGCGA-N9	0.037	6.98
Visible damage (70d)	T	I	117	p_2889b - p_575	0.001	12.65
	T	II	105	o_260 - p_2418	0.013	10.16

T	IV	84.8	p_2826 - CACTG-5	0.001	13.02
T	IX	9	o_023 - AGCGA-22	0.005	8.84
T	VI	0.2	CTCAG-2 - CCCAT-4	0.011	10.09
T	VIII(1)	27	o_381a - p_2610	0.044	6.51
T	X	62.2	o_149 - p_2786b	<.0001	16.33

Table 5.1: QTL mapped for physiological traits using composite interval mapping on 164 genotypes of Family 331 in 100 ppb ozone (T), ambient air (C), and in response to ozone (R), showing linkage group (LG) and centimorgan position (position (cM)), the identifiers of markers flanking the QTL, the statistical significance of the QTL (*p* value) and the percentage phenotypic variance explained by the QTL (PEV). Where traits were measured on two occasions, this is indicated by 30 d (30 days of exposure) or 70 d (70 days of exposure).

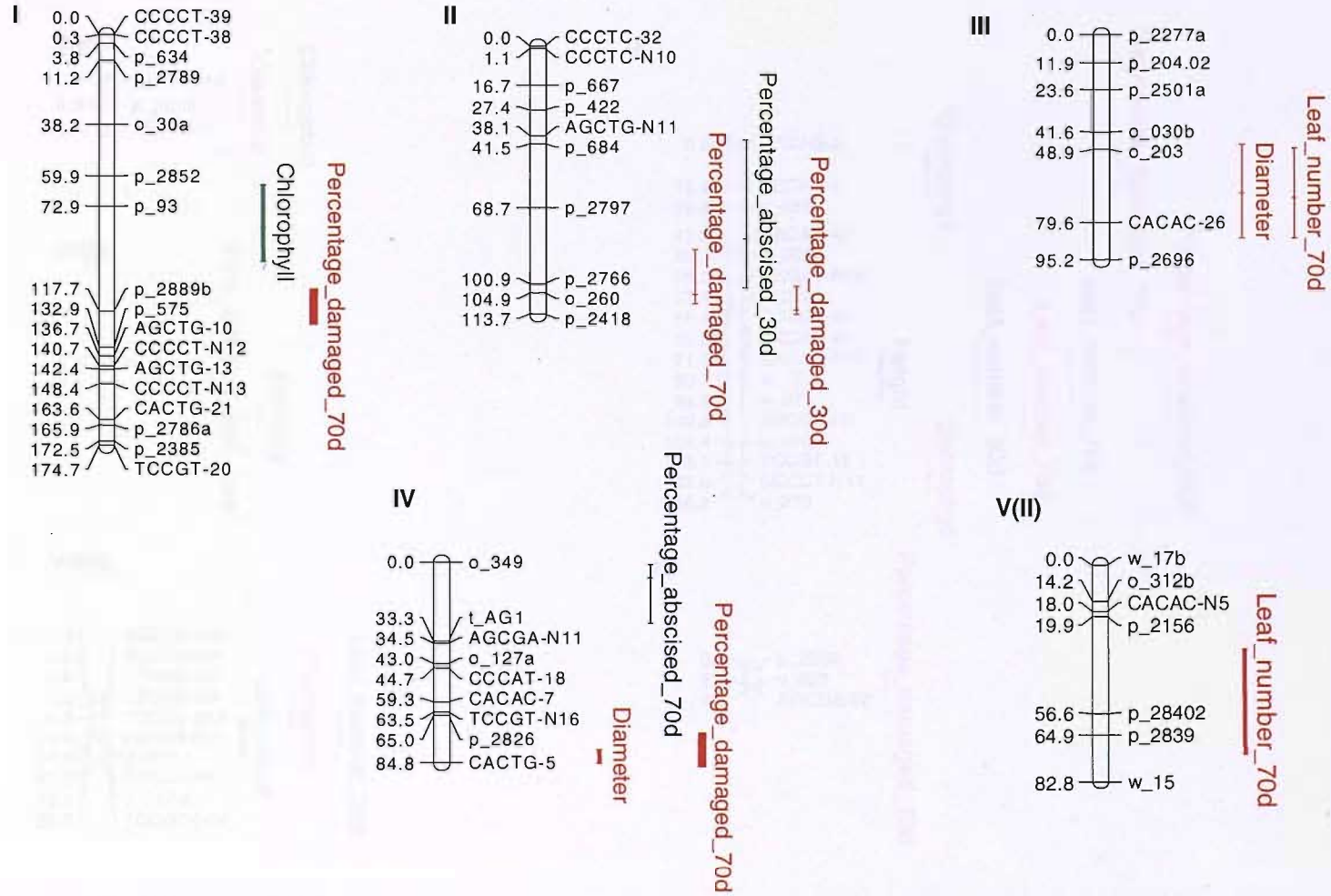

Figure 5.1 a: Location of QTL for traits in ambient air (green), 100 ppb ozone (red), and in response to ozone (blue). Centimorgan (cM) distance is shown on the right of the bars, and the marker names on the left. Confidence intervals represent the cM spread of 2 *F* values from the QTL location. For traits measured on two occasions, this is indicated by 30d (30 days of treatment) and 70d (70 days of treatment). Statisical significance of QTL is represented by thickness of the bars:
$p<0.05$ — $p<0.01$ — $p<0.001$ —

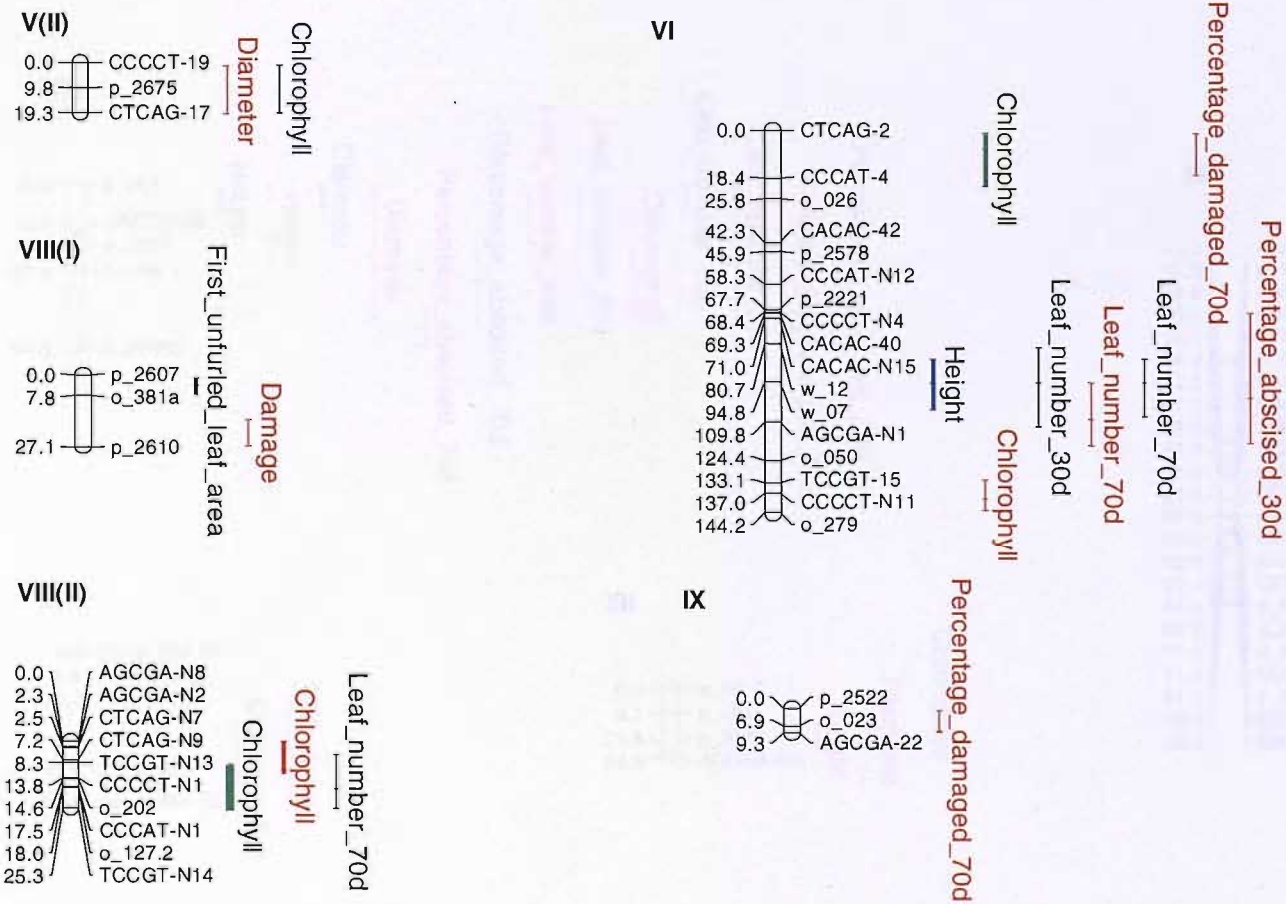

Figure 5.1 b: Location of QTL for traits in ambient air (green), 100 ppb ozone (red), and in response to ozone (blue). Centimorgan (cM) distance is shown on the right of the bars, and the marker names on the left. Confidence intervals represent the cM spread of 2 *F* values from the QTL location. For traits measured on two occasions, this is indicated by 30d (30 days of treatment) and 70d (70 days of treatment). Statisical significance of QTL is represented by thickness of the bars:
$p<0.05$ — $p<0.01$ — $p<0.001$ —

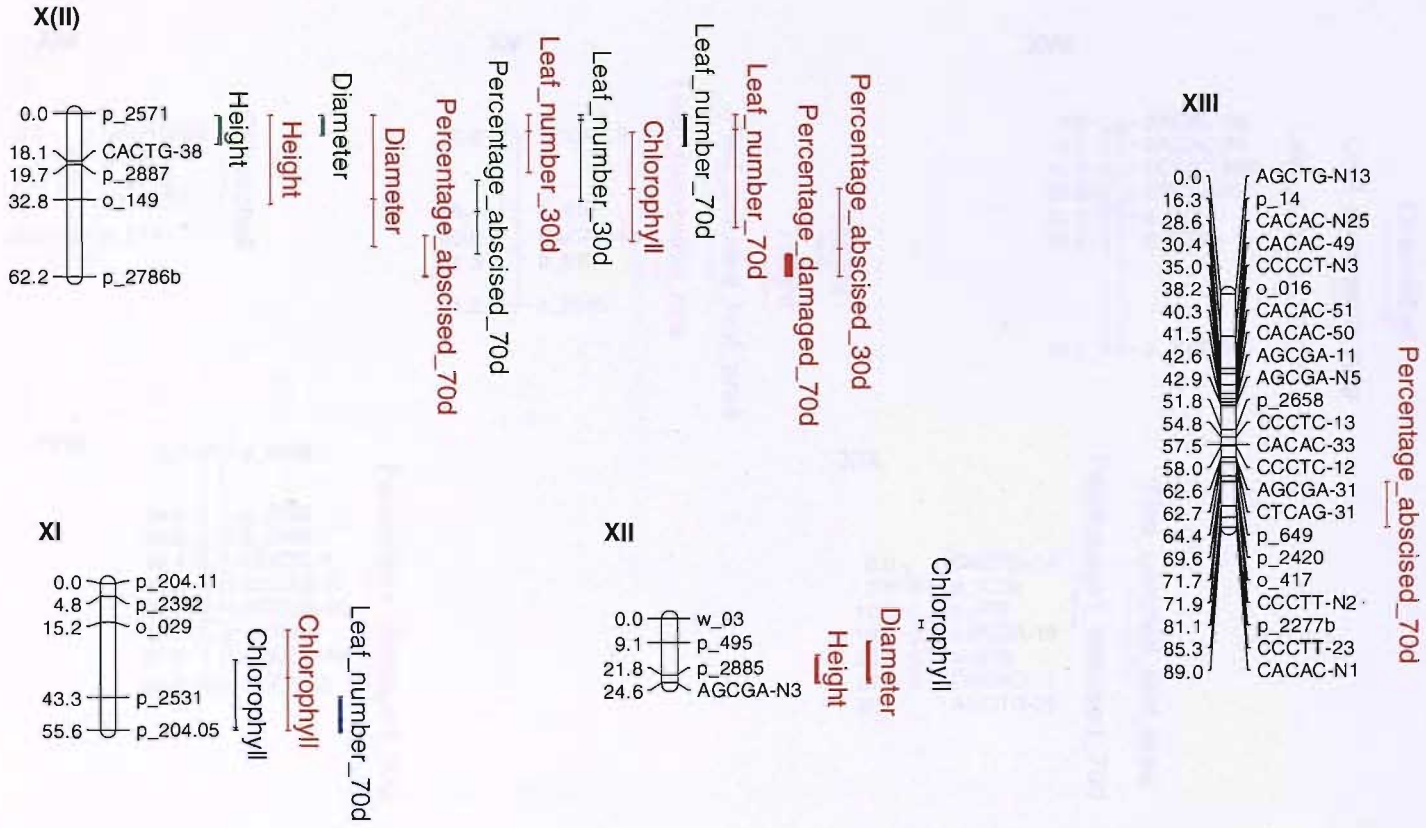

Figure 5.1 c: Location of QTL for traits in ambient air (green), 100 ppb ozone (red), and in response to ozone (blue). Centimorgan (cM) distance is shown on the right of the bars, and the marker names on the left. Confidence intervals represent the cM spread of 2 *F* values from the QTL location. For traits measured on two occasions, this is indicated by 30d (30 days of treatment) and 70d (70 days of treatment). Statisical significance of QTL is represented by thickness of the bars:
$p<0.05$ — $p<0.01$ — $p<0.001$ —

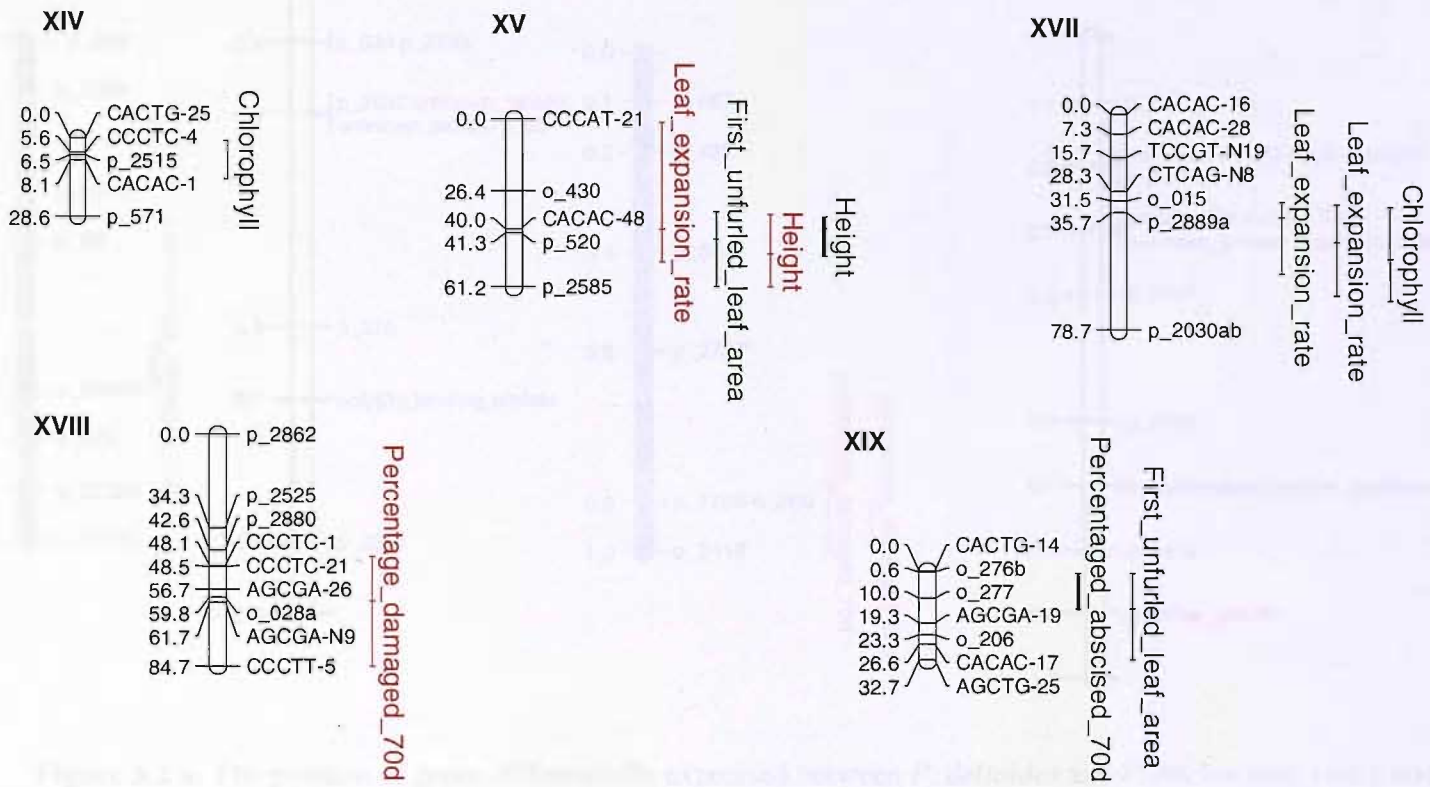

Figure 5.1 d: Location of QTL for traits in ambient air (green), 100 ppb ozone (red), and in response to ozone (blue). Centimorgan (cM) distance is shown on the right of the bars, and the marker names on the left. Confidence intervals represent the cM spread of 2 *F* values from the QTL location. For traits measured on two occasions, this is indicated by 30d (30 days of treatment) and 70d (70 days of treatment). Statisical significance of QTL is represented by thickness of the bars:
$p<0.05$ — $p<0.01$ — $p<0.001$ —

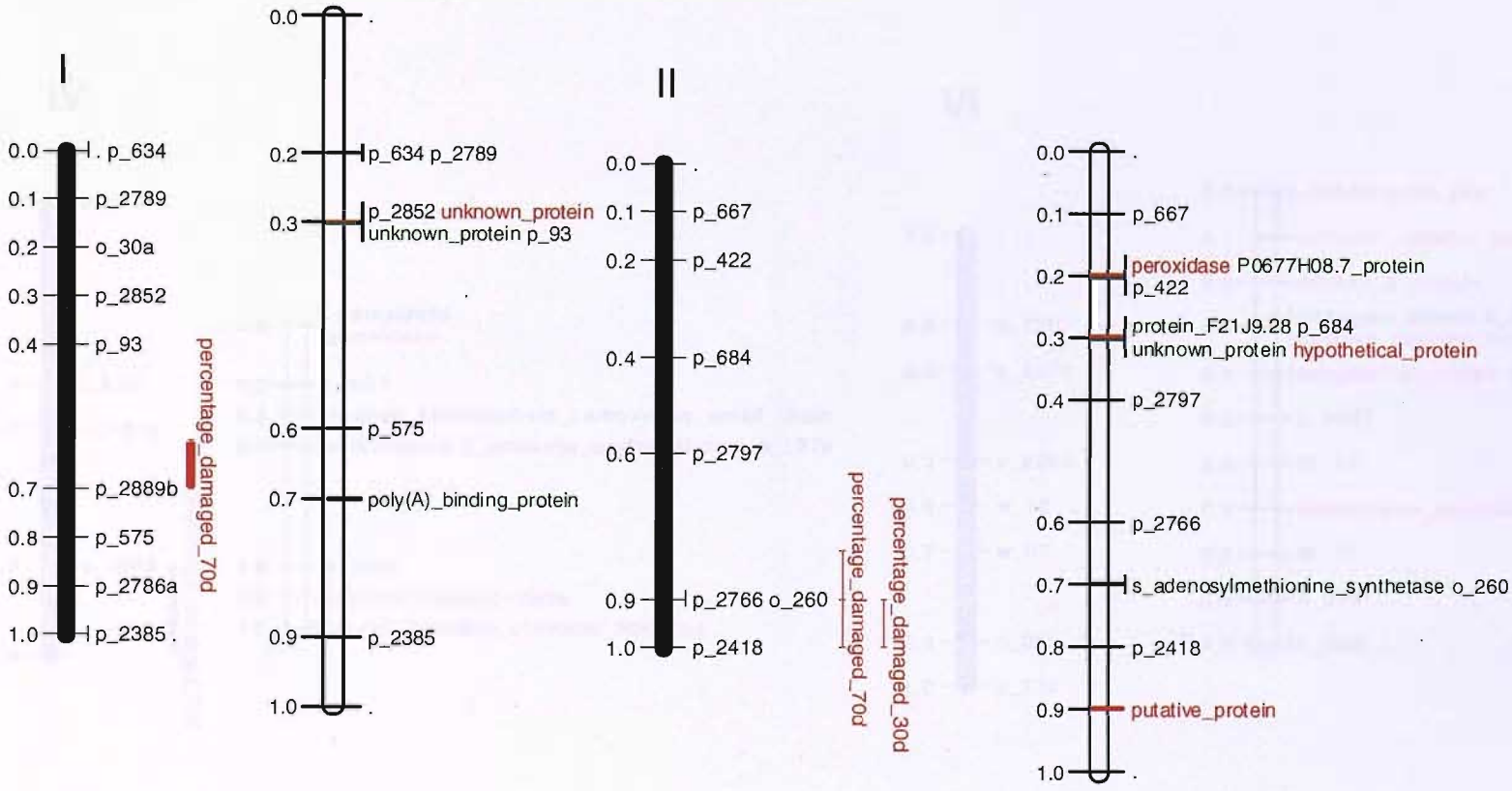

Figure 5.2 a: The position of genes differentially expressed between *P. deltoides* and *P. trichocarpa* (red), and between sensitive and tolerant genotypes of Family 331 (green) relative to QTL for visible damage on the genetic map. Linkage groups are represented by black bars, and chromosomes by white bars. The physical and genetic maps were aligned using the first and last SSR primer sequence that could be located on the physical map. SSR identifiers and their ratio position on the linkage group and chromosome are shown in black. Differentially expressed genes were identified through microarray analysis of plants exposed to 9 hrs 200 ppb ozone, and QTL were identified from a 100 ppb exposure of 164 genotypes of Family 331 in open-top chambers. Statisical significance of QTL is represented by thickness of the bars: $p<0.05$— $p<0.01$— $p<0.001$—

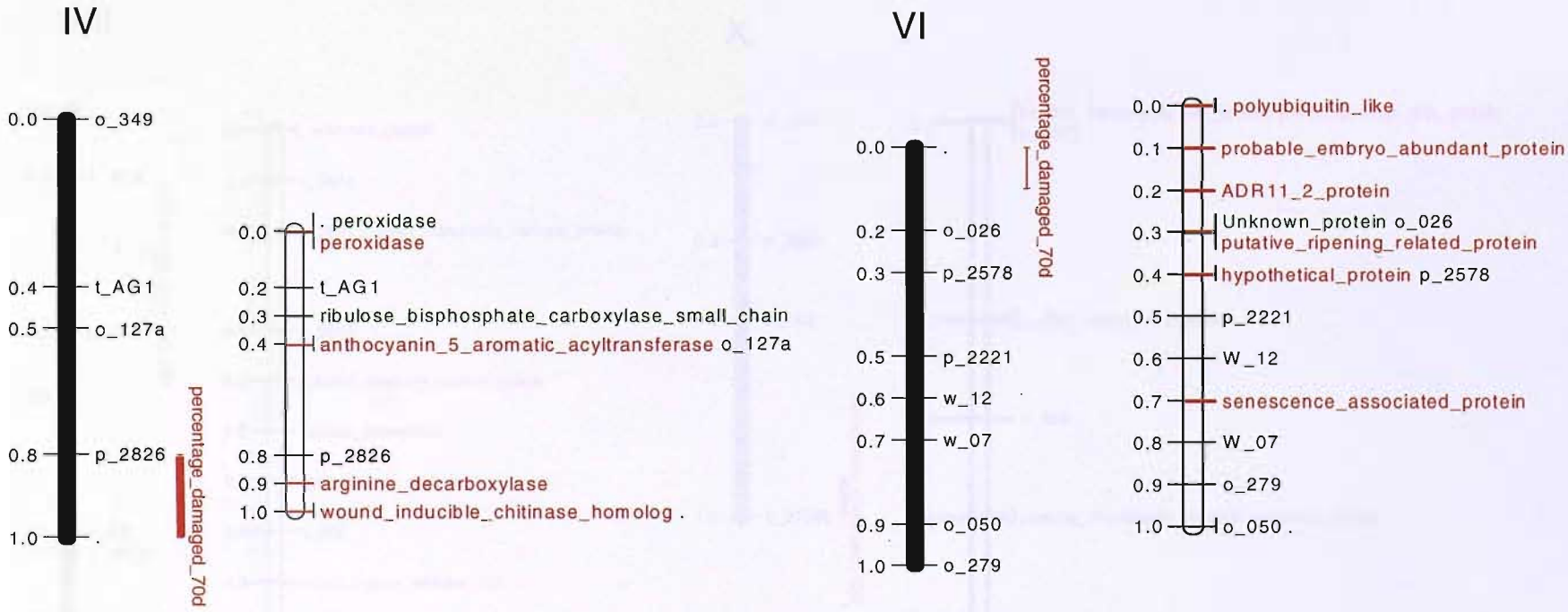

Figure 5.2 b: The position of genes differentially expressed between *P. deltoides* and *P. trichocarpa* (red), and between sensitive and tolerant genotypes of Family 331 (green) relative to QTL for visible damage on the genetic map. Linkage groups are represented by black bars, and chromosomes by white bars. The physical and genetic maps were aligned using the first and last SSR primer sequence that could be located on the physical map. SSR identifiers and their ratio position on the linkage group and chromosome are shown in black. Differentially expressed genes were identified through microarray analysis of plants exposed to 9 hrs 200 ppb ozone, and QTL were identified from a 100 ppb exposure of 164 genotypes of Family 331 in open-top chambers. Statisical significance of QTL is represented by thickness of the bars: $p<0.05$— $p<0.01$— $p<0.001$—

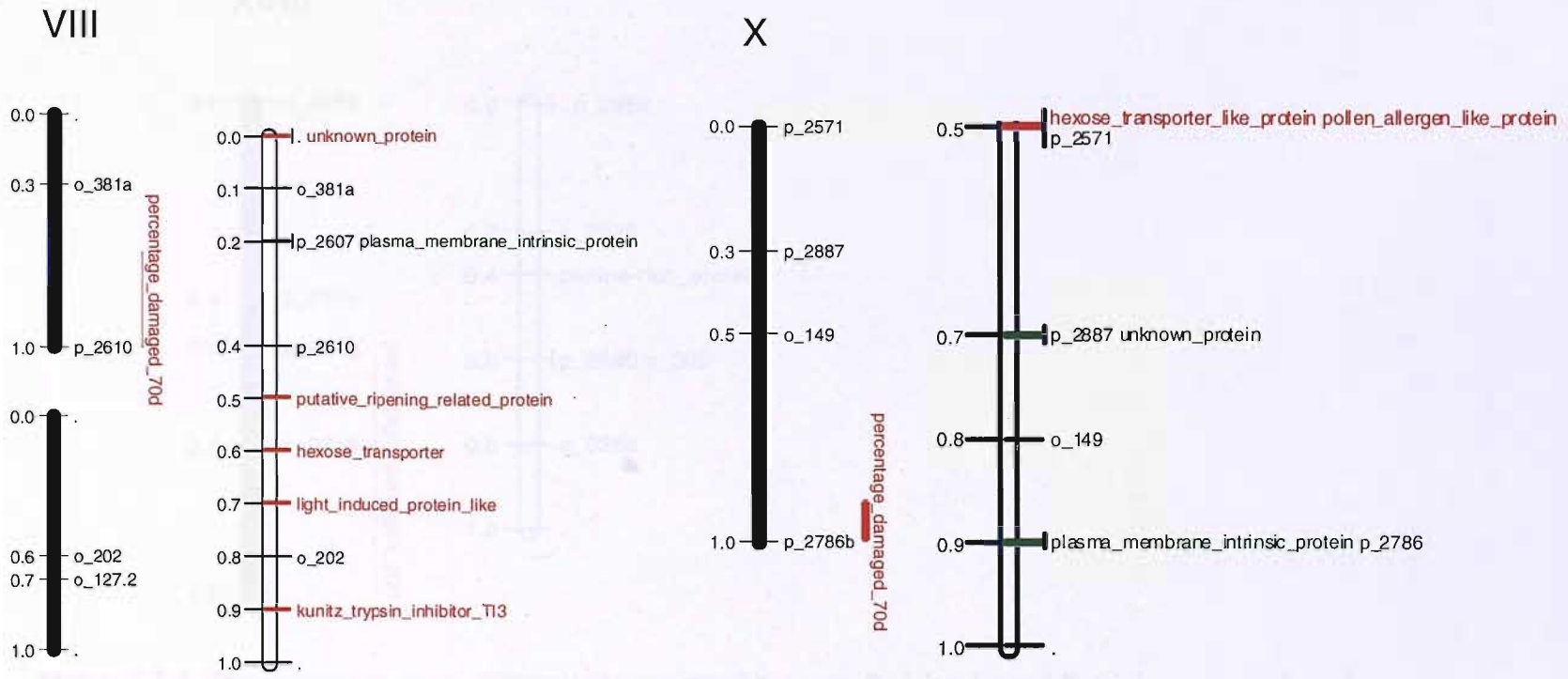

Figure 5.2 c: The position of genes differentially expressed between *P. deltoides* and *P. trichocarpa* (red), and between sensitive and tolerant genotypes of Family 331 (green) relative to QTL for visible damage on the genetic map. Linkage groups are represented by black bars, and chromosomes by white bars. The physical and genetic maps were aligned using the first and last SSR primer sequence that could be located on the physical map. SSR identifiers and their ratio position on the linkage group and chromosome are shown in black. Differentially expressed genes were identified through microarray analysis of plants exposed to 9 hrs 200 ppb ozone, and QTL were identified from a 100 ppb exposure of 164 genotypes of Family 331 in open-top chambers. Statisical significance of QTL is represented by thickness of the bars: $p<0.05$ $p<0.01$ $p<0.001$

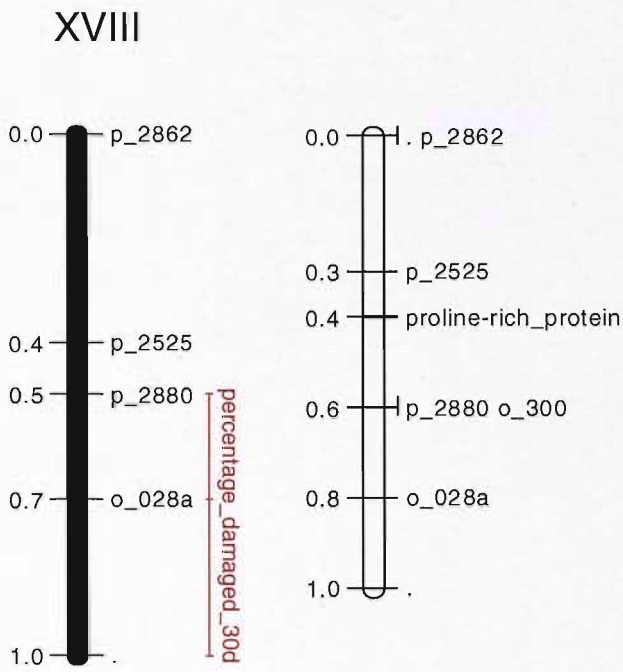

Figure 5.2 d: The position of genes differentially expressed between *P. deltoides* and *P. trichocarpa* (red), and between sensitive and tolerant genotypes of Family 331 (green) relative to QTL for visible damage on the genetic map. Linkage groups are represented by black bars, and chromosomes by white bars. The physical and genetic maps were aligned using the first and last SSR primer sequence that could be located on the physical map. SSR identifiers and their ratio position on the linkage group and chromosome are shown in black. Differentially expressed genes were identified through microarray analysis of plants exposed to 9 hrs 200 ppb ozone, and QTL were identified from a 100 ppb exposure of 164 genotypes of Family 331 in open-top chambers. Statisical significance of QTL is represented by thickness of the bars: $p<0.05$— $p<0.01$— $p<0.001$—

Figures 5.2 a-d show the linkage groups from the genetic map that contain QTL for visible damage aligned with the physical genome sequence on the basis of SSR markers. Of the 50 most differentially expressed genes between *P. deltoides* and *P. trichocarpa* and between the two sensitivity groups, four are located within QTL regions: those encoding arginine decarboxylase and a wound- inducible chitinase homologue from the grand-parental analysis; and S-adomethionine synthetase and a plasma membrane intrinsic protein from the extreme genotype analysis.

5.4 Discussion

QTL mapping

Of the 58 QTL detected, 20 were found to map only under ozone treatment or as response QTL. It is therefore likely that these represent genomic regions that are specifically involved in governing the response to ozone, and are the most encouraging candidates for further investigation. Such QTL were found for leaf necrosis, diameter, late-season leaf number, height, late season abscission, area of the first unfurled leaf and chlorophyll content, indicating that ozone responsive genomic regions exist that govern numerous traits. QTL that map both in ozone and control conditions are likely to correspond to regions that are of more fundamental importance in governing the trait under differing environmental conditions.

As growth traits are the end result of complex biological processes, including carbon assimilation and partitioning, it would be expected that they would also be under equally complex genetic control. The results presented here suggest that a relatively large proportion of the phenotypic variance can be explained by prospectively few QTL, indicating that a few genomic regions have a large effect, in concordance with the oligogenic model. It must be noted, however, that the QTL confidence spans are large, and may represent a large number of genes which have a small phenotypic effect, as opposed to one or a few genes with a large effect.

With reference to identification of the specific gene or genes underlying a QTL, it is of note that the QTL regions identified span an average confidence interval of approximately 30 cM, with the smallest being 14 cM. Although this narrows the

search for the genes involved, such a region will undoubtedly contain many genes, and strategies must be used to identify smaller genomic regions to target for further investigation. This study used 164 genotypes of Family 331. Improved resolution could be obtained by increasing the number of individuals, as the confidence interval is inversely proportional to the strength of the QTL and the square of the number of individuals (Darvasi et al., 1993; Darvasi, 1998). For example, a study by Rae et al. (submitted) used 285 genotypes to identify QTL in elevated CO_2, and showed improved resolution. This was not possible in this investigation due to space constraints. Increased marker coverage may also improve resolution, but this is subject to diminishing returns, and spacing of less than 10 cM will likely not give significant improvement. Association mapping can greatly improve resolution, and could be utilised by identifying SNP markers around a QTL region in a natural population. A SNP discovery program is currently underway in poplar, with an aim to identify candidate genes for wood quality and disease resistance (http://www.treenomix.ca). However, the logistics of exposing such a large population to elevated ozone are likely to be prohibitive. An alternative is to examine the QTL region for candidate genes. As the annotation of the physical sequence is currently underway, this will soon be possible.

As discussed in Chapter 3, considerable transgressive segregation was observed for several of the traits studied, with the phenotypes of the F_2 individuals varying more widely than the grandparents. In particular, 79 genotypes exceeded the late-season visible damage scores of *P. trichocarpa*. This may occur due to combinations of alleles arising in the F_2 generation which result in greater visible damage. Such a pattern is also seen for other traits, including leaf abscission.

As well as QTL particular to certain traits, there are numerous co-locating QTL, particularly for growth traits. In particular, there are overlapping QTL regions for height, diameter and leaf number on LG X. This could indicate that these QTL have pleiotropic effects and may be related to a fundamental growth process such as carbon assimilation. Co-locating QTL are also observed for visible damage and leaf abscission, which are both thought to be related to oxidative stress. Such QTL could therefore correspond to loci involved in governing sensitivity to such stress. Such interpretations should be made with caution, as the wide confidence spans of the QTL will result in more regions co-localising by chance. A higher mapping resolution would serve to ameliorate this problem.

Previous studies have found QTL that are consistent between heterogeneous environments to be comparatively rare. For example, of 22 QTL discovered for agronomic traits in a rice population, just 7 were found in the three environments tested (Lu et al., 1996). QTL that are robust between environments are likely to be of more interest commercially, as growth conditions can vary considerably. In this study, QTL for height and diameter co-localised to those for biomass from a study by Rae et al. (submitted) on LGs IV, X and XII, and QTL for area of first unfurled leaf, chlorophyll content and leaf abscission overlapped with those found by Street et al. (submitted) on LGs VIII, XI, XIV and XIX. This consistency across environments and growing seasons is indicative of robust QTL, and may represent those of the greatest interest for future studies. With regards to QTL specifically related to the response to ozone, it would be interesting to repeat the experiment in additional environments and growing seasons, or with different sets of genotypes, as suggested

by Xu et al. (2002). As the genetic maps of the populations used in the Popyomics project are being aligned, these other pedigrees could be used to identify ozone responsive QTL that are consistent across populations.

Candidate gene discovery

An aim of this study was to identify candidate genes through co-location of differentially expressed genes from microarray analysis with QTL identified from the population experiment. To achieve this, the top 50 most differentially expressed genes between *P. deltoides* and *P. trichocarpa*, and also between the groups of sensitive and tolerant F_2 genotypes, were located on the physical sequence. The physical and genetic maps were then aligned using sequenced SSR markers.

An EST with high similarity to Arabidopsis *arginine decarboxylase 2* (*ADC2*) was found to be significantly differentially expressed between *P. deltoides* and *P. trichocarpa*, and other ESTs representing this gene were also found to exhibit a similar pattern. Interrogation of the *P. trichocarpa* genome revealed this gene to be located on linkage group IV, and is coincident with a QTL for late-season visible damage under ozone treatment. As discussed, co-location of a differentially expressed gene with a QTL region provides additional evidence for the gene being important in governing the response (Borevitz et al., 2002). The maternal and paternal effects for the QTL were both negative, indicating that the QTL alleles from both parents serve a protective role against ozone damage. If the gene underlying the QTL is indeed *ADC*, this observation is consistent with the literature which has shown polyamine synthesis, and arginine decarboxylase itself, to ameliorate ozone damage (Ormrod et al., 1986; Rowland Bamford, 1989). In particular, application of a specific inhibitor of

ADC resulted in increased visible symptom formation in ozone exposed barley (Rowland-Bamford et al., 1989). A role for polyamines and ADC has been postulated for tolerance to a number of other stresses, including salt and osmotic stress (Legocka & Kluk, 2005) and chilling (Hao et al., 2005). It is of note that *ADC* is more up-regulated in *P. trichocarpa*, the ozone sensitive species. This could be considered as evidence against a key role for this gene in determining ozone sensitivity. However, it must be emphasised that alleles with a protective effect may be present in the sensitive parent and vice versa, and that this is considered a likely mechanism for transgressive segregation in the F_2 population.

S-adenosyl methionine (SAM) is the precursor molecule to both polyamines and ethylene, both of which are thought to be involved in the response to ozone. It is of interest, therefore, that *SAM synthetase (SAMS)* is co-located to QTL for both late and early season visible damage on LG II. Pandey et al. (2000) put forward a hypothesis for the interacting role of polyamines and ethylene in the control of senescence, with ethylene acting as a positive regulator and polyamines as a negative regulator. The authors put forward a model in which polyamine and ethylene biosynthetic pathways compete for a limited pool of SAM, with the interaction between the two determining the outcome. They also postulated that the product of one pathway could act to inhibit the opposing pathway. This presents the intriguing possibility that a similar mechanism could exist in the response to ozone, with the interaction between polyamine and ethylene biosynthesis serving to determine the extent of visible damage. The greater up-regulation of enzymes in the ethylene biosynthetic pathway for *P. trichocarpa* may be indicative of increased ethylene synthesis in this species. If this is the case, the second hypothesis of Pandey et al. (2000) could be of relevance, as

increased ethylene biosynthesis may serve to negatively regulate polyamine biosynthesis. If *SAMS* is indeed the gene underlying the QTL, it is possible that it plays an important role in this interaction through governing substrate availability. Also, increased ethylene synthesis could result in increased lesion spread in *P. trichocarpa*.

Plasma membrane intrinsic proteins are a subset of aquaporins that are located in the plasma membrane. Aquaporins are involved in water transport in plants (Maurel, 1997), and have achieved considerable attention concerning their role in response to abiotic stresses, in particular drought. Recently, it has been found that they are capable of transporting the signal molecule H_2O_2 across the plasma membrane, and as such may represent an interface between ROS generation in the apoplast and intracellular signalling (Pastori & Foyer, 2002). This opens up the possibility that they are involved in the response to ozone through transportation of H_2O_2 resulting from ozone exposure, and may contribute to sensitivity through initiation of downstream signal transduction cascades.

A wound inducible chitinase homologue co-locates to the same visible damage QTL as *ADC*. Chitinases are thought to play a role in defence against invading pathogens, and have also been found to be inducible by wounding in poplar (Clarke et al., 1994). As chitinase specifically acts to degrade chitin present in fungal cell walls, it is hard to envisage how it would play a role in the response to ozone. As mentioned, the QTL regions identified are relatively large, meaning that co-location to differentially expressed genes can occur by chance, by virtue of being linked to a gene or genes that do play a causal role. Therefore, although co-location of differentially expressed

genes with QTL provides evidence for their role, it does not prove a definite causal link. This emphasises the importance of an integration of these approaches with biological understanding. The value of such a multifaceted approach has been described in Borevitz et al. (2002).

5.5 Conclusions

This chapter successfully used physiological data for quantitatively distributed traits of Family 331 to identify QTL regions. Specifically, 20 QTL were mapped only under ozone treatment, and represent genomic regions for further investigation, through techniques such as association mapping. Sequenced SSR markers were used to align the physical and genetic maps, and upon completion of annotation of the *P. trichocarpa* genome, it will also be possible to screen all the genes residing within these regions, considerably narrowing the search for genes important in governing ozone sensitivity. QTL for visible damage were integrated with transcriptomic data for *P. trichocarpa* and *P. deltoides*, and also for groups of sensitive and tolerant F_2 genotypes. Several differentially expressed genes were found to collocate with QTL regions, and represent encouraging candidates for further investigation.

Chapter 6: General discussion

6.1 Overview of results

This work used a combination of phenotyping, QTL mapping and microarray analysis to investigate the mechanisms underlying the response of *Populus* to elevated ozone. An ozone fumigation system was successfully designed and constructed, and was used to demonstrate that the grandparents of the mapping population Family 331, *P. deltoides* and *P. trichocarpa,* were highly divergent in their response to an acute ozone treatment. A contrasting stomatal response was also found, with *P. deltoides* closing its stomata earlier than *P. trichocarpa.* As this could be involved in determining sensitivity, the stomatal response was further investigated in subsequent experiments. The contrasting response of the two species provided the basis for a large-scale QTL mapping and phenotyping experiment in open-top chambers on 164 individuals of the F_2 mapping population, and for gene expression studies in both the grandparental species and groups of sensitive and tolerant genotypes.

A recent study has shown variation in the response of genotypes of Family 331 to elevated ozone (Woo et al., 2005). However, as this work used just 36 F_2 genotypes, it was limited to phenotypic analysis. The work in this thesis used 164 genotypes, and was the first study to map QTL for the response of trees to elevated ozone. A total of 20 ozone-specific QTL were mapped for visible damage, stem diameter, leaf number, height, leaf abscission, leaf area and chlorophyll, indicating successful identification of genomic regions involved in mediating the response to elevated ozone.

The population exhibited marked transgressive segregation for numerous traits, allowing selection of subsets of ozone sensitive and tolerant genotypes with

contrasting patterns of visible damage, with the sensitive group exhibiting more severe visible damage than *P. trichocarpa*. This, coupled with the finding that these groups were not as divergent as the grandparents in traits other than visible damage, renders them a powerful model system for studying this particular response. (Borevitz, 2003). The stomatal conductance of sensitive and tolerant genotypes was also analysed, and no significant difference was found between the two groups. This may indicate that stomatal conductance is not in fact the primary determinant of sensitivity in this population.

With the advent of large poplar EST collections, considerable research has focussed on producing gene expression profiles using cDNA microarrays. Recent work by Street et al. (submitted) produced transcript profiles of drought-stressed *P. deltoides* and *P. trichocarpa*, and groups of sensitive and tolerant genotypes. Taylor et al. (2005) used microarrays to examine the response of *Populus euramericana* to elevated carbon dioxide, and discovered that the response at the transcriptional level was dependent on developmental stage. Previously, the only study to have produced a transcript profile of ozone stressed trees used a small scale 4600 EST macroarray (Gupta et al., 2005). This is the first investigation to use microarray analysis to probe the response of trees to elevated ozone. The study successfully identified 50 genes that were differentially expressed in response to an acute ozone treatment. Considerable similarity with previous work on other species was evident, such as changes in expression of genes encoding antioxidant and detoxification enzymes (Matsuyama et al., 2002; Mittler et al., 2002; Ludwikow et al., 2004), and those involved in photosynthesis and the phenypropanoid pathway. The results presented in this thesis provided a comprehensive view of the effect of acute ozone treatment upon

genes in the phenylpropanoid pathway, with a striking similarity seen between the two species in spite of their contrasting sensitivity.

A unique aspect of this investigation involved comparison of the gene expression profiles of two species exhibiting contrasting sensitivity to ozone. 50 genes that were differentially expressed between species were identified, including those encoding peroxidase, XET, and ACC oxidase. Microarray analysis was also used to compare gene expression profiles of the sensitive and tolerant groups of F_2 genotypes, which showed even greater divergence in sensitivity than *P. deltoides* and *P.trichocarpa.* Furthermore, this was one of the first investigations to use the recently available Picme microarrays, containing some 22,000 ESTs from three collections. Together, these experiments provided a valuable list of candidate genes that may be involved in governing sensitivity. The analysis also showed the utility of multivariate statistics for identifying gene expression patterns from plant microarray data. This technique has previously proved useful in gene expression studies in animals, and highlights the importance of a cross-disciplinary approach to microarray analysis.

Quantification of the phytohormones, jasmonic acid and salicylic acid, provided a link between gene expression data and the end products of biosynthetic pathways. Interestingly, although *P. trichocarpa* overall showed a greater upregulation of genes involved in JA biosynthesis, quantification of this hormone revealed levels to be elevated considerably earlier in *P. deltoides* than in *P. trichocarpa.* As jasmonic acid has previously found to attenuate ozone induced visible damage in poplar (Koch et al., 2000), this represents an encouraging mechanism for the differential sensitivity seen between the two species. These results highlight the importance of combining

expression studies with other approaches, as an upregulation at the transcriptional level do not necessarily translate into an increase in the end product.

In recent years, there has been considerable interest in the use of genetic and genomic techniques in combination, forming the unified field of "genetical genomics" (Janson and Nap, 2001). The work in this thesis capitalised on the abundance of genomic and genetic resources now available for *Populus*, and used QTL mapping and microarray analysis together to provide further insight into the genetic basis of ozone sensitivity. The completion of the physical genome sequence during my PhD has been of great benefit, as candidate genes and QTL regions could be located on the physical sequence. Furthermore, it was possible to align the physical and genetic maps using sequenced SSR markers, allowing the position of candidate genes to be compared to QTL locations relating to visible damage in ozone. Differentially expressed genes that were co-located with these QTL were considered to be encouraging candidates for mediating the response to ozone, and can be targeted for further investigation. These included genes encoding arginine decarboxylase, SAM synthetase, and a plasma membrane intrinsic protein. The results of this investigation therefore demonstrate the power of combining genetic and genomic techniques to provide a short-list of candidate genes for further research. Also, by locating QTL on the physical sequence, the search for genes that are important in governing ozone sensitivity is considerably narrowed.

6.2 Future work

Fine mapping

Although QTL mapping is capable of identifying regions of the genome associated with expression of a quantitative trait, it is limited in its resolution. As QTL regions may contain hundreds of genes, considerable work has focussed on improving resolution in order to find the specific gene or genes involved. These methods are commonly referred to as "fine mapping" procedures. One such approach, association mapping, takes advantage of the large number of meioses that have occurred in natural populations, due to a far greater number of elapsed generations. These recombination events act to reduce association of markers that are not strongly linked to a QTL.

Due to the high resolution achievable by association mapping, it is necessary to use markers that can accommodate this. SNPs, as discussed earlier, are highly abundant in the genome and can be used to produce saturated genetic maps. They can also easily be identified *in silico* from EST collections. A SNP discovery program is currently underway for candidate genes involved in wood quality and disease resistance in *Populus* (http://www.treenomix.ca), and Krutovsky et al. (2005) performed a SNP discovery study for cold tolerance and wood quality candidate genes in Douglas fir. The Euforgen collection represents a natural linkage disequilibrium population for poplar, and will be used for dissection of a number of complex traits.

Expression QTL

Analysing gene expression as a quantitative trait allows identification of QTL governing expression of that gene, known as expression QTL (eQTL) (Kirst et al, 2004), effectively allowing the regulation of the gene to be mapped. Although still in its infancy, this approach has been used with some success in *Eucalyptus* (Kirst et al, 2004) and maize (Hazen et al, 2003). As with traditional QTL analysis, eQTL will locate to the genetic region important in governing the trait, in this case gene expression. This may locate to the gene itself if a polymorphism in that gene is causing the expression differences. Perhaps more likely, it will map in *trans*, to another gene or genes that govern its transcription. It may therefore be a useful approach in identifying "master switches" that regulate the expression of candidate genes.

Transformation and RNA interference

Poplar was the first tree to be successfully transformed, and transgenes have been shown to be relatively stable (Peña et al., 2001). Agrobacterium-mediated transformation is now a routine procedure in a number of poplar species (Busov et al., 2005). Transformation presents an attractive approach for proving a causal link between gene and phenotype, particularly in trees where long generation times, large size and out-crossing render high resolution mapping techniques expensive and time consuming. A number of studies have successfully used genetic transformation to improve characteristics in *Populus*; for example, overexpression of glutamine synthetase has been shown to increase growth (Jing et al., 2004) and improve tolerance to drought (El Khatib et al., 2004), while Gill et al. (2006) demonstrated that

overexpression of tryptophan decarboxylase can improve resistance to an insect pest. RNA interference is a gene silencing technique that involving introduction of complementary double stranded RNA. It carries advantages over traditional knockout procedures, as it circumvents the problems such as redundancy and lethal phenotypes (Matthew, 2004). RNAi can also be induced at desired stages of development or during a particular treatment using an inducible promoter. Such methods have been shown to be viable in plants (Wielopolska et al., 2005), and vectors for the procedure have been designed for *Populus*.

6.3 Closing comments

The immense impact of genome sequencing on scientific research has been seen on all the organisms for which it has been achieved, and the recent sequencing of the *Populus trichocarpa* genome is likely to have a similar effect. Considerable genomic and genetic resources are already available for *Populus*, and the work in this thesis has capitalised on recent developments to provide a valuable insight into the underlying basis of ozone sensitivity, as well as grounding for further studies. However, the full potential of recent breakthroughs is yet to be realised, making this an exciting time for poplar research and the field of tree biology as a whole.

Appendix A: Publications and presentations

A1 Publications from work in this thesis

Tucker J, Street NR, Broschè M, Kangasjärvi J, Broadmeadow MSJ, Taylor G (2006) **The genetics and genomics of the response of *Populus* to elevated ozone.** *Submitted to Plant, Cell and Environment.*

Tucker J, Street NR, Broschè M, Kangasjärvi J, Broadmeadow MSJ, Taylor G (2005) **A genomics and quantitative genetics approach to understanding ozone sensitivity in poplar.** *SEB Conference, Barcelona.*

A2 Presentations on work in this thesis

Tucker J (2005) **A genomics and quantitative genetics approach to the response of poplar to elevated ozone.** *Oral presentation-* Postgraduate Symposium, University of Southampton.

Tucker J (2004) **The contrasting response of two *Populus* species to acute ozone stress- a genomic approach.** *Poster presentation-* Postgraduate Symposium, University of Southampton.

Tucker J, Tricker PJ, Street NR, Bradshaw HD, Taylor G (2003) **The contrasting response of *P. deltoides* and *P. trichocarpa* to acute ozone stress, and identification of associated patterns of gene expression using a novel microarray approach.** *Poster presentation-* Tree Biotechnology Conference

A3 Other work published or in press

Taylor G, Hanley ME, Graham LE, Street NR, Trewin H, Hughes J, **Tucker J**, Rae AM (2006) **Genetic control of plant growth response to elevated CO_2 in two model genera.** *In press.*

Street NR, Skogström O, Sjödin A, **Tucker J**, Rodríguez-Acosta M, Nilsson P, Jansson S, Taylor G (2006-) **The Genetics and Genomics of drought response in *Populus*.** *Submitted: Plant Physiology.*

Rae AM, Graham LE, Street NR, Hughes J, Hanley ME, **Tucker J**, Taylor G (2005-) **QTL for growth and development in elevated carbon dioxide in two model plant genera: a novel approach for understanding plant adaptation to climate change?** *Submitted: Global Change Biology*

Rae AM, Pinel MPC, Bastien C, Sabatti M, Street NR, **Tucker J**, Dixon C, Taylor G (2005) **Identifying G x E interactions influencing growth characteristics and QTL discovery for an F_2 population of hybrid *Populus* (*P. deltoides* x *P. trichocarpa*) grown at three contrasting sites.** *In preparation.*

Gardner SDL, Freer-Smith PH, **Tucker J**, Taylor G (2005) **Elevated CO_2 protects poplar (*Populus trichocarpa* x *P. deltoides*) from damage induced by ozone: identification of mechanisms.** Functional Plant Biology , 221-235

References

Agarawal GK, Rakwal R, Yonekura M, Kubo A, Saji H (2002) Proteome analysis of differentially displayed proteins as a tool for investigating ozone stress in rice (*Oryza sativa* L.) seedlings. Proteomics **2:** 947-959

Alonso-Blanco C, Peeters AJM, Koornneef M, Lister C, Dean C, van den Bosch N, Pot J, Kuiper MTR (1998) Development of an AFLP based linkage map of Ler, Col and Cvi Arabidopsis thaliana ecotypes and construction of a Ler/Cvi recombinant inbred line population. Plant Journal **14:** 259-271

Andaya VC, Mackill DJ (2003) QTLs conferring cold tolerance at the booting stage of rice using recombinant inbred lines from a japonica x indica cross. Theoretical and Applied Genetics **106:** 1084-1090

Annamalai P, Yanagihara S (1999) Identification and characterization of a heat-stress induced gene in cabbage encodes a Kunitz type protease inhibitor. Journal of Plant Physiology **155:** 226-233

Ashburner M, Bergman CM (2005) *Drosophila melanogaster*: A case study of a model genomic sequence and its consequences. Genome Research **15:** 1661-1667

Ashmore MR, Onal M (1984) Modification by sulphur dioxide of the responses of *Hordeum vulgare* to Ozone. Environmental Pollution (Series A) **36:** 31-43

Bahl A, Kahl G (1995) Air pollutant stress changes the steady-state transcript levels of 3 photosynthesis genes. Environmental Pollution **88:** 57-65

Benbella M, Paulsen GM (1998) Efficacy of treatments for delaying senescence of wheat leaves: I. Senescence under controlled conditions. Agronomy Journal **90:** 329-332

Berrang P, Karnosky DF, Bennett JP (1991) Natural selection for ozone tolerance in *Populus tremuloides* - an evaluation of nationwide trends. Canadian Journal of Forest Research **21:** 1091-1097

Bittner M, Meitzer P, Chen Y, Jiang Y, Seftor E, Hendrix M, Radmacher M, Simon R, Yakhini Z, Ben-Dor A, Sampas N, Dougherty E, Wang E, Marincola F, Gooden C, Lueders J, Glatfelter A, Pollock P, Carpten J, Gillanders E, Leja D, Dietrich K, Beaudry C, Berens M, Alberts D, Sondak V, Hayward N, Trent J (2000) Molecular classification of cutaneous malignant melanoma by gene expression profiling. Nature **406:** 536-540

Bleecker AB, Estelle MA, Somerville C, Kende H (1988) insensitivity to ethylene conferred by a dominant mutation in *Arabidopsis thaliana*. Science **241:** 1086-1089

Bolwell GP (1999) Role of active oxygen species and NO in plant defence responses. Current Opinion in Plant Biology **2:** 287-294

Bonello P, Heller W, Sandermann H (1993) Ozone effects on root-disease susceptibility and defense responses in mycorrhizal and nonmycorrhizal seedlings of scots pine (*Pinus sylvestris* L). New Phytologist **124:** 653-663

Booker FL, Anttonen S, Heagle AS (1996) Catechin, proanthocyanidin and lignin contents of loblolly pine (*Pinus taeda*) needles after chronic exposure to ozone. New Phytologist **132:** 483-492

Bradshaw HD, Villar M, Watson BD, Otto KG, Stewart S, Stettler RF (1994) Molecular-Genetics of Growth and Development in Populus .3. A Genetic-Linkage Map of a Hybrid Poplar Composed of Rflp, Sts, and Rapd Markers. Theoretical and Applied Genetics **89:** 167-178

Bradshaw HD, Stettler RF (1995) molecular-genetics of growth and development in *Populus* .4. Mapping QTLs with large effects on growth, form, and phenology traits in

a forest tree. Genetics **139:** 963-973

Bradshaw HD, Ceulemans R, Davis J, Stettler R (2000) Emerging model systems in plant biology: Poplar (*Populus*) as a model forest tree. Journal of Plant Growth Regulation **19:** 306-313

Brendley BW, Pell EJ (1998) Ozone-induced changes in biosynthesis of Rubisco and associated compensation to stress in foliage of hybrid poplar. Tree Physiology **18:** 81-90

Breyne P, Zabeau M (2001) Genome-wide expression analysis of plant cell cycle modulated genes. Current Opinion in Plant Biology **4:** 136-142

Broadmeadow MSJ, Heath J, Randle TJ (1999) Environmental limitations to O-3 uptake - Some key results from young trees growing at elevated CO2 concentrations. Water Air and Soil Pollution **116:** 299-310

Brosche M, Vinocur B, Alatalo ER, Lamminmaki A, Teichmann T, Ottow EA, Djilianov D, Afif D, Bogeat-Triboulot MB, Altman A, Polle A, Dreyer E, Rudd S, Lars P, Auvinen P, Kangasjarvi J (2005) Gene expression and metabolite profiling of *Populus euphratica* growing in the Negev desert. Genome Biology **6**

Brunner AM, Busov VB, Strauss SH (2004) Poplar genome sequence: functional genomics in an ecologically dominant plant species. Trends in Plant Science **9:** 49-56

Buchanan-Wollaston V, Earl S, Harrison E, Mathas E, Navabpour S, Page T, Pink D (2003) The molecular analysis of leaf senescence - a genomics approach. Plant Biotechnology Journal **1:** 3-22

Cabane M, Pireaux JC, Leger E, Weber E, Dizengremel P, Pollet B, Lapierre C (2004) Condensed lignins are synthesized in poplar leaves exposed to ozone. Plant Physiology **134:** 586-594

Cervera MT, Storme V, Ivens B, Gusmao J, Liu BH, Hostyn V, Van Slycken J,

Van Montagu M, Boerjan W (2001) Dense genetic linkage maps of three *Populus* species (*Populus deltoides*, *P. nigra* and *P. trichocarpa*) based on AFLP and microsatellite markers. Genetics **158:** 787-809

Chevone BI, Yang YS (1985) CO_2 exchange rates and stomatal diffusive resistance in soybean exposed to O_3 and SO_2. Canadian Journal of Plant Science **65:** 267-274

Cho RJ, Campbell MJ, Winzeler EA, Steinmetz L, Conway A, Wodicka L, Wolfsberg TG, Gabrielian AE, Landsman D, Lockhart DJ, Davis RW (1998) A genome-wide transcriptional analysis of the mitotic cell cycle. Molecular Cell **2:** 65-73

Ciardi JA, Tieman DM, Lund ST, Jones JB, Stall RE, Klee HJ (2000) Response to Xanthomonas campestris pv. vesicatoria in tomato involves regulation of ethylene receptor gene expression. Plant Physiology **123:** 81-92

Clayton H, Knight MR, Knight H, McAinsh MR, Hetherington AM (1999) Dissection of the ozone-induced calcium signature. Plant Journal **17:** 575-579

Cleveland WS (1981) Lowess - a program for smoothing scatterplots by robust locally weighted regression. American Statistician **35:** 54-54

Coleman MD, Isebrands JG, Dickson RE, Karnosky DF (1995) Photosynthetic productivity of aspen clones varying in sensitivity to tropospheric ozone. Tree Physiology **15:** 585-592

Coleman MD, Dickson RE, Isebrands JG, Karnosky DF (1996) Root growth and physiology of potted and field-grown trembling aspen exposed to tropospheric ozone. Tree Physiology **16:** 145-152

Conklin PL, Last RL (1995) Differential Accumulation of Antioxidant Messenger-Rnas in Arabidopsis-Thaliana Exposed to Ozone. Plant Physiology **109:** 203-212

Cooley DR, Manning WJ (1987) The Impact of ozone on assimilate partitioning in

plants - a review. Environmental Pollution **47:** 95-113

Corpas FJ, Barroso JB, del Rio LA (2001) Peroxisomes as a source of reactive oxygen species and nitric oxide signal molecules in plant cells. Trends in Plant Science **6:** 145-150

Cregan PB, Jarvik T, Bush AL, Shoemaker RC, Lark KG, Kahler AL, Kaya N, VanToai TT, Lohnes DG, Chung L, Specht JE (1999) An integrated genetic linkage map of the soybean genome. Crop Science **39:** 1464-1490

Cui XQ, Churchill GA (2003) Statistical tests for differential expression in cDNA microarray experiments. Genome Biology **4:** art. no.-210

Dangl JL, Dietrich RA, Richberg MH (1996) Death don't have no mercy: Cell death programs in plant-microbe interactions. Plant Cell **8:** 1793-1807

Darvasi A (1998) Experimental strategies for the genetic dissection of complex traits in animal models. Nature Genetics **18:** 19-24

Darvasi A, Weinreb A, Minke V, Weller JI, Soller M (1993) detecting marker QTL linkage and estimating QTL gene effect and map location using a saturated genetic map. Genetics **134:** 943-951

Davies KM, Grierson D (1989) Identification of cDNA clones for tomato (*Lycopersicon esculentum* Mill.) messenger RNAs that accumulate during fruit ripening and leaf senescence in response to ethylene. Planta **179:** 73-80

Deikman J (1997) Molecular mechanisms of ethylene regulation of gene transcription. Physiologia Plantarum **100:** 561-566

Delaney TP, Uknes S, Vernooij B, Friedrich L, Weymann K, Negrotto D, Gaffney T, Gutrella M, Kessmann H, Ward E, Ryals J (1994) A central role of salicylic acid in plant disease resistance. Science **266:** 1247-1250

Delledonne M, Xia YJ, Dixon RA, Lamb C (1998) Nitric oxide functions as a signal

in plant disease resistance. Nature **394:** 585-588

DeRisi JL, Iyer VR, Brown PO (1997) Exploring the metabolic and genetic control of gene expression on a genomic scale. Science **278:** 680-686

Desikan R, Mackerness SAH, Hancock JT, Neill SJ (2001) Regulation of the *Arabidopsis* transcriptome by oxidative stress. Plant Physiology **127:** 159-172

DeSilva DLR, Hetherington AM, Mansfield TA (1996) Where does all the calcium go? Evidence of an important regulatory role for trichomes in two calcicoles. Plant Cell and Environment **19:** 880-886

Devey ME, Bell JC, Smith DN, Neale DB, Moran GF (1996) A genetic linkage map for Pinus radiata based on RFLP, RAPD, and microsatellite markers. Theoretical and Applied Genetics **92:** 673-679

Doebley J, Stec A, Hubbard L (1997) The evolution of apical dominance in maize. Nature **386:** 485-488

Dixon RA, Paiva NL (1995) Stress-induced phenylpropanoid metabolism. Plant Cell **7:** 1085-1097

Doke N, Miura Y, Sanchez LM, Park HJ, Noritake T, Yoshioka H, Kawakita K (1996) The oxidative burst protects plants against pathogen attack: Mechanism and role as an emergency signal for plant bio-defence - A review. Gene **179:** 45-51

Dominy PJ, Heath RL (1985) Inhibition of the K^+-stimulated ATPase of the plasmalemma of pinto bean leaves by ozone. Plant Physiology **77:** 43-45

Drew MC, He CJ, Morgan PW (2000) Programmed cell death and aerenchyma formation in roots. Trends in Plant Science **5:** 123-127

Dudley JW, Lambert RJ (1992) 90 generations of selection for oil and protein in maize. Maydica **37:** 81-87

Durner J, Klessig DF (1995) Inhibition of ascorbate peroxidase by salicylic acid and

2,6- dichloroisonicotinic acid, 2 inducers of plant defense responses. Proceedings of the National Academy of Sciences of the United States of America **92:** 11312-11316

Durner J, Klessig DF (1996) Salicylic acid is a modulator of tobacco and mammalian catalases. Journal of Biological Chemistry **271:** 28492-28501

Durner J, Wendehenne D, Klessig DF (1998) Defense gene induction in tobacco by nitric oxide, cyclic GMP, and cyclic ADP-ribose. Proceedings of the National Academy of Sciences of the United States of America **95:** 10328-10333

Eckardt NA, Pell EJ (1994) O_3-induced degradation of Rubisco protein and loss of Rubisco messenger RNA in relation to leaf age in *Solanum tuberosum* L. New Phytologist **127:** 741-748

Ecker JR, Davis RW (1987) Plant defense genes are regulated by ethylene. Proceedings of the National Academy of Sciences of the United States of America **84:** 5202-5206

Eckeykaltenbach H, Grosskopf E, Sandermann H, Ernst D (1994) Induction of pathogen defense genes in parsley (*Petroselinum crispum* L.) plants by ozone. Proceedings of the Royal Society of Edinburgh (Section B) **102:** 63-74

Eckeykaltenbach H, Ernst D, Heller W, Sandermann H (1994) Biochemical-plant responses to ozone .4. Cross-induction of defensive pathways in parsley (*Petroselinum crispum* L.) plants. Plant Physiology **104:** 67-74

Edwards NT (1991) Root and soil respiration responses to ozone in *Pinus taeda* seedlings. New Phytologist **118:** 315-321

Elstner EF (1987) Ozone and ethylene stress. Nature **328:** 482-482

Farage PK, Long SP, Lechner EG, Baker NR (1991) The sequence of change within the photosynthetic apparatus of wheat following short-term exposure to ozone. Plant Physiology **95:** 529-535

Farage PK (1996) The effect of ozone fumigation over one season on photosynthetic processes of *Quercus robur* seedlings. New Phytologist **134:** 279-285

Ferris R, Long L, Bunn SM, Robinson KM, Bradshaw HD, Rae AM, Taylor G (2002) Leaf stomatal and epidermal cell development: identification of putative quantitative trait loci in relation to elevated carbon dioxide concentration in poplar. Tree Physiology **22:** 633-640

Fink S (1991) Unusual patterns in the distribution of calcium oxalate in spruce needles and their possible relationships to the impact of pollutants. New Phytologist **119:** 41-51

Fry SC (1998) Oxidative scission of plant cell wall polysaccharides by ascorbate-induced hydroxyl radicals. Biochemical Journal **332:** 507-515

Fry SC, Smith RC, Renwick KF, Martin DJ, Hodge SK, Matthews KJ (1992) Xyloglucan endotransglycosylase, a new wall-loosening enzyme activity from plants. Biochemical Journal **282:** 821-828

Furukawa A, Park SY, Fujinuma Y (1990) Hybrid poplar stomata unresponsive to changes in environmental conditions. Trees-Structure and Function **4:** 191-197

Galliano H, Heller W, Sandermann H (1993) Ozone induction and purification of spruce cinnamyl alcohol dehydrogenase. Phytochemistry **32:** 557-563

Ganesan V, Thomas G (2001) Salicylic acid response in rice: influence of salicylic acid on H_2O_2 accumulation and oxidative stress. Plant Science **160:** 1095-1106

Gelang J, Pleijel H, Sild E, Danielsson H, Younis S, Sellden G (2000) Rate and duration of grain filling in relation to flag leaf senescence and grain yield in spring wheat (*Triticum aestivum*) exposed to different concentrations of ozone. Physiologia Plantarum **110:** 366-375

Glazebrook J, Rogers EE, Ausubel FM (1997) Use of *Arabidopsis* for genetic

dissection of plant defense responses. Annual Review of Genetics **31:** 547-569

Glazener JA, Orlandi EW, Baker CJ (1996) The active oxygen response of cell suspensions to incompatible bacteria is not sufficient to cause hypersensitive cell death. Plant Physiology **110:** 759-763

Glick RE, Schlagnhaufer CD, Arteca RN, Pell EJ (1995) Ozone-induced ethylene emission accelerates the loss of ribulose-1,5-bisphosphate carboxylase oxygenase and nuclear-encoded messenger RNAs in senescing potato leaves. Plant Physiology **109:** 891-898

Golub TR, Slonim DK, Tamayo P, Huard C, Gaasenbeek M, Mesirov JP, Coller H, Loh ML, Downing JR, Caligiuri MA, Bloomfield CD, Lander ES (1999) Molecular classification of cancer: Class discovery and class prediction by gene expression monitoring. Science **286:** 531-537

Grattapaglia D, Sederoff R (1994) genetic-linkage maps of *Eucalyptus grandis* and *Eucalyptus urophylla* using a pseudo-testcross mapping strategy and RAPD markers. Genetics **137:** 1121-1137

Grbic V, Bleecker AB (1995) Ethylene regulates the timing of leaf senescence in *Arabidopsis*. Plant Journal **8:** 595-602

Grimmig B, Gonzalez-Perez MN, Leubner-Metzger G, Vogeli-Lange R, Meins F, Hain R, Penuelas J, Heidenreich B, Langebartels C, Ernst D, Sandermann H (2003) Ozone-induced gene expression occurs via ethylene-dependent and -independent signalling. Plant Molecular Biology **51:** 599-607

Guderian R (1985) Air pollution by photochemical oxidants: formation, transport, control and effects on plants. Air Pollution by Photochemical Oxidants, Springer-Verlag, Berlin: 129–334.

Gunthardtgoerg MS, Matyssek R, Scheidegger C, Keller T (1993) Differentiation

and structural decline in the leaves and bark of birch (*Betula pendula*) under low ozone concentrations. Trees-Structure and Function **7:** 104-114

Guo Y, Cai Z, Gan S (2004) Transcriptome of *Arabidopsis* leaf senescence. Plant Cell and Environment **27:** 521-549

Gupta P, Duplessis S, White H, Karnosky DF, Martin F, Podila GK (2005) Gene expression patterns of trembling aspen trees following long-term exposure to interacting elevated CO_2 and tropospheric O_3. New Phytologist **167:** 129-142

Guzy MR, Heath RL (1993) Responses to ozone of varieties of common bean (*Phaseolus vulgaris* L). New Phytologist **124:** 617-625

Hadfield KA, Dang T, Guis M, Pech JC, Bouzayen M, Bennett AB (2000) Characterization of ripening-regulated cDNAs and their expression in ethylene-suppressed Charentais melon fruit. Plant Physiology **122:** 977-983

HammondKosack KE, Jones DA, Jones JDG (1996) Ensnaring microbes: The components of plant disease resistance. New Phytologist **133:** 11-24

Hao YJ, Kitashiba H, Honda C, Nada K, Moriguchi T (2005) Expression of arginine decarboxylase and ornithine decarboxylase genes in apple cells and stressed shoots. Journal of Experimental Botany **56:** 1105-1115

Hays JB (2002) *Arabidopsis thaliana*, a versatile model system for study of eukaryotic genome-maintenance functions. DNA Repair **1:** 579-600

Hazen SP, Hawley RM, Davis GL, Henrissat B, Walton JD (2003) Quantitative trait loci and comparative genomics of cereal cell wall composition. Plant Physiology **132:** 263-271

Heath MC (1997) Signalling between pathogenic rust fungi and resistant or susceptible host plants. Annals of Botany **80:** 713-720

Heath MC, Nimchuk ZL, Xu HX (1997) Plant nuclear migrations as indicators of

critical interactions between resistant or susceptible cowpea epidermal cells and invasion hyphae of the cowpea rust fungus. New Phytologist **135:** 689-700

Heggestad HM, JT (1959) Ozone in high concentrations as cause of tobacco leaf injury. Science **129:** 208-210

Held AA, Mooney HA, Gorham JN (1991) Acclimation to ozone stress in radish - leaf demography and photosynthesis. New Phytologist **118:** 417-423

Hwang EW, Kim KA, Park SC, Jeong MJ, Byun MO, Kwon HB (2005) Expression profiles of hot pepper (*Capsicum annuum*) genes under cold stress conditions. Journal of Biosciences **30:** 657-667

Ilami G, Nespoulous C, Huet JC, Vartanian N, Pernollet JC (1997) Characterization of BnD22, a drought-induced protein expressed in *Brassica napus* leaves. Phytochemistry **45:** 1-8

Jakob B, Heber U (1998) Apoplastic ascorbate does not prevent the oxidation of fluorescent amphiphilic dyes by ambient and elevated concentrations of ozone in leaves. Plant and Cell Physiology **39:** 313-322

Jansen RC, Stam P (1994) High resolution of quantitative traits into multiple loci via interval mapping. Genetics **136:** 1447-1455

Jansen RC, Nap JP (2001) Genetical genomics: the added value from segregation. Trends in Genetics **17:** 388-391

Jorde LB (2000) Linkage disequilibrium and the search for complex disease genes. Genome Research **10:** 1435-1444

Kaletta T, Hengartner MO (2006) Finding function in novel targets: *C. elegans* as a model organism. Nature Reviews Drug Discovery **5:** 387-398

Kangasjarvi J, Jaspers P, Kollist H (2005) Signalling and cell death in ozone-exposed plants. Plant Cell and Environment **28:** 1021-1036

Kangasjarvi J, Talvinen J, Utriainen M, Karjalainen R (1994) Plant defense systems induced by ozone. Plant Cell and Environment **17:** 783-794

Kargiolaki H, Osborne DJ, Thompson FB (1991) Leaf abscission and stem lesions (intumescences) on poplar clones after SO_2 and O_3 Fumigation - a link with ethylene release. Journal of Experimental Botany **42:** 1189-1198

Karnosky DF, Pregitzer KS, Zak DR, Kubiske ME, Hendrey GR, Weinstein D, Nosal M, Percy KE (2005) Scaling ozone responses of forest trees to the ecosystem level in a changing climate. Plant Cell and Environment **28:** 965-981

Karnosky DF, Gagnon ZE, Dickson RE, Coleman MD, Lee EH, Isebrands JG (1996) Changes in growth, leaf abscission, and biomass associated with seasonal tropospheric ozone exposures of *Populus tremuloides* clones and seedlings. Canadian Journal of Forest Research **26:** 23-37

Kauss H, Jeblick W (1995) Pre-treatment of parsley suspension cultures with salicylic acid enhances spontaneous and elicited production of H_2O_2. Plant Physiology **108:** 1171-1178

Kawasaki S, Borchert C, Deyholos M, Wang H, Brazille S, Kawai K, Galbraith D, Bohnert HJ (2001) Gene expression profiles during the initial phase of salt stress in rice. Plant Cell **13:** 889-905

Keller T (1988) Growth and premature leaf fall in American aspen as bioindications for ozone. Environmental Pollution **52:** 183-192

Kende H (1993) Ethylene biosynthesis. Annual Review of Plant Physiology and Plant Molecular Biology **44:** 283-307

Kirst M, Myburg AA, De Leon JPG, Kirst ME, Scott J, Sederoff R (2004) Coordinated genetic regulation of growth and lignin revealed by quantitative trait locus analysis of cDNA microarray data in an interspecific backcross of *Eucalyptus*.

Plant Physiology **135:** 2368-2378

Klessig DF, Durner J, Noad R, Navarre DA, Wendehenne D, Kumar D, Zhou JM, Shah J, Zhang SQ, Kachroo P, Trifa Y, Pontier D, Lam E, Silva H (2000) Nitric oxide and salicylic acid signaling in plant defense. Proceedings of the National Academy of Sciences of the United States of America **97:** 8849-+

Koch JR, Scherzer AJ, Eshita SM, Davis KR (1998) Ozone sensitivity in hybrid poplar is correlated with a lack of defense gene activation. Plant Physiology **118:** 1243-1252

Koch JR, Creelman RA, Eshita SM, Seskar M, Mullet JE, Davis KR (2000) Ozone sensitivity in hybrid poplar correlates with insensitivity to both salicylic acid and jasmonic acid. The role of programmed cell death in lesion formation. Plant Physiology **123:** 487-496

Kollist H, Moldau H, Mortensen L, Rasmussen SK, Jorgensen LB (2000) Ozone flux to plasmalemma in barley and wheat is controlled by stomata rather than by direct reaction of ozone with cell wall ascorbate. Journal of Plant Physiology **156:** 645-651

Koornneef M, Alonso-Blanco C, Vreugdenhil D (2004) Naturally occurring genetic variation in *Arabidopsis thaliana*. Annual Review of Plant Biology **55:** 141-172

Kovtun Y, Chiu WL, Tena G, Sheen J (2000) Functional analysis of oxidative stress-activated mitogen-activated protein kinase cascade in plants. Proceedings of the National Academy of Sciences of the United States of America **97:** 2940-2945

Koyama ML, Levesley A, Koebner RMD, Flowers TJ, Yeo AR (2001) Quantitative trait loci for component physiological traits determining salt tolerance in rice. Plant Physiology **125:** 406-422

Langebartels C, Wohlgemuth H, Kschieschan S, Grun S, Sandermann H (2002)

Oxidative burst and cell death in ozone-exposed plants. Plant Physiology and Biochemistry **40:** 567-575

Le Dantec L, Chagne D, Pot D, Cantin O, Garnier-Gere P, Bedon F, Frigerio JM, Chaumeil P, Leger P, Garcia V, Laigret F, de Daruvar A, Plomion C (2004) Automated SNP detection in expressed sequence tags: statistical considerations and application to maritime pine sequences. Plant Molecular Biology **54:** 461-470

Lee S, Yun SC (2006) The ozone stress transcriptome of pepper (*Capsicum annuum* L.). Molecules and Cells **21:** 197-205

Legocka J, Kluk A (2005) Effect of salt and osmotic stress on changes in polyamine content and arginine decarboxylase activity in *Lupinus luteus* seedlings. Journal of Plant Physiology **162:** 662-668

Lehnherr B, Grandjean A, Machler F, Fuhrer J (1987) The effect of ozone in ambient air on ribulose bisphosphate carboxylase oxygenase activity decreases photosynthesis and grain yield in wheat. Journal of Plant Physiology **130:** 189-200

Lethiec D, Dixon M, Garrec JP (1994) The effects of slightly elevated ozone concentrations and mild drought stress on the physiology and growth of Norway spruce (*Picea abies* L.) and beech (*Fagus sylvatica* L.), in Open-top chambers. New Phytologist **128:** 671-678

Li PH, Mane SP, Sioson AA, Robinet CV, Heath LS, Bohnert HJ, Grene R (2006) Effects of chronic ozone exposure on gene expression in *Arabidopsis thaliana* ecotypes and in *Thellungielia halophila*. Plant Cell and Environment **29:** 854-868

Loreto F, Mannozzi M, Maris C, Nascetti P, Ferranti F, Pasqualini S (2001) Ozone quenching properties of isoprene and its antioxidant role in leaves. Plant Physiology **126:** 993-1000

Loudet O, Chaillou S, Camilleri C, Bouchez D, Daniel-Vedele F (2002) Bay-0 x Shahdara recombinant inbred line population: a powerful tool for the genetic dissection of complex traits in *Arabidopsis*. Theoretical and Applied Genetics **104:** 1173-1184

Lu C, Shen L, Tan Z, Xu Y, He P, Chen Y, Zhu L (1996) Comparative mapping of QTLs for agronomic traits of rice across environments using a doubled haploid population. Theoretical and Applied Genetics **93:** 1211-1217

Ludwikow A, Gallois P, Sadowski J (2004) Ozone-induced oxidative stress response in *Arabidopsis*: Transcription profiling by microarray approach. Cellular & Molecular Biology Letters **9:** 829-842

Maccarrone M, Veldink GA, Vliegenthart JFG, Agro AF (1997) Ozone stress modulates amine oxidase and lipoxygenase expression in lentil (*Lens culinaris*) seedlings. Febs Letters **408:** 241-244

Maleck K, Levine A, Eulgem T, Morgan A, Schmid J, Lawton KA, Dangl JL, Dietrich RA (2000) The transcriptome of *Arabidopsis thaliana* during systemic acquired resistance. Nature Genetics **26:** 403-410

Matsuyama T, Tamaoki M, Nakajima N, Aono M, Kubo A, Moriya S, Ichihara T, Suzuki O, Saji H (2002) cDNA microarray assessment for ozone-stressed *Arabidopsis thaliana*. Environmental Pollution **117:** 191-194

McAinsh MR, Clayton H, Mansfield TA, Hetherington AM (1996) Changes in stomatal behavior and guard cell cytosolic free calcium in response to oxidative stress. Plant Physiology **111:** 1031-1042

McCamant T, Black RA (2000) Cold hardiness in coastal, montane, and inland populations of *Populus trichocarpa*. Canadian Journal of Forest Research **30:** 91-99

Mehlhorn H, Wellburn AR (1987) Stress ethylene formation determines plant-sensitivity to ozone. Nature **327:** 417-418

Mehlhorn H (1990) Ethylene-promoted ascorbate peroxidise activity protects plants against hydrogen peroxide, ozone and paraquat. Plant Cell and Environment **13:** 971-976

Miller JD, Arteca RN, Pell EJ (1999) Senescence-associated gene expression during ozone-induced leaf senescence in *Arabidopsis*. Plant Physiology **120:** 1015-1023

Mittler R (2002) Oxidative stress, antioxidants and stress tolerance. Trends in Plant Science **7:** 405-410

Moeder W, Barry CS, Tauriainen AA, Betz C, Tuomainen J, Utriainen M, Grierson D, Sandermann H, Langebartels C, Kangasjarvi J (2002) Ethylene synthesis regulated by biphasic induction of 1- aminocyclopropane-1-carboxylic acid synthase and 1- aminocyclopropane-1-carboxylic acid oxidase genes is required for hydrogen peroxide accumulation and cell death in ozone- exposed tomato. Plant Physiology **130:** 1918-1926

Morris K, Mackerness SAH, Page T, John CF, Murphy AM, Carr JP, Buchanan-Wollaston V (2000) Salicylic acid has a role in regulating gene expression during leaf senescence. Plant Journal **23:** 677-685

Mould MJR, Heath MC (1999) Ultrastructural evidence of differential changes in transcription, translation, and cortical microtubules during *in planta* penetration of cells resistant or susceptible to rust infection. Physiological and Molecular Plant Pathology **55:** 225-236

Mur LAJ, Naylor G, Warner SAJ, Sugars JM, White RF, Draper J (1996) Salicylic acid potentiates defence gene expression in tissue exhibiting acquired resistance to pathogen attack. Plant Journal **9:** 559-571

Musumarra G, Barresi V, Condorelli DF, Fortuna CG, Scire S (2004) Potentialities of multivariate approaches in genome-based cancer research: identification of candidate genes for new diagnostics by PLS discriminant analysis. Journal of Chemometrics **18:** 125-132

Naot D, Benhayyim G, Eshdat Y, Holland D (1995) Drought, heat and salt stress induce the expression of a citrus homolog of an atypical late-embryogenesis LEA5 gene. Plant Molecular Biology **27:** 619-622

Nelson CD, Nance WL, Doudrick RL (1993) A partial genetic-linkage map of slash pine (*Pinus elliottii* Engelm) based on random amplified polymorphic DNAs. Theoretical and Applied Genetics **87:** 145-151

Nguyen DV, Rocke DM (2002) Tumor classification by partial least squares using microarray gene expression data. Bioinformatics **18:** 39-50

Nie GY, Tomasevic M, Baker NR (1993) Effects of ozone on the photosynthetic apparatus and leaf proteins during leaf development in wheat. Plant Cell and Environment **16:** 643-651

Niki T, Mitsuhara I, Seo S, Ohtsubo N, Ohashi Y (1998) Antagonistic effect of salicylic acid and jasmonic acid on the expression of pathogenesis-related (PR) protein genes in wounded mature tobacco leaves. Plant and Cell Physiology **39:** 500-507

Ohtake Y, Takahashi T, Komeda Y (2000) Salicylic acid induces the expression of a number of receptor-like kinase genes in *Arabidopsis thaliana*. Plant and Cell Physiology **41:** 1038-1044

Oliver SG, Vanderaart QJM, Agostonicarbone ML, Aigle M, Alberghina L, Alexandraki D, Antoine G, Anwar R, Ballesta JPG, Benit P, Berben G, Bergantino E, Biteau N, Bolle PA, Bolotinfukuhara M, Brown A, Brown AJP,

Buhler JM, Carcano C, Carignani G, Cederberg H, Chanet R, Contreras R, Crouzet M, Daignanfornier B, Defoor E, Delgado M, Demolder J, Doira C, Dubois E, Dujon B, Dusterhoft A, Erdmann D, Esteban M, Fabre F, Fairhead C, Faye G, Feldmann H, Fiers W, Francinguesgaillard MC, Franco L, Frontali L, Fukuhara H, Fuller LJ, Galland P, Gent ME, Gigot D, Gilliquet V, Glansdorff N, Goffeau A, Grenson M, Grisanti P, Grivell LA, Dehaan M, Haasemann M, Hatat D, Hoenicka J, Hegemann J, Herbert CJ, Hilger F, Hohmann S, Hollenberg CP, Huse K, Iborra F, Indge KJ, Isono K, Jacq C, Jacquet M, James CM, Jauniaux JC, Jia Y, Jimenez A, Kelly A, Kleinhans U, Kreisl P, Lanfranchi G, Lewis C, Vanderlinden CG, Lucchini G, Lutzenkirchen K, Maat MJ, Mallet L, Mannhaupt G, Martegani E, Mathieu A, Maurer CTC, McConnell D, McKee RA, Messenguy F, Mewes HW, Molemans F, Montague MA, Falconi MM, Navas L, Newlon CS, Noone D, Pallier C, Panzeri L, Pearson BM, Perea J, Philippsen P, Pierard A, Planta RJ, Plevani P, Poetsch B, Pohl F, Purnelle B, Rad MR, Rasmussen SW, Raynal A, Remacha M, Richterich P, Roberts AB, Rodriguez F, Sanz E, Schaaffgerstenschlager I, Scherens B, Schweitzer B, Shu Y, Skala J, Slonimski PP, Sor F, Soustelle C, Spiegelberg R, Stateva LI, Steensma HY, Steiner S, Thierry A, Thireos G, Tzermia M, Urrestarazu LA, Valle G, Vetter I, Vanvlietreedijk JC, Voet M, Volckaert G, Vreken P, Wang H, Warmington JR, Vonwettstein D, Wicksteed BL, Wilson C, Wurst H, Xu G, Yoshikawa A, Zimmermann FK, Sgouros JG (1992) The complete DNA sequence of yeast chromosome-Iii. Nature **357:** 38-46

Olszyk DM, Tibbitts TW (1981) Stomatal response and leaf injury of *Pisum Sativum* L. with SO_2 and O_3 exposures .1. Influence of pollutant level and leaf maturity. Plant Physiology **67:** 539-544

Orvar BL, McPherson J, Ellis BE (1997) Pre-activating wounding response in tobacco prior to high-level ozone exposure prevents necrotic injury. Plant Journal **11:** 203-212

Orzaez D, Granell A (1997) DNA fragmentation is regulated by ethylene during carpel senescence in *Pisum sativum*. Plant Journal **11:** 137-144

Overmyer K, Tuominen H, Kettunen R, Betz C, Langebartels C, Sandermann H, Kangasjarvi J (2000) Ozone-sensitive *Arabidopsis* rcd1 mutant reveals opposite roles for ethylene and jasmonate signaling pathways in regulating superoxide-dependent cell death. Plant Cell **12:** 1849-1862

Paakkonen E, Seppanen S, Holopainen T, Kokko H, Karenlampi S, Karenlampi L, Kangasjarvi J (1998) Induction of genes for the stress proteins PR-10 and PAL in relation to growth, visible injuries and stomatal conductance in birch (*Betula pendula*) clones exposed to ozone and/or drought. New Phytologist **138:** 295-305

Pandey S, Ranade SA, Nagar PK, Kumar N (2000) Role of polyamines and ethylene as modulators of plant senescence. Journal of Biosciences **25:** 291-299

Pastori GM, Foyer CH (2002) Common components, networks, and pathways of cross-tolerance to stress. The central role of "redox" and abscisic acid-mediated controls. Plant Physiology **129:** 460-468

Pearson M, Mansfield TA (1993) Interacting effects of ozone and water stress on the stomatal resistance of beech (*Fagus sylvatica* L). New Phytologist **123:** 351-358

Pei ZM, Murata Y, Benning G, Thomine S, Klusener B, Allen GJ, Grill E, Schroeder JI (2000) Calcium channels activated by hydrogen peroxide mediate abscisic acid signalling in guard cells. Nature **406:** 731-734

Pell EJ, Pearson NS (1983) Ozone-induced reduction in quantity of ribulose-1,5-bisphosphate carboxylase in alfalfa foliage. Plant Physiology **73:** 185-187

Pell EJ, Schlagnhaufer CD, Arteca RN (1997) Ozone-induced oxidative stress: Mechanisms of action and reaction. Physiologia Plantarum **100:** 264-273

Pena L, Seguin A (2001) Recent advances in the genetic transformation of trees. Trends in Biotechnology **19:** 500-506

Perou CM, Sorlie T, Eisen MB, van de Rijn M, Jeffrey SS, Rees CA, Pollack JR, Ross DT, Johnsen H, Aksien LA, Fluge O, Pergamenschikov A, Williams C, Zhu SX, Lonning PE, Borresen-Dale AL, Brown PO, Botstein D (2000) Molecular portraits of human breast tumours. Nature **406:** 747-752

Piikki K, Sellden G, Pleijel H (2004) The impact of tropospheric O_3 on leaf number duration and tuber yield of the potato (*Solanum tuberosum* L.) cultivars Bintje and Kardal. Agriculture Ecosystems & Environment **104:** 483-492

Pons TL, Pearcy RW (1994) Nitrogen reallocation and photosynthetic acclimation in response to partial shading in soybean plants. Physiologia Plantarum **92:** 636-644

Price AH, Taylor A, Ripley SJ, Griffiths A, Trewavas AJ, Knight MR (1994) Oxidative signals in tobacco increase cytosolic calcium. Plant Cell **6:** 1301-1310

Price A, Courtois B (1999) Mapping QTLs associated with drought resistance in rice: Progress, problems and prospects. Plant Growth Regulation **29:** 123-133

Ramakers C, Ruijter JM, Deprez RHL, Moorman AFM (2003) Assumption-free analysis of quantitative real-time polymerase chain reaction (PCR) data. Neuroscience Letters **339:** 62-66

Ranieri A, Giuntini D, Ferraro F, Nali C, Baldan B, Lorenzini G, Soldatini GF, Soldatini F (2001) Chronic ozone fumigation induces alterations in thylakoid functionality and composition in two poplar clones. Plant Physiology and Biochemistry **39:** 999-1008

Rao MV, Davis KR (1999) Ozone-induced cell death occurs via two distinct mechanisms in *Arabidopsis*: the role of salicylic acid. Plant Journal **17:** 603-614

Rao MV, Lee H, Creelman RA, Mullet JE, Davis KR (2000) Jasmonic acid signaling modulates ozone-induced hypersensitive cell death. Plant Cell **12:** 1633-1646

Rao MV, Davis KR (2001) The physiology of ozone induced cell death. Planta **213:** 682-690

Ravanel S, Gakiere B, Job D, Douce R (1998) The specific features of methionine biosynthesis and metabolism in plants. Proceedings of the National Academy of Sciences of the United States of America **95:** 7805-7812

Reddy GN, Arteca RN, Dai YR, Flores HE, Negm FB, Pell EJ (1993) Changes in ethylene and polyamines in relation to messenger RNA levels of the large and small subunits of ribulose-bisphosphate carboxylase oxygenase in ozone-stressed potato foliage. Plant Cell and Environment **16:** 819-826

Reich PB, Schoettle AW, Amundson RG (1985) Effects of low concentrations of O_3, leaf age and water stress on leaf diffusive conductance and water use efficiency in soybean. Physiologia Plantarum **63:** 58-64

Reiling K, Davison AW (1995) Effects of ozone on stomatal conductance and photosynthesis in populations of *Plantago major* L. New Phytologist **129:** 587-594

Reinert RA, Shafer SR, Eason G, Schoeneberger MM, Horton SJ (1996) Responses of loblolly pine to ozone and simulated acidic rain. Canadian Journal of Forest Research **26:** 1715-1723

Reymond P, Weber H, Damond M, Farmer EE (2000) Differential gene expression in response to mechanical wounding and insect feeding in *Arabidopsis*. Plant Cell **12:** 707-719

Richael C, Gilchrist D (1999) The hypersensitive response: A case of hold or fold? Physiological and Molecular Plant Pathology **55:** 5-12

Riikonen J, Lindsberg MM, Holopainen T, Oksanen E, Lappi J, Peltonen P, Vapaavuori E (2004) Silver birch and climate change: variable growth and carbon allocation responses to elevated concentrations of carbon dioxide and ozone. Tree Physiology **24:** 1227-1237

Risch NJ (2000) Searching for genetic determinants in the new millennium. Nature **405:** 847-856

Rosemann D, Heller W, Sandermann H (1991) Biochemical plant responses to ozone .2. Induction of stilbene biosynthesis in scots pine (*Pinus sylvestris* L.) seedlings. Plant Physiology **97:** 1280-1286

Rowlandbamford AJ, Borland AM, Lea PJ, Mansfield TA (1989) The role of arginine decarboxylase in modulating the sensitivity of barley to ozone. Environmental Pollution **61:** 95-106

Samuel MA, Miles GP, Ellis BE (2000) Ozone treatment rapidly activates MAP kinase signalling in plants. Plant Journal **22:** 367-376

Sandermann H, Ernst D, Heller W, Langebartels C (1998) Ozone: an abiotic elicitor of plant defence reactions. Trends in Plant Science **3:** 47-50

Sandermann H (1996) Ozone and plant health. Annual Review of Phytopathology **34:** 347-366

Schena M, Shalon D, Heller R, Chai A, Brown PO, Davis RW (1996) Parallel human genome analysis: Microarray-based expression monitoring of 1000 genes. Proceedings of the National Academy of Sciences of the United States of America **93:** 10614-10619

Schenk PM, Kazan K, Wilson I, Anderson JP, Richmond T, Somerville SC, Manners JM (2000) Coordinated plant defense responses in Arabidopsis revealed by microarray analysis. Proceedings of the National Academy of Sciences of the United States of America **97:** 11655-11660

Schlagnhaufer CD, Glick RE, Arteca RN, Pell EJ (1995) Molecular cloning of an ozone-induced 1-aminocyclopropane-1- carboxylate synthase cDNA and its relationship with a loss of Rbcs in potato (*Solanum tuberosum* L.) plants. Plant Molecular Biology **28:** 93-103

Seaton G, Haley CS, Knott SA, Kearsey M, Visscher PM (2002) QTL Express: mapping quantitative trait loci in of simple and complex pedigrees. Bioinformatics **18:** 339-340

Seki M, Narusaka M, Ishida J, Nanjo T, Fujita M, Oono Y, Kamiya A, Nakajima M, Enju A, Sakurai T, Satou M, Akiyama K, Taji T, Yamaguchi-Shinozaki K, Carninci P, Kawai J, Hayashizaki Y, Shinozaki K (2002) Monitoring the expression profiles of 7000 *Arabidopsis* genes under drought, cold and high-salinity stresses using a full- length cDNA microarray. Plant Journal **31:** 279-292

Shafer SR, Heagle AS (1989) Growth responses of field grown loblolly pine to chronic doses of ozone during multiple growing seasons. Canadian Journal of Forest Research **19:** 821-831

Shah J, Kachroo P, Klessig DF (1999) The *Arabidopsis* ssi1 mutation restores pathogenesis-related gene expression in npr1 plants and renders defensin gene expression salicylic acid dependent. Plant Cell **11:** 191-206

Sharma YK, Davis KR (1996) Molecular and genetic basis of ozone-induced responses in *Arabidopsis thaliana*. Plant Physiology **111:** 507-507

Shimazaki K, Iino M, Zeiger E (1986) Blue light-dependent proton extrusion by guard cell protoplasts of *Vicia faba*. Nature **319:** 324-326

Snyder KA, Richards JH, Donovan LA (2003) Night-time conductance in C-3 and C-4 species: do plants lose water at night? Journal of Experimental Botany **54:** 861-865

Spellman PT, Sherlock G, Zhang MQ, Iyer VR, Anders K, Eisen MB, Brown PO, Botstein D, Futcher B (1998) Comprehensive identification of cell cycle-regulated genes of the yeast *Saccharomyces cerevisiae* by microarray hybridization. Molecular Biology of the Cell **9:** 3273-3297

Storey JD (2002) A direct approach to false discovery rates. Journal of the Royal Statistical Society Series B-Statistical Methodology **64:** 479-498

Stoyanova R, Querec TD, Brown TR, Patriotis C (2004) Normalization of single-channel DNA array data by principal component analysis. Bioinformatics **20:** 1772-1784

Strohm M, Eiblmeier M, Langebartels C, Jouanin L, Polle A, Sandermann H, Rennenberg H (1999) Responses of transgenic poplar (*Populus tremula* x *P. alba*) overexpressing glutathione synthetase or glutathione reductase to acute ozone stress: visible injury and leaf gas exchange. Journal of Experimental Botany **50:** 365-374

Taylor G, Street NR, Tricker PJ, Sjodin A, Graham L, Skogstrom O, Calfapietra C, Scarascia-Mugnozza G, Jansson S (2005) The transcriptome of *Populus* in elevated CO_2. New Phytologist **167:** 143-154

Taylor G (2002) *Populus*: *Arabidopsis* for forestry. Do we need a model tree? Annals of Botany **90:** 681-689

Taylor G, Dobson MC (1989) Photosynthetic characteristics, stomatal responses and water relations of *Fagus sylvatica* - Impact of air quality at a site in Southern Britain.

New Phytologist **113:** 265-273

Tschaplinski TJ, Tuskan GA, Sewell MM, Gebre GM, Donald ETI, Pendleyi C (2006) Phenotypic variation and quantitative trait locus identification for osmotic potential in an interspecific hybrid inbred F-2 poplar pedigree grown in contrasting environments. Tree Physiology **26:** 595-604

Torsethaugen G, Pell EJ, Assmann SM (1999) Ozone inhibits guard cell K^+ channels implicated in stomatal opening. Proceedings of the National Academy of Sciences of the United States of America **96:** 13577-13582

Tricker PJ, Trewin H, Kull O, Clarkson GJJ, Eensalu E, Tallis MJ, Colella A, Doncaster CP, Sabatti M, Taylor G (2005) Stomatal conductance and not stomatal density determines the long-term reduction in leaf transpiration of poplar in elevated CO_2. Oecologia **143:** 652-660

Tulsieram LK, Glaubitz JC, Kiss G, Carlson JE (1992) Single tree genetic-linkage mapping in conifers using haploid DNA from megagametophytes. Biotechnology **10:** 686-690

Tuomainen J, Betz C, Kangasjarvi J, Ernst D, Yin ZH, Langebartels C, Sandermann H (1997) Ozone induction of ethylene emission in tomato plants: regulation by differential accumulation of transcripts for the biosynthetic enzymes. Plant Journal **12:** 1151-1162

Turcsanyi E, Lyons T, Plochl M, Barnes J (2000) Does ascorbate in the mesophyll cell walls form the first line of defence against ozone? Testing the concept using broad bean (*Vicia faba* L.). Journal of Experimental Botany **51:** 901-910

Tuskan GA, DiFazio SP, Teichmann T (2004) Poplar genomics is getting popular: The impact of the poplar genome project on tree research. Plant Biology **6:** 2-4

Vahala J, Keinanen M, Schutzendubel A, Polle A, Kangasjarvi J (2003) Differential effects of elevated ozone on two hybrid aspen genotypes predisposed to chronic ozone fumigation. Role of ethylene and salicylic acid. Plant Physiology **132:** 196-205

van Hove LWA, Bossen ME, San Gabino BG, Sgreva C (2001) The ability of apoplastic ascorbate to protect poplar leaves against ambient ozone concentrations: a quantitative approach. Environmental Pollution **114:** 371-382

Vranova E, Atichartpongkul S, Villarroel R, Van Montagu M, Inze D, Van Camp W (2002) Comprehensive analysis of gene expression in *Nicotiana tabacum* leaves acclimated to oxidative stress. Proceedings of the National Academy of Sciences of the United States of America **99:** 10870-10875

Wang Y, Lu JP, Lee R, Gu ZP, Clarke R (2002) Iterative normalization of cDNA microarray data. IEEE Transactions on Information Technology in Biomedicine **6:** 29-37

Wang XJ, Hessner MJ, Wu Y, Pati N, Ghosh S (2003) Quantitative quality control in microarray experiments and the application in data filtering, normalization and false positive rate prediction. Bioinformatics **19:** 1341-1347

Wang HY, Luo MJ, Tereshchenko IV, Frikker DM, Cui XF, Li JY, Hu GH, Chu Y, Azaro MA, Lin Y, Shen L, Yang QF, Kambouris ME, Gao RC, Shih WC, Li HH (2005) A genotyping system capable of simultaneously analyzing > 1000 single nucleotide polymorphisms in a haploid genome. Genome Research **15:** 276-283

Weaver LM, Gan SS, Quirino B, Amasino RM (1998) A comparison of the expression patterns of several senescence- associated genes in response to stress and hormone treatment. Plant Molecular Biology **37:** 455-469

Wilson DL, Buckley MJ, Helliwell CA, Wilson IW (2003) New normalization methods for cDNA microarray data. Bioinformatics **19:** 1325-1332

Wohlgemuth H, Mittelstrass K, Kschieschan S, Bender J, Weigel HJ, Overmyer K, Kangasjarvi J, Sandermann H, Langebartels C (2002) Activation of an oxidative burst is a general feature of sensitive plants exposed to the air pollutant ozone. Plant Cell and Environment **25:** 717-726

Woo SY, Hinckley TM (2005) The effects of ozone on growth and stomatal response in the F_2 generation of hybrid poplar (*Populus trichocarpa* x *Populus deltoides*). Biologia Plantarum **49:** 395-404

Yalpani N, Enyedi AJ, Leon J, Raskin I (1994) Ultraviolet light and ozone stimulate accumulation of salicylic acid, pathogenesis-related proteins and virus resistance in tobacco. Planta **193:** 372-376

Yang YH, Dudoit S, Luu P, Lin DM, Peng V, Ngai J, Speed TP (2002) Normalization for cDNA microarray data: a robust composite method addressing single and multiple slide systematic variation. Nucleic Acids Research **30:** art. no.-e15

Zacarias L, Reid MS (1990) Role of growth regulators in the senescence of *Arabidopsis thaliana* leaves. Physiologia Plantarum **80:** 549-554

Zeng ZB (1994) Precision mapping of quantitative trait loci. Genetics **136:** 1457-1468

Zhang SQ, Klessig DF (1997) Salicylic acid activates a 48-kD MAP kinase in tobacco. Plant Cell **9:** 809-824

Zheng YB, Lyons T, Ollerenshaw JH, Barnes JD (2000) Ascorbate in the leaf apoplast is a factor mediating ozone resistance in Plantago major. Plant Physiology and Biochemistry **38:** 403-411